Periodic time-dependent Kondo model

Markus Philip Ludwig Heyl

München 2009

Periodic time-dependent Kondo model

Markus Philip Ludwig Heyl

Diplomarbeit
an der Fakultät für Physik
der Ludwig–Maximilians–Universität
München

vorgelegt von
Markus Philip Ludwig Heyl
aus Starnberg

München, den 7. April 2009

Erstgutachter: Prof. Stefan Kehrein
Zweitgutachter: Prof. Erwin Frey

Contents

Chapter 1

Introduction

The fundamental assumption in statistical physics demands that systems evolve into a unique configuration, an equilibrium or thermal state, after a sufficiently long time. For the description of the statistical properties of these equilibrium configurations only a small set of macroscopic quantities like energy, total particle number or confining volume have to be prescribed. The methods of statistical physics that enable this simplified description, however, fail for the description of states that are driven out of equilibrium posing the question of how to characterize these nonequilibrium states.

Recently, nonequilibrium dynamics in quantum systems have gained considerable interest due to their observation in experiments. Nanodevices like single electron transistors or quantum dots offer the possibility to control microscopic parameters. It was realized soon that these nanodevices can display Kondo physics [11], the paradigm model for strongly correlated electron systems. The huge flexibility in control over the microsocopic parameters in these nanodevices leads to the question of how the system's properties are affected in a nonequilibrium setting. In principle, two different ways of creating a nonequilibrium situation for a quantum dot can be distinguished. First, a source drain voltage can be applied across the nanodevice, creating a window of scattering channels that are not accessible in an equilibrium setting. Alternatively, the microscopic parameters can be varied in time leading to a time-dependent nonequilibrium setup. Another way of experimentally realizing nonequilibrium quantum many-body systems is to use cold atoms in optical lattices. Optical lattices are arrays of standing light waves that create a periodic potential background in which atoms can be trapped. In contrast to bulk solids the lattice spacing as well as the ratio between kinetic and potential energy can be varied in time.

A way of generating a nonequilibrium setting is a so-called interaction quench. An interaction quench describes a scenario in which a system is initially prepared in the ground state of some Hamiltonian H_0. Then at $t = 0$ a parameter of the Hamiltonian is changed instantaneously, much faster than any internal time scale in an actual experiment, such that the ground state of the initial Hamiltonian evolves in time due to a new Hamiltonian. In general, the prepared state is not an eigenstate of the system's Hamiltonian any more leading to nontrivial dynamics. The time evolution for interacting quantum many-body systems subject to such an interaction quench has been studied for a variety of model systems, e.g. for the Hubbard model [30], the Falicov-Kimball model [9], the Kondo model [26][27] and the related Anderson model [31], the Richardson model [10] or for Luttinger liquids [5]. Another important example for a system

subject to an interaction quench is the Fermi-edge singularity problem where the X-ray absorption spectrum for bulk metals is studied. As it turned out, it is possible to map this problem onto a nonequilibrium problem where a sea of conduction band electrons has to adapt to a suddenly created local scatterer [33].

One may ask the question of how a system's properties are affected if it is quenched not only once, but infinitely often in a periodic fashion. In this case a quasi-steady state is generated, a state such that all correlation functions are invariant under a discrete time shift of one period τ in all their time arguments, i.e. $\langle \mathcal{O}(t)\mathcal{P}(t')\rangle = \langle \mathcal{O}(t+\tau)\mathcal{P}(t'+\tau)\rangle$ for a two-time correlation function. In general, states that are created by a periodic driving of a system are different from states that are accessible by thermal activation such that states with new properties may be generated. The characterization of such states, however, poses a new challenge. The dynamics of periodically driven strongly interacting many-body systems have been addressed only in a rather small number of model systems, e.g. the Falicov-Kimball model [42], the Anderson model [29][32] or the Kondo model [12][20][21]. The complexity of these driven quasi-steady states, however, is accompanied by mathematical and technical difficulties restricting the number of analytical and numerical methods that are suitable to tackle these time-dependent problems.

In this thesis a quasi-steady state in the Kondo model will be analyzed. The Kondo model, the paradigm model for strongly correlated electron systems, describes a local two level system, a spin $1/2$, that is coupled to a bath of fermions via an exchange interaction. The quasi-steady state is generated by periodically switching on and off the exchange interaction. The Kondo model exhibits a special point in parameter space, the so-called Toulouse limit, where it becomes exactly solvable such that its dynamics can be studied nonperturbatively. Moreover, the real-time dynamics are accessible analytically on all time scales for a wide range of parameters of the external driving. Especially, it is possible to analyze the buildup of the quasi-steady state whose features will be characterized by analyzing the dynamical properties of the local two state system, that is the magnetization of the local spin $\langle S_z(t)\rangle$ and the spin-spin correlation function $\langle S_z(t)S_z(t')\rangle$. The exact solvability of the Kondo model in the Toulouse limit may open the possibility to gain key insights into the properties of quasi-steady states in the Kondo model.

Recently, there have been attempts to characterize nonequilibrium settings by introducing effective thermodynamic quantities like effective temperatures [28][32]. It will be shown that it is not possible to define an effective temperature in the present setup since the excitations in a periodically driven system are fundamentally different from those induced by temperature. A periodic driving creates a discrete excitation spectrum corresponding to the absorption and emission of multiple quanta of the driving frequency whereas a finite temperature leads to a smearing of the Fermi surface.

Although new parameters appear in a nonequilibrium configuration, a universal description is expected to be possible in the Kondo model. Kaminski et al. [21] proposed a universal function for the conductance through a Kondo impurity in nonequilibrium. Moreover, they showed that the Kondo temperature remains the only relevant energy scale. In the periodic time-dependent setting used in this thesis, the spin-spin correlation function also exhibits a universal description revealing that the only relevant energy scale indeed is the Kondo scale.

Moreover, the asymptotic behavior of the periodically driven Kondo system in the

fast and slow driving case will be analyzed. As expected, the system is not able to follow a fast external driving. The spin-spin correlation function approaches a shape that is similar to an equilibrium one. A careful analysis, however, shows that it is not possible to find a time-independent effective Hamiltonian that generates the same dynamics. In the opposite case of very slow driving, the system relaxes during each time interval in which the Kondo Hamiltonian is constant in time. Therefore, the system behaves as for a single interaction quench in the Kondo model, a situation that has already been addressed in the work by Lobaskin and Kehrein [27][28].

The outline of this thesis is as follows. In Chapter 2, the basic concepts of impurity models in equilibrium will be explained, including the Anderson impurity model and Kondo model as well as their connection via the Schrieffer-Wolff transformation. The experimental realization of tunable Kondo impurities in form of quantum dots embedded in two-dimensional electron gases will be presented. Moreover, known results of time-dependent Kondo and Anderson impurity models will be discussed. Chapter 3 is devoted to the bosonization technique and its application to the Kondo model. Using the bosonization method it is shown how the Kondo Hamiltonian in the Toulouse limit can be mapped onto an exactly solvable noninteracting resonant level model Hamiltonian. Chapter 4 deals with the periodic time-dependent setup that is used to generate the quasi-steady state in the Kondo model, namely the periodic switch on and off of the Kondo interaction. Moreover, a possible experimental realization using a quantum dot is presented. The exact single-particle dynamics in the time-dependent resonant level model Hamiltonian are determined in Chapter 5 on all time scales. This enables the exact evaluation of correlation functions on all times like the magnetization of the impurity spin and the spin-spin correlation function in the full many-body situation in Chapter 6. Based on these quantities the quasi-steady state will be characterized. The thesis closes with a short summary and outlook in Chapter 7.

Chapter 2

Kondo effect

The Kondo effect was observed for the first time in 1934 in an experiment by de Haas et al. where the temperature dependence of the resistivity of a bulk gold sample was investigated. The measurement unexpectedly showed an increase of resistivity for decreasing temperature. Phonons, that commonly provide the dominant scattering mechanism for electrons, die out rapidly as one approaches low temperatures. Therefore, the resistivity was expected to decline monotonically and to saturate at a nonzero value due to scattering off lattice imperfections. The deviation from this behavior suggested the existence of a new scattering mechanism that becomes more efficient at lower temperatures. In 1964 the Japanese physicist Jun Kondo achieved a first theoretical explanation for this anomalous behavior in terms of scattering induced by magnetic impurities, impurities with a net spin in the electronic environment. Using the *s-d-* model, also named Kondo model, Kondo showed using perturbation theory up to the second order in the coupling that a new contribution $\propto \ln(1/T)$ appears in the resistivity increasing logarithmically at low temperatures. While perturbation theory describes the increase of resistivity, the logarithmic divergence for $T \to 0$ suggested that for low temperatures perturbation theory breaks down such that this problem becomes nonperturbative. In the early 70's, Anderson [2] proposed a scaling method, named poor man's scaling, by which the most relevant logarithmic terms in the perturbation series can be summed up. This approach confirmed the existence of an energy scale, the Kondo temperature T_K, below which the problem becomes nonperturbative. Based on the idea of scaling, Wilson [44] with the invention of the numerical renormalization group method was able to calculate thermodynamic low-temperature properties of the Kondo model nonperturbatively. In 1980, Andrei [4] gave an analytical and nonperturbative solution of the Kondo model by use of the Bethe ansatz that allowed to determine thermodynamic properties exactly. In the same year, Wiegman [43] applied the Bethe ansatz to the closely related Anderson impurity model and showed its integrability. Dynamical properties, however, have not been accessible using this approach. For a detailed introduction to the Kondo effect, see for example [16].

2.1 The Kondo effect in equilibrium

As already mentioned in the introductory remarks, the Kondo effect emerges when a local spin is coupled to a metallic environment. The Hamiltonian that models a physical situation in which a local two state system in form of a spin $\frac{1}{2}$ is coupled to a fermionic
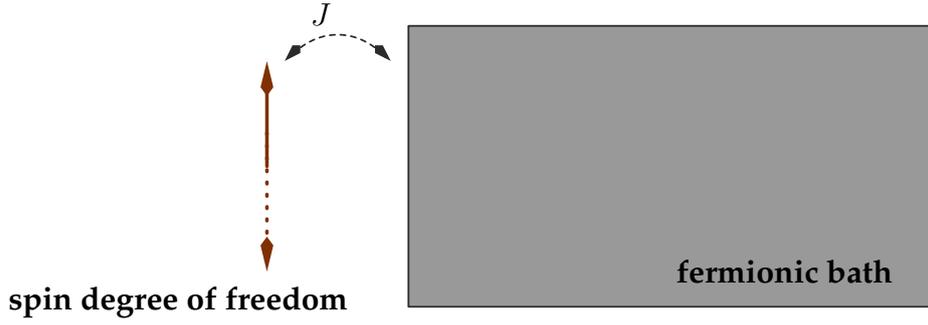
Figure 2.1: Two state system coupled to a fermionic bath via an exchange interaction J leading to spin-flips of the local spin.

bath of electrons via an exchange interaction is the *s-d*-Hamiltonian, or Kondo Hamiltonian:

$$H_K = \sum_{\mathbf{k},\eta=\uparrow,\downarrow} \epsilon_{\mathbf{k}} : c_{\mathbf{k}\eta}^{\dagger} c_{\mathbf{k}\eta} : + J \sum_{\mathbf{kk'}} \left[c_{\mathbf{k}\uparrow}^{\dagger} c_{\mathbf{k'}\uparrow} - c_{\mathbf{k}\downarrow}^{\dagger} c_{\mathbf{k'}\downarrow} \right] S_z +$$
$$+ J \sum_{\mathbf{kk'}} \left[c_{\mathbf{k}\downarrow}^{\dagger} c_{\mathbf{k'}\uparrow} S_+ + c_{\mathbf{k}\uparrow}^{\dagger} c_{\mathbf{k'}\downarrow} S_- \right]. \tag{2.1}$$

Here, $c_{\mathbf{k}\eta}^{\dagger}$ creates an electron with wave vector $\mathbf{k}$ and spin η in the reservoir. The colons : ... : denote normal ordering with respect to the Fermi sea. The operator S_z measures the spin on the local level that can be flipped by the spin ladder operators S_+ and S_-. The first term thus describes a sea of noninteracting fermions with a dispersion relation ϵ_k. The second contribution causes scattering of electrons off the impurity by changing their momenta but retaining their spins. The spin dynamics are introduced by the term in the second line where the spin of the scattered electron is flipped while simultaneously flipping the spin of the impurity.

The characteristic energy scale of the Kondo model is the Kondo temperature T_K that is connected to the parameters in the Hamiltonian through the following relation:

$$T_K = D \, e^{-\frac{1}{\rho J}} \tag{2.2}$$

where D denotes an ultra-violet cutoff and ρ the electron's density of states at the Fermi energy.

The low energy excitations of a Kondo system are complicated spin excitations in the vicinity of the local level resulting from multiple spin flip processes of the conduction band electrons. Due to these subsequent scattering events the electrons become strongly correlated. As electrons try to screen Coulomb potentials the surrounding electrons try to screen the local spin. Therefore, electrons with opposite spin gather in the vicinity of the impurity forming the so called Kondo cloud thereby partially compensating the excess spin. Renormalization group approaches show that for decreasing temperature $T \to 0$ the Kondo model flows to a strong coupling fixed point Hamiltonian that is dominated by the Kondo interaction. In the zero temperature limit one ends up in a situation where itinerant electrons with opposite spin are bound to the local level resulting in a perfectly screened spin. The ground state in the Kondo model can be thought of as a superposition of two states each of which contains a bound pair
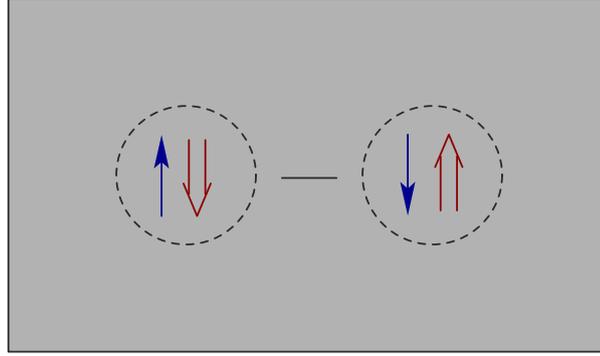
Figure 2.2: Schematic picture of the ground state of the Kondo model: superposition of two bound pairs of the impurity spin (marked by the blue arrow) with a collective bath electron spin (marked as the red arrow) embedded in an otherwise unpolarized background

of an impurity spin with a collective localized spin of conduction band electrons as indicated in Fig. (2.2). This bound pair of a local spin and a collective spin of the bath electrons is called the Kondo singlet with an associated binding energy of the order T_K. Due to the formation of the Kondo singlet it is not possible any more for the impurity to flip spins. Nevertheless, this new local impurity acts as a static scatterer. The conduction band electrons constitue a Fermi liquid where the phase shift associated with this local potential scatterer approaches the value $\delta_\uparrow (\epsilon_F) = \pi/2$ at the Fermi level.

At low temperatures, the striking feature of the Kondo effect is a sharp resonance in the local density of states that is pinned exactly at the Fermi energy of the conduction band. As transport properties depend crucially on the available states at the Fermi level it is clear that this sharp resonance will have an important impact on those quantities.

2.1.1 Anderson impurity model

The Kondo model describes the low energy physics of the local level coupled to a fermionic environment, but it does not explain how such a single spin can develop in a sea of fermions. For this purpose, the more general Anderson impurity model can be employed [1]:

$$
\begin{aligned}
H_{\text{AIM}} &= H_{el} + H_{dot} + H_t \\
H_{el} &= \sum_{\mathbf{k}\eta=\uparrow,\downarrow} \epsilon_{\mathbf{k}} : c^\dagger_{\mathbf{k}\eta} c_{\mathbf{k}\eta} : \\
H_{dot} &= \sum_{\eta} \epsilon_d d^\dagger_\eta d_\eta + U \hat{n}_\uparrow \hat{n}_\downarrow \\
H_t &= \sum_{\mathbf{k}\eta} \left[t_{\mathbf{k}} c^\dagger_{\mathbf{k}\eta} d_\eta + t^*_{\mathbf{k}} d^\dagger_\eta c_{\mathbf{k}\eta} \right] .
\end{aligned}
\tag{2.3}
$$

The Anderson impurity model describes a situation where a central region with a level at an energy ε_d is coupled to a sea of electrons via tunnel coupling. The local level
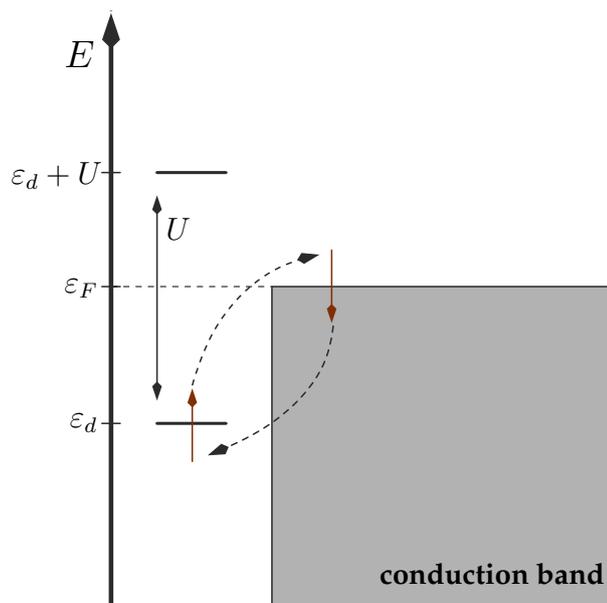
Figure 2.3: Schematic picture of a Quantum Dot in the local moment regime. The arrows indicate a virtual process leading to a spin flip in the central region.

hybridizes with the surrounding bath of conduction band states with an associated level broadening of half width $\Gamma = 2\pi \sum_k |t_{\mathbf{k}}|^2 \delta(\varepsilon_F - \varepsilon_k)$. The Anderson impurity model is able to describe a variety of different physical situations depending on the parameters. Important for the present work is the so called local-moment regime where

$$\varepsilon_d \ll 0, \quad \varepsilon_d + U \gg 0, \quad \Gamma, k_B T \ll |\varepsilon_d|, \varepsilon_d + U. \tag{2.4}$$

A schematic picture of this situation is shown in Fig. (2.3). Here, all energies are measured in their distance from the Fermi energy of the lead, i.e. $\varepsilon_F = 0$. The probability for the local level ε_d to be occupied in the local-moment regime will be nearly one. The first condition ensures that it is favorable for the local level to be occupied since the energy can always be minimized due to a process where a conduction band electron hops onto the local level with energy ε_d if no electron is present in the central region. The second condition prohibits double occupancy at low temperatures since a conduction band electron has to pay a lot of energy for hopping onto the central region if already another electron is occupying the level ε_d. The third restriction ensures that the level broadening as well as the temperature are small enough not to cause strong fluctuations in the occupation of the local levels such that the occupation number is a good quantum number. Consequently, the large on-site Coulomb interaction U causes single occupancy. Since single occupancy implies a net spin in the central region, the Anderson impurity model provides the explanation for the question of how a single spin can develop in a fermionic environment.

As already emphasized in the previous paragraph, the Kondo effect originates from multiple spin-flip processes of conduction band electrons. In the Anderson impurity model such processes can happen in the following way. Suppose the local level is occupied with a spin up electron as indicated in Fig. (2.3). Although double occupancy is unfavorable virtual processes can lead to spin flips. According to the Heisenberg uncertainty relation it is possible for the local electron to hop into the conduction band for a

short but finite time. In the meanwhile, it is possible for an electron with opposite spin to tunnel onto the local level thereby effectively flipping the spin of the central region. Besides this example, various other virtual processes can lead to a spin-flip of the local electron.

2.1.2 Schrieffer-Wolff transformation

In the local-moment regime the effective low energy Hamiltonian of the Anderson impurity model is the Kondo Hamiltonian. This can be shown by the so-called Schrieffer-Wolff transformation that maps onto the subspace of states that are relevant for the low energy properties of the Anderson impurity Hamiltonian [40]. Suppose there is a unitary transformation

$$U = e^W \tag{2.5}$$

where the generator W is chosen to be proportional to the hopping element $t_{\mathbf{k}}$. Due to the condition $\Gamma \ll |\varepsilon_d|, \varepsilon_d + U$, see Eq. (2.4), the tunneling matrix element $t_{\mathbf{k}}$ is small such that the transformed Hamiltonian can be expanded according to the Baker-Hausdorff formula where the expansion parameter is $t_{\mathbf{k}}$:

$$e^W H_{\mathrm{AIM}} e^{-W} = H_{\mathrm{AIM}} + [W, H_{\mathrm{AIM}}] + \frac{1}{2}[W, [W, H_{\mathrm{AIM}}]] + \mathcal{O}\left[t_{\mathbf{k}}^3\right]. \tag{2.6}$$

Grouping together those terms that are of the same order in the expansion parameter $t_{\mathbf{k}}$ leads to:

$$e^W H_{\mathrm{AIM}} e^{-W} = H_{el} + H_{dot} + (H_t + [W, H_{el} + H_{dot}])$$

$$+ \left([W, H_t] + \frac{1}{2}[W, [W, H_{el} + H_{dot}]]\right) + \mathcal{O}\left[t_{\mathbf{k}}^3\right]. \tag{2.7}$$

Suppose one can choose the generator W in such a way, that the term linear in the tunnel coupling vanishes

$$[H_{el} + H_{dot}, W] = H_t. \tag{2.8}$$

Then the resulting transformed operator will be of the order $t_{\mathbf{k}}^2$:

$$e^W H_{\mathrm{AIM}} e^{-W} = H_{el} + H_{dot} + \frac{1}{2}[W, H_t] + \mathcal{O}\left[t_{\mathbf{k}}^3\right]. \tag{2.9}$$

This is achieved by the choice:

$$W = \sum_{\mathbf{k}\eta} t_{\mathbf{k}} \left[\frac{1}{\varepsilon_{\mathbf{k}} - \varepsilon_d} c_{\mathbf{k}\eta}^\dagger d_\eta + \frac{U}{(\varepsilon_d - \varepsilon_{\mathbf{k}})(\varepsilon_d + U - \varepsilon_{\mathbf{k}})} d_{-\eta}^\dagger d_{-\eta} c_{\mathbf{k}\eta}^\dagger d_\eta\right] - h.c. \tag{2.10}$$

Additionally, another projection is performed simplifying the resulting Hamilton operator substantially. The occupation of the local level is nearly one in the local-moment regime. Due to the conditions $\varepsilon_d \ll 0, \varepsilon_d + U \gg 0$, see Eq. (2.4), the subspace of the Hilbert space that contains zero and double occupancy is irrelevant for the low energy properties. Therefore, one can project onto the subspace of single occupation. As a result of the unitary transformation and the projection one ends up with the following

Kondo Hamiltonian as the effective Hamiltonian for the low energy properties of the Anderson impurity model:

$$
H_K = \sum_{\mathbf{k},\eta=\uparrow,\downarrow} \epsilon_{\mathbf{k}} : c_{\mathbf{k}\eta}^\dagger c_{\mathbf{k}\eta} : + J \sum_{\mathbf{k}\mathbf{k}'} \left[c_{\mathbf{k}\uparrow}^\dagger c_{\mathbf{k}'\uparrow} - c_{\mathbf{k}\downarrow}^\dagger c_{\mathbf{k}'\downarrow} \right] S_z +
$$
$$
+ J \sum_{\mathbf{k}\mathbf{k}'} \left[c_{\mathbf{k}\downarrow}^\dagger c_{\mathbf{k}'\uparrow} S_+ + c_{\mathbf{k}\uparrow}^\dagger c_{\mathbf{k}'\downarrow} S_- \right] + \sum_{\mathbf{k}\mathbf{k}'\eta} K_{\mathbf{k}\mathbf{k}'} c_{\mathbf{k}\eta}^\dagger c_{\mathbf{k}'\eta},
\tag{2.11}
$$

where the couplings are related to the parameters of the Anderson impurity Hamiltonian [16]:

$$
J_{\mathbf{k}\mathbf{k}'} = t_{\mathbf{k}} t_{\mathbf{k}'} \left[\frac{1}{\varepsilon_{\mathbf{k}} - \varepsilon_d} + \frac{1}{\varepsilon_d + U - \varepsilon_{\mathbf{k}'}} \right],
$$
$$
K_{\mathbf{k}\mathbf{k}'} = \frac{t_{\mathbf{k}} t_{\mathbf{k}'}}{2} \left[\frac{1}{\varepsilon_{\mathbf{k}} - \varepsilon_d} - \frac{1}{\varepsilon_d + U - \varepsilon_{\mathbf{k}'}} \right].
\tag{2.12}
$$

Since only electrons near the Fermi level, $\varepsilon_{\mathbf{k}} = 0$, contribute to the low energy properties of the Kondo model, one can neglect the $\mathbf{k}$-dependence of the coupling $J_{\mathbf{k}\mathbf{k}'}$ thereby replacing it by the structureless constant $J = J_{00}$. In the particle-hole symmetric case, $\varepsilon_d = -U/2$, the potential scattering term vanishes.

2.2 The anisotropic Kondo model in *1-d*

In the case where the coupling J in the Kondo Hamiltonian shows no dependence on the momenta the local spin acts as a pointlike scatterer located at the origin, such that only s-wave scattering occurs. By expanding the electron's plane waves with wave vector $\mathbf{k}$ in spherical waves around $x = 0$ one can show that only those spherical waves that have angular momentum quantum numbers $l = m = 0$ are affected by the local scatterer [25]. All other spherical waves decouple from the scattering problem and propagate freely. As a consequence, the states that are relevant for the dynamics can be characterized by the absolute value $|\mathbf{k}|$ of their momenta. Thus, the problem is effectively a one-dimensional one.

Since the excitations that are relevant for the Kondo effect are low energy excitations in the vicinity of the Fermi level, one may linearize the spectrum of the conduction band electrons around the Fermi energy $\varepsilon_F = 0$ leading to

$$
\varepsilon_k \approx v_F k,
\tag{2.13}
$$

where v_F is the Fermi velocity. In the low temperature limit the interaction in the Kondo Hamiltonian becomes dominant leading to the buildup of the Kondo singlet. In this regime one can replace the usual Kondo Hamiltonian by its anisotropic counterpart in the Toulouse limit [27]:

$$
H_K = \sum_{k,\eta=\uparrow\downarrow} v_F k : c_{k\eta}^\dagger c_{k\eta} : + \frac{J_\parallel}{2} \left[: \Psi_\uparrow^\dagger(0)\Psi_\uparrow(0) : - : \Psi_\downarrow^\dagger(0)\Psi_\downarrow(0) : \right] S_z +
$$
$$
+ \frac{J_\perp}{2} \left[\Psi_\uparrow^\dagger(0)\Psi_\downarrow(0) S^- + \Psi_\downarrow^\dagger(0)\Psi_\uparrow(0) S^+ \right],
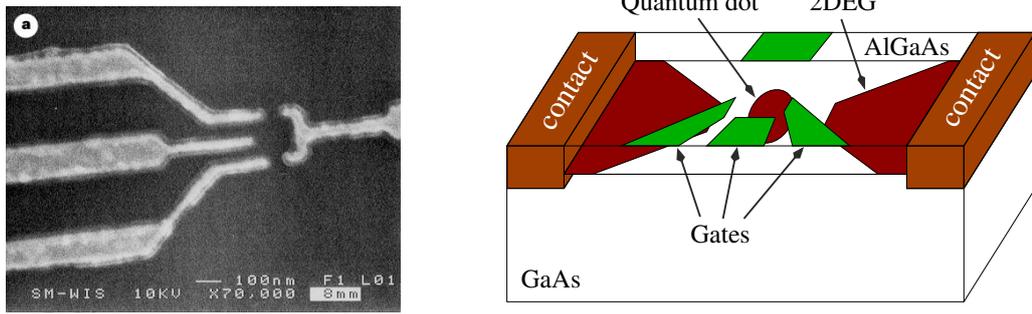\tag{2.14}
$$

Figure 2.4: The left picture shows a scanning electron microscope image of a quantum dot that is created in the confined region between the electrodes. The picture is taken from Goldhaber-Gordon et al. [11]. The two outer metallic gates can be used to tune the tunnel coupling of the dot to the surrounding 2DEG. The metallic gate in between, the so-called back-gate, enables to control the energy levels of the dot relative to the conduction band electrons. Additionally, contacts for source and drain, not shown in the left picture, can be placed upon the heterostructure in order to create a current through the device. A schematic picture of the experimental situation is shown on the right hand side.

that can be viewed as a generalization of the usual isotropic Kondo Hamiltonian. Here, the perpendicular coupling $J_\perp$ and the parallel coupling $J_\parallel$ are not necessarily identical. This is in contrast to the Kondo Hamiltonian that emerges from the Anderson impurity model after the Schrieffer-Wolff transformation. Initially, the anisotropic Kondo Hamiltonian was introduced by Anderson and coworkers [3] in the beginning of the 70's merely as a calculational tool while rotational invariance, i.e. $J_\parallel = J_\perp$, was always demanded in the end. Here, the anisotropic Kondo Hamiltonian in the Toulouse limit serves as an effective Hamiltonian for the strong coupling limit of the Kondo model. Under this replacement, however, the meaning of the coupling constant changes. The parallel coupling $J_\parallel$ is fixed at a special value, $J_\parallel = 2 - \sqrt{2}$, the so-called Toulouse limit, where the Hamiltonian can be diagonalized exactly using the bosonization technique. The Kondo scale T_K is still linked to a coupling constant in the Kondo model, namely to the perpendicular coupling $J_\perp$. The exact relation will be discussed later.

2.3 The Kondo effect in nonequilibrium

Originally, measurements on the Kondo effect were restricted to metallic or semiconducting bulk samples in which magnetic impurities have been embedded. In order to observe their impact on bulk properties like conductance or magnetic susceptibility, for example, a sufficient concentration of impurities was needed. The influence of a single impurity, however, has not been accessible by such an experiment. Moreover, a variation of the microscopic parameters was achievable only by fabricating different samples with different kinds of impurities.

The advent of quantum dots opened up the possibility to study the Kondo effect with a high tunability of the microscopic parameters. Quantum dots can be thought

of as small islands that are confined within a two dimensional electron gas (2DEG) in a semiconductor heterostructure. Connecting two semiconducting materials with different band structures leads to a deformation of the conduction and valence band in the vicinity of the interface. For a proper combination of materials, like GaAs/AlGaAs, a two-dimensional electron gas (2DEG) forms in the interface region. Additionally, metallic gates can be placed upon the top of the heterostructure as can be seen in Fig. (2.4). By a proper tuning of the gates the filling of the dot as well as the tunnel coupling can be controlled. Moreover, contacts can be placed upon the heterostructure such that a current can be induced by applying a source-drain voltage across the dot. Mathematically, a quantum dot can be modeled by an Anderson impurity Hamiltonian.

The flexibility in control over these systems automatically led to the question of how the Kondo effect is influenced by a nonequilibrium setting. Such a nonequilibrium situation can be created in different ways. One may apply a source-drain voltage across the dot that may be chosen time-dependent. Moreover, the back gate voltage can varied in time leading to a modulation of the energy levels in the dot. In this work the influence of a special periodic time-dependent back-gate voltage, that leads to a periodic switch on and off of the Kondo interaction in the Kondo model, onto local properties of the quantum dot will be analyzed. During the last two decades numerous theoretical works have addressed the properties of the Kondo or Anderson impurity model in nonequilibrium settings with time-dependent gate voltages.

Nordlander and coworkers [31] investigated a scenario in which the local level position ε_d, by a proper tuning of the back gate voltage, is suddenly pushed into the local-moment regime in which a Kondo effect can emerge. This amounts to the instantaneous switch on of the Kondo interaction. As a result of their calculation using the noncrossing approximation (NCA) they could confirm the existence of a time scale $1/T_K$ for the buildup of the Kondo effect.

In an earlier work, Nordlander and coworkers [32] addressed a situation in which the local level position of a quantum dot is varied sinusoidally with a period Ω. Depending on the driving frequency Ω they found three different regimes. For slow driving, i.e. small Ω, the system behaves adiabatically such that at any time the system is in perfect equilibrium. In an intermediate regime, the Kondo effect survives and additional side peaks appear in the local density of states placed at multiples of the driving frequency Ω. For fast switching an equilibrium-like situation is created. The local density of states approaches an equilibrium form of a setting where the local level position ε_d is given by its time averaged value. In the case of fast driving, they conjectured that the additional decay rate for the electrons on the dot due to the periodic driving has the same effect as an increased effective temperature for leads.

Goldin and Avishai [12] derived an explicit formula for the current through a quantum dot in the Kondo regime for the case of a strong source-drain voltage with a slowly varying periodic modulation by use of third order perturbation theory in the Kondo coupling. They found that the zero bias anomaly in the differential conductance is suppressed and side peaks appear at multiples of the driving frequency.

In a work by Kaminski et.al. [20] [21] the influence of an ac source-drain voltage and a periodic shifting of the local level in a quantum dot onto the differential conductance was investigated for various regimes. Despite the appearance of new parameters in this nonequilibrium setup, they conjectured that a universal description of the differential conductance is achievable. Moreover, they found that the Kondo temperature remains

the only relevant energy scale even under these nonequilibrium conditions. They could attribute the suppression of the Kondo effect to a mechanism called spin-flip cotunneling leading to decoherence of the local spin under the periodic driving.

The dynamical quantities characterizing the local two state system are the magnetization of the impurity spin $\langle S_z(t) \rangle$ and the spin-spin correlation function $\langle S_z(t)S_z(t') \rangle$ whose properties have been addressed in numerous works [15] [25] [26] [27]. Those dynamical quantities, however, have only been studied in equilibrium settings or interaction quench scenarios. The influence of a periodic driving onto their properties will be investigated in this work. Due to the periodic driving, a quasi-steady state will emerge that may be fundamentally different from an equilibrium state or factorized initial preparation as for an interaction quench scenario. A characterization of this quasi-steady state with the help of the magnetization and spin-spin correlation function will be the task of this work.

Leggett and coworkers [25] studied those dynamical quantities in the context of the spin-boson model that is unitarily equivalent to the Kondo model. In this formulation of the problem they calculated the magnetization and spin-spin correlation function by using the so-called noninteracting-blip approximation. Preparing the system in a nonequilibrium state with a nonvanishing initial impurity spin orientation, $\langle S_z \rangle = \frac{1}{2}$, they found that the magnetization decays exponentially:

$$P(t) = \langle S_z(t) \rangle = \frac{1}{2} e^{-t/\tau} \tag{2.15}$$

where τ is a characteristic time scale of the system. This result has been confirmed by Lesage and Saleur [26] using the form-factor approach. Lobaskin and Kehrein [27] derived the magnetization after an interaction quench in the limit of small Kondo couplings, i.e. away from the Toulouse limit, for all times using the flow equation method. They found that, initially, $P(t)$ decays faster, but approaches the exponential behavior as in Eq. (2.15) asymptotically for long times. The question of how the magnetization of the impurity spin relaxes in a scenario of periodic driving will be a basic issue addressed in this work.

A local dynamical quantity that carries more information about the local two state system is the spin-spin correlation function $\langle S_z(t)S_z(t') \rangle$. As has been shown by Leggett and coworkers [25] it asymptotically decays algebraically at zero temperature in equilibrium:

$$\langle S_z(t)S_z(t') \rangle \overset{t-t' \to \infty}{\propto} 1/(t-t')^2 \tag{2.16}$$

For finite temperatures, however, the spin-spin correlation function decays exponentially. Guinea [15] derived an analytical expression for the Fourier transform of this function for zero temperature in equilibrium in the Toulouse limit. The behavior of the spin-spin correlation function in a nonequilibrium situation due to an interaction quench in the Kondo model was addressed in the work by Lobaskin and Kehrein [27]. They found that both in the Toulouse limit and in the limit of small Kondo couplings this correlation function decays algebraically for nonzero waiting times, that is the time of the first spin measurement. Additionally, the nonequilibrium to equilibrium crossover happens exponentially fast as a function of the waiting time.

Chapter 3

Bosonization: Kondo model

One striking feature of one dimensional systems is the possibility to completely span the full fermionic Fock space in terms of bosonic operators and Klein factors resulting in the bosonization identity relating fermionic fields with bosonic ones as an operator identity in Fock space [37]. The bosonization identity is a fundamental property of fermionic fields in one dimension and is completely independent of the structure of the Hamiltonian that is responsible for the dynamics of the physical system. Nevertheless, the question, if it is of advantage to use the bosonization identity, relies on the detailed structure of the Hamilton operator. Bosonizing a Hamiltonian with quadratic dispersion, for example, leads to an interaction between bosons that is not tractable in the bosonic language [35]. Despite these difficulties of quadratic dispersion relations, strongly correlated systems with linear dispersion such as the Luttinger liquid or the Kondo model in the Toulouse limit can be solved exactly using the bosonization technique. Therefore, bosonization has become a very useful analytical tool to study one-dimensional systems. Recently, there have been attempts to also treat quadratic dispersion relations in Luttinger liquids in combination with the bosonization method [18][35][22]. All those attempts are based on a projection scheme, that is related to the solution of the Fermi-edge singularity problem, mapping the Luttinger liquid Hamiltonian onto an effective Hamiltonian with appropriately linearized spectrum such that in the end the problem can be solved using the bosonization technique.

Since the bosonization technique does not rely on the structure of the Hamiltonian, it can also be used for the treatment of time-dependent nonequilibrium systems. The Fermi-edge singularity problem [33], for example, can be solved easily by use of the bosonization technique [39]. This is in big contrast to the first analytical solution where a Parquet expansion has been used [33]. The Fermi-edge singularity problem addresses a nonequilibrium situation where conduction band electrons have to adapt to a suddenly created local Coulomb potential. Recently, it has been shown by Lobaskin and Kehrein that it is possible to determine the spin dynamics in the Kondo model after an interaction quench by use of the bosonization technique [27].

For the bosonization technique to be applicable the only prerequisite has to be a given field theory in one dimension with fermionic fields $\Psi_\eta(x)$ defined on an interval $[-L/2, L/2]$. In general, such a field theory contains M different species η of fermions. These may be spins as in the Kondo model, $\eta = \uparrow, \downarrow$, or left- and right-movers in a Luttinger liquid, $\eta = L, R$. Since the domain of the fermionic fields is compact, one can

perform a mode expansion defining the operators $c_{k\eta}$

$$\Psi_\eta(x) = \sqrt{\frac{2\pi}{L}} \sum_k e^{-ikx} c_{k\eta}, \tag{3.1}$$

$$c_{k\eta} = \frac{1}{\sqrt{2\pi L}} \int_{L/2}^{L/2} \mathrm{d}x\, e^{ikx}\, \Psi_\eta(x), \tag{3.2}$$

obeying fermionic commutation relations

$$\left\{\Psi_\eta(x), \Psi_{\eta'}^\dagger(x')\right\} = 2\pi\delta_{\eta,\eta'}\delta(x-x'), \qquad \left\{c_{k\eta}, c_{k'\eta'}^\dagger\right\} = \delta_{\eta,\eta'}\delta_{k,k'}. \tag{3.3}$$

Here, the fermionic fields are normalized to 2π instead of 1. Depending on the periodicity condition characterized by the parameter $\delta_B \in [0,2)$:

$$\Psi_\eta(x+L/2) = e^{i\pi\delta_B}\Psi_\eta(x-L/2), \tag{3.4}$$

the momentum index k obeys the following relation:

$$k = \frac{2\pi}{L}\left[n_k - \frac{1}{2}\delta_B\right], \quad n_k \in \mathbb{Z}. \tag{3.5}$$

It is important for the derivation of the bosonization identity, that the wave-vector k is unbounded. In the case of a momentum bounded from below as in a Luttinger liquid one introduces unphysical positron states and extends k to $-\infty$. These positron states typically lie well below the Fermi surface. Therefore, they don't contribute to the low energy properties of the system. Since the physical properties of a bulk system in the thermodynamic limit should not depend on the boundary conditions, one is free to choose δ_B. From now on, δ_B will be set equal to 0 corresponding to periodic boundary conditions.

Given a set of annihilation and creation operators $c_{k\eta}, c_{k\eta}^\dagger$ there is a unique state, the vacuum state $|0\rangle$, such that

$$c_{k\eta}|0\rangle = 0, \quad k > 0 \tag{3.6}$$

$$c_{k\eta}^\dagger|0\rangle = 0, \quad k \leq 0. \tag{3.7}$$

One can think of $|0\rangle$ as a Fermi sea filled up to $k=0$. Given the vacuum state one can define the procedure of normal-ordering, to be denoted by : ... :

$$: ABC... : = ABC... - \langle 0|ABC...|0\rangle, \quad A, B, C, ... \in \left\{c_{k\eta}, c_{k\eta}^\dagger\right\}. \tag{3.8}$$

A function of annihilation and creation operators is called normal-ordered if all $c_{k\eta}$ with $k > 0$ and $c_{k\eta}^\dagger$ with $k \leq 0$ are located right of all other operators.

The number operator

$$\hat{N}_\eta = \sum_{k=-\infty}^{\infty} : c_{k\eta}^\dagger c_{k\eta} : \tag{3.9}$$

counts the number of fermions of species η with respect to the reference state $|0\rangle$ such that the eigenvalues of this symmetric operator are integer numbers. Given an M-tuple $\mathbf{N} = (N_1, ..., N_M)$ of integers, M is the number of different species, the space $\mathcal{H}_\mathbf{N}$

spanned by the set of all eigenvectors with the same set of eigenvalues will be called the **N**-particle Hilbert space. For each $\mathcal{H}_{\mathbf{N}}$ there exists one unique state $|\mathbf{N}\rangle_0$ up to a sign that contains no particle-hole excitations. Thus, it can be viewed as a vacuum of the Hilbert space $\mathcal{H}_{\mathbf{N}}$. Here, this state $|\mathbf{N}\rangle_0$ is defined in the following way, prescribing a definite ordering of the fermionic operators in order to resolve sign ambiguities:

$$|\mathbf{N}\rangle_0 = [\mathcal{C}_1]^{N_1} ... [\mathcal{C}_M]^{N_M} |0\rangle, \tag{3.10}$$

$$[\mathcal{C}_\eta]^{N_\eta} = \begin{cases} c^\dagger_{N_\eta \, \eta} c^\dagger_{(N_\eta-1) \, \eta} ... c^\dagger_{1 \, \eta} & \text{for } N_\eta > 0, \\ 1 & \text{for } N_\eta = 0, \\ c_{N_\eta \, \eta} c_{(N_\eta-1) \, \eta} ... c_{1 \, \eta} & \text{for } N_\eta < 0. \end{cases} \tag{3.11}$$

For ease of notation, n_k instead of k is used at this point as an index for the creation and annihilation operators. The fact that the fermionic Fock space $\mathcal{F}$ can be decomposed into a direct sum over all **N**-particle Hilbert spaces:

$$\mathcal{F} = \oplus_{\mathbf{N}} \mathcal{H}_{\mathbf{N}}, \tag{3.12}$$

will be of great importance for the derivation of the bosonization identity.

3.1 Bosonization technique

Based on these introductory remarks, it is possible to establish a relation between fermionic and bosonic fields in one dimension called the bosonization identity whose derivation will be given below following the work of Schöller and von Delft [37]. The basic ingredient is the observation that the particle-hole excitations in a bath of fermions display bosonic character by defining proper so-called bosonic particle-hole operators. Most importantly, the fermionic fields acting on states of the Hilbert space are similar to coherent states of these bosonic particle-hole operators. As a consequence, one can find a coherent state representation of the fermionic fields that leads to the bosonization identity. As mentioned before, for the applicability of the bosonization technique only a fermionic field theory is required. Importantly, the bosonization method is independent of the structure of the Hamilton operator determining the physical properties of the system of interest.

3.1.1 Bosonic particle-hole operators

As mentioned before, the basic building block of the bosonization technique is the observation that the particle-hole excitations possess bosonic character. The operators

$$b_{q\eta} = -\frac{i}{\sqrt{n_q}} \sum_{k=-\infty}^{\infty} c^\dagger_{k-q \, \eta} c_{k\eta}, \qquad b^\dagger_{q\eta} = \frac{i}{\sqrt{n_q}} \sum_{k=-\infty}^{\infty} c^\dagger_{k+q \, \eta} c_{k\eta} \tag{3.13}$$

create a superposition of particle-hole pairs with momentum transfer $q = \frac{2\pi}{L} n_q > 0$ where $n_q \in \mathbb{N}$. These operators obey bosonic commutation rules

$$\left[b_{q\eta}, b^\dagger_{q'\eta'} \right] = \delta_{\eta,\eta'} \delta_{q,q'}, \qquad \left[b_{q\eta}, b_{q'\eta'} \right] = 0, \qquad \left[b^\dagger_{q\eta}, b^\dagger_{q'\eta'} \right] = 0, \tag{3.14}$$

as can be checked by using the known commutation relations of the original fermions, although some care is needed not to subtract off infinite expressions in an uncontrollable way [37]. Since the states $|\mathbf{N}\rangle_0$, see Eq. (3.10), contain no particle-hole excitations the action of all the $b_{q\eta}$'s on those gives 0:

$$b_{q\eta}|\mathbf{N}\rangle_0 = 0 \quad \text{for all } q, \eta, \mathbf{N}. \tag{3.15}$$

Therefore, $|\mathbf{N}\rangle_0$ serves as a vacuum state for the bosonic excitations in each $\mathbf{N}$-particle Hilbert space $\mathcal{H}_\mathbf{N}$. Moreover, a very important and nontrivial statement can be made, namely that every state $|\mathbf{N}\rangle$ in an $\mathbf{N}$-particle Hilbert space $\mathcal{H}_\mathbf{N}$ can be obtained by the action of the $b_{q\eta}^\dagger$ operators on the $\mathbf{N}$-particle ground state $|\mathbf{N}\rangle_0$. Thus, given a state $|\mathbf{N}\rangle \in \mathcal{H}_\mathbf{N}$, there exists a function $f(b^\dagger)$ of bosonic creation operators such that

$$|\mathbf{N}\rangle = f(b^\dagger)|\mathbf{N}\rangle_0. \tag{3.16}$$

A proof of this relation can be found in [37].

3.1.2   Klein factors

Using the statement before, each $\mathbf{N}$-particle Hilbert space can be spanned by the bosonic operators $b_{q\eta}^\dagger$ acting on $|\mathbf{N}\rangle_0$. In order to completely recast the full Fock space, ladder operators are needed that connect the various $\mathbf{N}$-particle Hilbert spaces. These operators are called Klein factors and will be labeled $F_\eta^\dagger$ and F_η. They are uniquely defined through, firstly, their commutation relations with the bosonic particle-hole operators:

$$\left[b_{q\eta}, F_\eta^\dagger\right] = \left[b_{q\eta}^\dagger, F_\eta^\dagger\right] = [b_{q\eta}, F_\eta] = \left[b_{q\eta}^\dagger, F_\eta\right] = 0, \tag{3.17}$$

and, secondly, through their action on the $\mathbf{N}$-particle ground states:

$$F_\eta^\dagger|\mathbf{N}\rangle_0 \quad = c_{N_\eta+1\,\eta}^\dagger|N_1,...,N_\eta,...,N_M\rangle_0 = \hat{T}_\eta|N_1,...,N_\eta+1,...,N_M\rangle_0, \tag{3.18}$$

$$F_\eta|\mathbf{N}\rangle_0 \quad = c_{N_\eta\,\eta}|N_1,...,N_\eta,...,N_M\rangle_0 = \hat{T}_\eta|N_1,...,N_\eta-1,...,N_M\rangle_0. \tag{3.19}$$

The operator $\hat{T}_\eta$ counts the (-1) factors for the fermions that the creation or annihilation operators have to pass until they arrive at the position on which they act on. The Klein factors can be used to map different $\mathbf{N}$-particle ground states onto each other. Using the properties of the Klein factors above, one can show that they fulfill the following anticommutation relations:

$$\left\{F_\eta, F_{\eta'}^\dagger\right\} = 2\delta_{\eta,\eta'} \qquad \text{, since } F_\eta^\dagger F_\eta = 1, \tag{3.20}$$

$$\left\{F_\eta, F_{\eta'}\right\} = \left\{F_\eta^\dagger, F_{\eta'}^\dagger\right\} = 0, \tag{3.21}$$

$$\left[\hat{N}_\eta, F_{\eta'}^\dagger\right] = \delta_{\eta,\eta'} F_\eta^\dagger. \tag{3.22}$$

3.1.3   Bosonic fields

Based on the bosonic annihilation and creation operators $b_{q\eta}$ and $b_{q\eta}^\dagger$ one can introduce bosonic fields:

$$\varphi_\eta(x) = -\sum_{q>0} \frac{1}{\sqrt{n_q}} e^{-iqx} b_{q\eta}\, e^{-aq/2}, \qquad \varphi_\eta^\dagger(x) = -\sum_{q>0} \frac{1}{\sqrt{n_q}} e^{iqx} b_{q\eta}^\dagger\, e^{-aq/2}, \tag{3.23}$$

$$\phi_\eta(x) = \varphi_\eta(x) + \varphi_\eta^\dagger(x) = -\sum_{q>0} \frac{1}{\sqrt{n_q}} \left[e^{-iqx} b_{q\eta} + e^{iqx} b_{q\eta}^\dagger\right] e^{-aq/2}. \tag{3.24}$$

At this stage, a regularization scheme for the theory has been introduced in terms of an ultra-violet cutoff $a > 0$ in the bosonic fields. The cutoff a can be thought of as the maximum momentum transfer that is possible in the physical system of interest. In principle, there are various ways to regularize a given theory. Depending on the regularization scheme that is chosen, however, the meaning of the coupling constants in the Hamiltonian changes [45]. The bosonic fields obey the following commutation relations:

$$\left[\varphi_\eta^\dagger(x), \varphi_{\eta'}^\dagger(x')\right] = \left[\varphi_\eta(x), \varphi_{\eta'}(x')\right] = 0, \tag{3.25}$$

$$\left[\varphi_\eta(x), \varphi_{\eta'}^\dagger(x')\right] = -\delta_{\eta,\eta'} \ln\left[1 - e^{-i\,2\pi/L\,(x-x'-ia)}\right] \tag{3.26}$$

$$\xrightarrow{L\to\infty} -\delta_{\eta,\eta'} \ln\left[i\frac{2\pi}{L}\left(x - x' - ia\right)\right], \tag{3.27}$$

$$\left[\phi_\eta(x), \partial_{x'}\phi_{\eta'}(x')\right] \xrightarrow{L\to\infty} \delta_{\eta,\eta'} 2\pi i \left[\frac{a/\pi}{(x-x')^2 + a^2} - \frac{1}{L}\right] \tag{3.28}$$

$$\xrightarrow{a\to 0} 2\pi i \delta_{\eta,\eta'} \left[\delta(x - x') - \frac{1}{L}\right], \tag{3.29}$$

$$\left[\phi_\eta(x), \phi_{\eta'}(x')\right] \xrightarrow{L\to\infty} -\delta_{\eta,\eta'} 2i \arctan\left[\frac{x-x'}{a}\right] \tag{3.30}$$

$$\xrightarrow{a\to 0} -\delta_{\eta,\eta'} i\pi \operatorname{sgn}(x - x'). \tag{3.31}$$

One very important property of the bosonic field $\phi_\eta(x)$ is the relation to the local density $\rho_\eta(x)$ of η-fermions:

$$\rho_\eta(x) =: \Psi_\eta^\dagger(x)\Psi_\eta(x) := \partial_x\phi(x) + \frac{2\pi}{L}\hat{N}_\eta. \tag{3.32}$$

In the thermodynamic limit the last term in this expression can be neglected:

$$\lim_{L\to\infty} \frac{2\pi}{L}\hat{N}_\eta = 0. \tag{3.33}$$

The great importance of the relation in Eq. (3.32) is, that the electron's density, which is quadratic in fermion operators, becomes linear in the bosonic ones. Therefore, a density-density interaction as it appears in a Luttinger liquid, which is quartic in the fermion operators, becomes quadratic in the bosonic language and therefore exactly solvable. Moreover, one can think of the bosonic field $\phi_\eta(x)$ as a charge since $\rho_\eta(x)/2\pi$ is the charge density. The factor 2π is included for the actual charge density since the fermionic fields defined in Eq. (3.2) are normalized to 2π instead of 1, see Eq. (3.3)

3.1.4   Bosonization identity

The derivation of the bosonization identity, as it is presented in the work by von Delft and Schöller [37], is based on the observation that the fermionic fields $\Psi_\eta(x)$ acting on the **N**-particle ground states $|\mathbf{N}\rangle_0$ are coherent states of the bosonic particle-hole operators $b_{q\eta}$. The essential commutators needed to verify this property of the operators $\hat{\Psi}_\eta(x)$ are direct consequences of the definitions of the fermionic fields in Eq. (3.2) and

the bosonic particle-hole operators, see Eq. (3.13):

$$\left[b_{q\eta'}, \Psi_\eta(x)\right] = \delta_{\eta,\eta'}\alpha_q(x)\Psi_\eta(x),$$
$$\left[b_{q\eta'}^\dagger, \Psi_\eta(x)\right] = \delta_{\eta,\eta'}\alpha_q^*(x)\Psi_\eta(x). \tag{3.34}$$

Here, $\alpha_q(x) = \frac{i}{\sqrt{n_q}}e^{iqx}$. Using these relations together with $b_{q\eta}|\mathbf{N}\rangle_0 = 0$, see Eq. (3.15), leads to the following expression:

$$b_{q\eta'}\Psi_\eta(x)|\mathbf{N}\rangle_0 = \delta_{\eta,\eta'}\alpha_q(x)\Psi_\eta(x)|\mathbf{N}\rangle_0. \tag{3.35}$$

Therefore, $\Psi_\eta(x)|\mathbf{N}\rangle_0$ is a coherent state of the bose operators $b_{q\eta}$. Since the fermionic field annihilates one η-electron, $\Psi_\eta(x)|\mathbf{N}\rangle_0$ is an element of $\mathcal{H}_{\mathbf{N}'}$ where $\mathbf{N}'$ is the same M-tuple as $\mathbf{N}$ except that $N_\eta' = N_\eta - 1$. Due to Eq. (3.16) one can find a function $f\left(b^\dagger\right)$ such that the relation $\Psi_\eta(x)|\mathbf{N}\rangle_0 = f(b^\dagger)|\mathbf{N}'\rangle_0$ holds. The right-hand side of Eq. (3.35) can also be expressed through the function f such that one ends up with a relation, that clarifies in which $\mathbf{N}$-particle Hilbert space we work in:

$$b_{q\eta'}f(b^\dagger)|\mathbf{N}'\rangle_0 = \delta_{\eta,\eta'}\alpha_q(x)f(b^\dagger)|\mathbf{N}'\rangle_0. \tag{3.36}$$

Therefore:

$$\Psi_\eta(x)|\mathbf{N}\rangle_0 = f(b^\dagger)|\mathbf{N}'\rangle_0 = e^{\sum_{q>0}\alpha_q(x)b_{q\eta}^\dagger}\lambda_\eta(x)|\mathbf{N}'\rangle_0 = e^{-i\varphi_\eta^\dagger(x)}\lambda_\eta(x)F_\eta|\mathbf{N}\rangle_0. \tag{3.37}$$

Strictly speaking, the last equality is true only if the ultra-violet cutoff $a = 0$, see the definition of the bosonic fields $\varphi_\eta^\dagger(x)$ in Eq. (3.23). Thus, all statements below are only valid in this limit.

Any coherent state is defined up to a multiplicative factor, called $\lambda_\eta(x)$ here, that is included at this stage of the derivation of the bosonization identity since it will be of great importance as we shall see now. The expectation value ${}_0\langle\mathbf{N}|F_\eta^\dagger\Psi_\eta(x)|\mathbf{N}\rangle_0$ determines the value of $\lambda_\eta(x)$ uniquely. Firstly, plugging in Eq. (3.37), the outcome of this expectation value is $\lambda_\eta(x)$ itself:

$$_0\langle\mathbf{N}|F_\eta^\dagger\Psi_\eta(x)|\mathbf{N}\rangle_0 = \lambda_\eta(x), \tag{3.38}$$

since the Klein factors and the bosonic fields $\varphi_\eta^\dagger(x)$ commute due to Eq. (3.17). Additionally, $\exp\left[-i\varphi_\eta(x)\right]|\mathbf{N}\rangle_0 = 1$ and $F_\eta^\dagger F_\eta = 1$. Alternatively, one can insert the original definition of the fermionic field, see Eq. (3.1), as a mode expansion. Using Eq. (3.19) ${}_0\langle\mathbf{N}|F_\eta^\dagger = {}_0\langle\mathbf{N}|c_{N_\eta}^\dagger$ the only term in the mode expansion that gives a non zero contribution is the one with $n_k = N_\eta$:

$$_0\langle\mathbf{N}|F_\eta^\dagger\Psi_\eta(x)|\mathbf{N}\rangle_0 = \sqrt{\frac{2\pi}{L}}\sum_k e^{-ikx}\,{}_0\langle\mathbf{N}|c_{N_\eta\,\eta}^\dagger c_{n_k\,\eta}|\mathbf{N}\rangle_0 = \sqrt{\frac{2\pi}{L}}e^{-i\frac{2\pi}{L}N_\eta x}. \tag{3.39}$$

Therefore, the multiplicative factor $\lambda_\eta(x)$ depends on the $\mathbf{N}$-particle ground state $|\mathbf{N}\rangle_0$ such that one can introduce the following operator:

$$\hat{\lambda}_\eta(x) = \sqrt{\frac{2\pi}{L}}e^{-i\frac{2\pi}{L}\hat{N}_\eta x}. \tag{3.40}$$

As a result, Eq. (3.37) is equivalent to the following relation:

$$\Psi_\eta(x)|\mathbf{N}\rangle_0 = e^{-i\varphi_\eta^\dagger(x)} F_\eta \,\hat{\lambda}_\eta(x)|\mathbf{N}\rangle_0. \tag{3.41}$$

The bosonization identity can be derived by regarding the action of $\Psi_\eta(x)$ onto an arbitrary state $|\mathbf{N}\rangle$. Using Eq. (3.16), the quantity to analyze is

$$\Psi_\eta(x)\, f(\{b_{q\eta'}^\dagger\})|\mathbf{N}\rangle_0. \tag{3.42}$$

The aim is to commute $\Psi_\eta(x)$ past the function f. Then Eq. (3.41) can be inserted. Using Eq. (3.34) together with the elementary operator identity

$$[A, B] = DB \text{ and } [A, D] = [B, D] = 0 \quad \Rightarrow \quad Bf(A) = f(A - D)B \tag{3.43}$$

leads to

$$\Psi_\eta(x)\, f(\{b_{q\eta'}^\dagger\}) = f(\{b_{q\eta'}^\dagger - \delta_{\eta,\eta'}\alpha_q^*(x)\})\Psi_\eta(x). \tag{3.44}$$

Additionally, Eq. (3.23) together with

$$[A, B] = C \text{ and } [A, C] = [B, C] = 0 \quad \Rightarrow \quad e^{-B}f(A)e^B = f(A + C) \tag{3.45}$$

implies

$$f(\{b_{q'\eta}^\dagger - \delta_{\eta,\eta'}\alpha_q^*(x)\}) = e^{-i\varphi_\eta(x)} f(\{b_{q'\eta}^\dagger\})e^{i\varphi_\eta(x)}. \tag{3.46}$$

Using all these relations, the bosonization identity can be easily shown [37]:

$$\begin{aligned}
\Psi_\eta(x)|\mathbf{N}\rangle &= \Psi_\eta(x)f(\{b_{q\eta'}^\dagger\})|\mathbf{N}\rangle_0\\
&= f(\{b_{q\eta'}^\dagger - \delta_{\eta,\eta'}\alpha_q^*(x)\})\Psi_\eta(x)|\mathbf{N}\rangle_0\\
&= f(\{b_{q\eta'}^\dagger - \delta_{\eta,\eta'}\alpha_q^*(x)\})e^{-i\varphi_\eta^\dagger(x)} F_\eta\hat{\lambda}_\eta(x)|\mathbf{N}\rangle_0\\
&= F_\eta\hat{\lambda}_\eta(x)e^{-i\varphi_\eta^\dagger(x)} f(\{b_{q\eta'} - \delta_{\eta,\eta'}\alpha_q^*(x)\})|\mathbf{N}\rangle_0\\
&= F_\eta\hat{\lambda}_\eta(x)e^{-i\varphi_\eta^\dagger(x)} \left[e^{-i\varphi_\eta(x)} f(\{b_{q\eta'}^\dagger\})e^{i\varphi_\eta(x)}\right]|\mathbf{N}\rangle_0\\
&= F_\eta\hat{\lambda}_\eta(x)e^{-i\varphi_\eta^\dagger(x)}e^{-i\varphi_\eta(x)} f(\{b_{q\eta'}\})|\mathbf{N}\rangle_0\\
&= F_\eta\hat{\lambda}_\eta(x)e^{-i\varphi_\eta^\dagger(x)}e^{-i\varphi_\eta(x)}|\mathbf{N}\rangle.
\end{aligned} \tag{3.47}$$

Since the state $|\mathbf{N}\rangle$ has been chosen to be arbitrary, there exists a representation of $\Psi_\eta(x)$ in terms of bosonic fields that is called the bosonization identity

$$\boxed{\Psi_\eta(x) = F_\eta\hat{\lambda}_\eta(x)e^{-i\varphi_\eta^\dagger(x)}\, e^{-i\varphi_\eta(x)} \qquad (3.48)}.$$

Due to the operator identity:

$$[A, B] = \text{const.} \quad \Rightarrow \quad e^A e^B = e^{A+B}e^{[A,B]/2} \tag{3.49}$$

and Eq. (3.27) the above equality can be rewritten in terms of the field $\phi_\eta(x)$ defined in Eq. (3.24)

$$\Psi_\eta(x) \;=\; \sqrt{\frac{2\pi}{L}} F_\eta e^{-i\frac{2\pi}{L}\hat{N}_\eta x} e^{-i\varphi_\eta^\dagger(x)} e^{-i\varphi_\eta(x)} \tag{3.50}$$

$$=\; \frac{1}{\sqrt{a}} F_\eta e^{-i\frac{2\pi}{L}\hat{N}_\eta x} e^{-i\phi_\eta(x)}. \tag{3.51}$$

Strictly speaking, this equality is not valid since the bosonization identity is exact only in the limit $a \to 0$ as already mentioned before. The prefactor $1/\sqrt{a}$ appears since the expression in Eq. (3.51) is not normal ordered. Nevertheless, Eq. (3.51) can be used by implicitly assuming that the limit $a \to 0$ is to be taken in the end. In the thermodynamic limit the phase operator can be replaced by unity, see Eq. (3.33):

$$e^{-i\frac{2\pi}{L}\hat{N}_\eta x} \overset{L\to\infty}{\longrightarrow} 1. \tag{3.52}$$

In this case, the bosonization identity reduces to:

$$\Psi_\eta(x) \overset{L\to\infty}{=} \sqrt{\frac{2\pi}{L}} F_\eta e^{-i\varphi_\eta(x)} e^{-i\varphi_\eta^\dagger(x)} \tag{3.53}$$

$$=\; \frac{1}{\sqrt{a}} F_\eta e^{-i\phi_\eta(x)} \tag{3.54}$$

.

Concluding, starting from a fermionic field theory one can define bosonic particle-hole operators, the corresponding bosonic fields and Klein factors such that in the end one can express the fermionic fields in terms of Klein factors and bosonic fields. The inverse procedure named refermionization is also possible. Suppose that bosonic fields and Klein factors are given, as will be the case for the Kondo model, one can introduce a new fermionic field out of those quantities by just using the inverse of the bosonization identity.

3.1.5   Bosonizing a Hamiltonian with linear dispersion

So far, only the properties of fermionic fields have been exploited. The goal of this section will be to express a Hamiltonian with linear dispersion:

$$H_0 = \sum_\eta H_{0\eta}, \qquad H_{0\eta} = \sum_k v_F \hbar k : c_{k\eta}^\dagger c_{k\eta} := v_F \hbar \int_{L/2}^{L/2} \frac{\mathrm{d}x}{2\pi} : \Psi_\eta^\dagger(x)\, i\partial_x \Psi_\eta(x) : \tag{3.55}$$

in terms of bosonic operators. From now on, $v_F \hbar$ will be set equal to 1. Normal ordering regularizes operators in momentum space, the regularization technique in position space is a procedure called point splitting. The product of two local operators $\mathcal{O}(x)$ and $\mathcal{P}(x)$ at the same point x is regularized by evaluating the operators a short distance ia

apart from each other and then subtracting off their expectation value with respect to a reference state $|0\rangle$:

$$: \mathcal{O}(x)\mathcal{P}(x) := \lim_{a \to 0} \left[\mathcal{O}(x - ia)\mathcal{P}(x) - \langle 0 | \mathcal{O}(x - ia)\mathcal{P}(x) | 0 \rangle \right]. \tag{3.56}$$

Here, a is not necessarily related to the ultra-violet cutoff introduced in the definition of the bosonic fields [45]. In this section, however, we will identify both for simplicity [37]. By use of the bosonization identity the operators of the operator product $\Psi_\eta^\dagger(x - ia)\, i\partial_x \Psi_\eta(x)$ can be written in terms of the bosonic fields:

$$\Psi_\eta^\dagger(x - ia)\, i\partial_x \Psi_\eta(x) = \frac{1}{a} e^{i\phi_\eta(x-ia)} e^{-i\phi_\eta(x)} \left[\partial_x \phi_\eta(x) - \left(\frac{1}{a} - \frac{\pi}{L} \right) \right]. \tag{3.57}$$

where the identity

$$i\partial_x e^{-i\Phi_\eta(x)} = e^{-i\Phi_\eta(x)} \left[\partial_x \Phi_\eta(x) + \frac{[\partial_x \Phi_\eta(x), \Phi_\eta(x)]}{2} \right] \tag{3.58}$$

has been used. An additional decomposition of the exponentials leads to:

$$\Psi_\eta^\dagger(x - ia)\, i\partial_x \Psi_\eta(x) =$$
$$= \frac{2\pi}{L} e^{i\varphi_\eta^\dagger(x-ia)} e^{i\varphi_\eta(x-ia)} e^{-i\varphi_\eta^\dagger(x)} e^{-i\varphi_\eta(x)} \left[\partial_x \phi_\eta(x) - \left(\frac{1}{a} - \frac{\pi}{L} \right) \right]. \tag{3.59}$$

Interchanging the two exponentials in the middle and a subsequent Taylor expansion yield:

$$\Psi_\eta^\dagger(x - ia)\, i\partial_x \Psi_\eta(x) =$$
$$= \frac{2\pi}{L} e^{i[\varphi_\eta^\dagger(x-ia)-\varphi_\eta^\dagger(x)]} e^{i[\varphi_\eta(x-ia)-\varphi_\eta(x)]} \left[\frac{L}{4\pi a} \right] \left[\partial_x \phi_\eta(x) - \left(\frac{1}{a} - \frac{\pi}{L} \right) \right]$$
$$= \frac{1}{2a} \left[1 + \partial_x \varphi_\eta^\dagger(x)a \right] \left[1 + \partial_x \varphi_\eta(x)a \right] \left[\partial_x \phi_\eta(x) - \left(\frac{1}{a} - \frac{\pi}{L} \right) \right]$$
$$= \frac{1}{2a} \partial_x \phi_\eta(x) + \frac{1}{2} \left(\partial_x \phi_\eta(x) \right)^2 - \frac{1}{2a} \left(\frac{1}{a} - \frac{\pi}{L} \right) \partial_x \phi_\eta(x) - \frac{1}{2a} \left(\frac{1}{a} - \frac{\pi}{L} \right) + \mathcal{O}\left(\frac{a}{L} \right). \tag{3.60}$$

Subtracting off the ground state expectation value $\langle 0 | \Psi_\eta^\dagger(x - ia)\, i\partial_x \Psi_\eta(x) | 0 \rangle$ eliminates the divergent constant. Therefore, the Hamiltonian in Eq. (3.55) reads:

$$H_{0\eta} = \int_{L/2}^{L/2} \frac{dx}{2\pi}\; : \Psi_\eta^\dagger(x)\, i\partial_x \Psi_\eta(x) :$$
$$= \lim_{a \to 0} \int_{L/2}^{L/2} \frac{dx}{2\pi} \left[\frac{1}{2} : \left(\partial_x \phi_\eta(x) \right)^2 : + \left(\frac{1}{2a} - \frac{1}{2a^2} + \frac{\pi}{2aL} \right) \partial_x \phi_\eta(x) \right]. \tag{3.61}$$

The normal-ordering colons can be neglected for the operator $\partial_x \phi_\eta$, since it is already normal-ordered. Due to the periodic boundary condition of the bosonic fields [37]

$$\phi_\eta(x + L/2) = \phi_\eta(x - L/2) \tag{3.62}$$

the integral $\int_{L/2}^{L/2} \mathrm{d}x\, \partial_x \phi_\eta(x) = \phi_\eta(L/2) - \phi_\eta(-L/2) = 0$ gives zero such that in the end only one term survives:

$$H_{0\eta} = \int_{L/2}^{L/2} \frac{\mathrm{d}x}{2\pi} \frac{1}{2} : [\partial_x \phi_\eta(x)]^2 : . \tag{3.63}$$

Expanding $\partial_x \phi_\eta(x)$ in a Fourier series leads to an expression for the Hamiltonian in terms of the bosonic particle-hole operators:

$$H_{0\eta} = \int_{-L/2}^{L/2} \frac{\mathrm{d}x}{2\pi} \frac{1}{2} : [\partial_x \phi_\eta(x)]^2 : = \sum_{q>0} q b_{q\eta}^\dagger b_{q\eta}. \tag{3.64}$$

Therefore, a linear dispersion for the initial fermionic Hamiltonian results in a linear dispersion for the bosonic particle-hole operators. As mentioned in the introduction to bosonization, a Hamilton operator with a quadratic dispersion relation would lead to an additional scattering of the bosons that is not tractable in a bosonic language.

3.2 Bosonization: Anisotropic Kondo model

One of the physical systems whose Hamiltonian can be diagonalized analytically by use of the bosonization technique is the anisotropic Kondo Hamiltonian for a special line in parameter space, the so-called Toulouse limit. This diagonalization procedure will be shown in this section. As already mentioned in Sec. (2.2), strong coupling properties of the Kondo model are described by the anisotropic Kondo Hamiltonian in one dimension with a linearized dispersion relation:

$$
\begin{aligned}
H_K = \sum_{k,\eta=\uparrow\downarrow} k : c_{k\eta}^\dagger c_{k\eta} : + \frac{J_\parallel}{2} \left[: \Psi_\uparrow^\dagger(0)\Psi_\uparrow(0) : - : \Psi_\downarrow^\dagger(0)\Psi_\downarrow(0) : \right] S_z + \\
+ \frac{J_\perp}{2} \left[\Psi_\uparrow^\dagger(0)\Psi_\downarrow(0)S_- + \Psi_\downarrow^\dagger(0)\Psi_\uparrow(0)S_+ \right].
\end{aligned}
\tag{3.65}
$$

The kinetic part of the Hamiltonian can be expressed in terms of bosonic operators using Eq. (3.64). Due to Eq. (3.32) the fermionic charge density $: \Psi_\eta^\dagger(0)\Psi_\eta(0) :$ can be replaced by the derivative of the bosonic field $\partial_x \phi_\eta(0)$. Additionally, inserting the bosonization identity in the thermodynamic limit, see Eq. (3.54), into Eq. (3.65) yields the anisotropic Kondo Hamiltonian in a bosonic representation:

$$
\begin{aligned}
H_K = \sum_\eta \int_{-L/2}^{L/2} \frac{\mathrm{d}x}{2\pi} \frac{1}{2} : [\partial_x \phi_\eta(x)]^2 : + \frac{J_\parallel}{2} \partial_x \left[\phi_\uparrow(0) - \phi_\downarrow(0) \right] S_z \\
+ \frac{J_\perp}{2a} \left[F_\uparrow^\dagger F_\downarrow e^{i\phi_\uparrow(0)} e^{-i\phi_\downarrow(0)} S_- + F_\downarrow^\dagger F_\uparrow e^{i\phi_\downarrow(0)} e^{-i\phi_\uparrow(0)} S_+ \right]
\end{aligned}
\tag{3.66}
$$

This operator may now be written in a form in which the spin and charge degrees of freedom can be separated, a characteristic feature of one dimensional systems. Since the bosonic fields of different species commute with each other, the product of the exponentials can be recast into a single exponential of the sum of the two exponents due

to Eq. (3.49):

$$
\begin{aligned}
H_K = & \sum_{q>0} q \frac{1}{2} [b_{q\uparrow}^\dagger + b_{q\downarrow}^\dagger][b_{q\uparrow} + b_{q\downarrow}] + \sum_{q>0} q \frac{1}{2} [b_{q\uparrow}^\dagger - b_{q\downarrow}^\dagger][b_{q\uparrow} - b_{q\downarrow}] \\
& + \frac{J_\parallel}{2} \partial_x [\phi_\uparrow(0) - \phi_\downarrow(0)] S_z \\
& + \frac{J_\perp}{2a} \left[F_\uparrow^\dagger F_\downarrow e^{i[\phi_\uparrow(0) - \phi_\downarrow(0)]} S_- + F_\downarrow^\dagger F_\uparrow e^{-i[\phi_\uparrow(0) - i\phi_\downarrow(0)]} S_+ \right].
\end{aligned}
\tag{3.67}
$$

3.2.1 Spin-charge separation

A unitary transformation of the bosonic particle-hole operators that mixes the two spin species reduces the degrees of freedom that couple to the local level from two to one. Define [46]

$$
\begin{aligned}
b_{qc}^\dagger &= \frac{1}{\sqrt{2}} \left[b_{q\uparrow}^\dagger + b_{q\downarrow}^\dagger \right], \\
b_{qs}^\dagger &= \frac{1}{\sqrt{2}} \left[b_{q\uparrow}^\dagger - b_{q\downarrow}^\dagger \right].
\end{aligned}
\tag{3.68}
$$

This rotation in the space of the b operators conserves the bosonic commutation relations. According to these new bosonic operators, new bosonic fields can be introduced that share the same relation to the original bosonic fields as the new bosonic operators to their old ones:

$$
\begin{aligned}
\phi_c(x) &= -\sum_{q>0} \frac{1}{\sqrt{n_q}} \left[e^{-iqx} b_{qc} + e^{iqx} b_{qc}^\dagger \right] e^{-aq/2} = \frac{1}{\sqrt{2}} \left[\phi_\uparrow(x) + \phi_\downarrow(x) \right], \\
\phi_s(x) &= -\sum_{q>0} \frac{1}{\sqrt{n_q}} \left[e^{-iqx} b_{qs} + e^{iqx} b_{qs}^\dagger \right] e^{-aq/2} = \frac{1}{\sqrt{2}} \left[\phi_\uparrow(x) - \phi_\downarrow(x) \right].
\end{aligned}
\tag{3.69}
$$

As indicated by the subscript (c,s) those two new species of bosons describe the charge (c) and the spin (s) degrees of freedom of the model. Most evidently this connection can be visualized regarding the corresponding densities. The quantity that measures the total charge density at a point x is : $\Psi_\uparrow^\dagger(x)\Psi_\uparrow(x)$: + : $\Psi_\downarrow^\dagger(x)\Psi_\downarrow(x)$:= $\sqrt{2}\partial_x\phi_c(x)$. Accordingly, the spin density at x, that describes the spin polarization of the bath of fermions, is connected to the bosonic field $\phi_s(x)$: : $\Psi_\uparrow^\dagger(x)\Psi_\uparrow(x)$: $-$: $\Psi_\downarrow^\dagger(x)\Psi_\downarrow(x)$:= $\sqrt{2}\partial_x\phi_s(x)$. A Fourier transformation of $\partial_x\phi_s(x)$ shows that $\sqrt{n_q}b_{qs}^\dagger$ and $\sqrt{n_q}b_{qs}$ are the modes of the spin density. Insertion of the bosonic spin and charge operators defined above into the Kondo Hamiltonian leads to spin-charge separation, a phenomenon that is typical for one-dimensional systems:

$$
\begin{aligned}
H_K =& H_c + H_s, \\
H_c =& \sum_{q>0} q b_{qc}^\dagger b_{qc}, \\
H_s =& \sum_{q>0} q b_{qs}^\dagger b_{qs} + \frac{J_\parallel}{\sqrt{2}} \partial_x \phi_s(0) S_z \\
& + \frac{J_\perp}{2a} \left[F_\uparrow^\dagger F_\downarrow e^{i\sqrt{2}\phi_s(0)} S_- + F_\downarrow^\dagger F_\uparrow e^{-i\sqrt{2}\phi_s(0)} S_+ \right].
\end{aligned}
\tag{3.70}
$$

The charge sector of the Kondo Hamiltonian H_c decouples completely from the local level. Moreover, the dynamics of the charge degree of freedom are trivial as they are determined by a set of uncoupled harmonic oscillators with a linear dispersion. Therefore, the charge sector will be disregarded from now on.

The fact that the charge dynamics are completely irrelevant for the Kondo effect is not surprising since the excitations that are causing the Kondo effect are spin excitations in the vicinity of the local level. Those emerge from scattering events where the spin of a conduction band electron is flipped. Such a process, as it happens instantaneously, conserves the local particle density. The spin density, however, changes.

For systems, where it is not sufficient to consider the particle-hole symmetric case, see Eq. (2.1.2), i.e. $U \neq -\varepsilon_d/2$, an additional scattering term has to be included in the Kondo Hamiltonian. This may be the case for a quantum dot in a real experiment. The dynamics of such a scatterer do not produce spin flips, but charge excitations. As a consequence, the charge sector will not be trivial any more and will contain an additional local scatterer $\propto \partial_x \phi_c(0)$. The spin sector and consequently the spin dynamics, however, will not be affected.

3.2.2 Emery-Kivelson transformation

The bosonized Hamiltonian in Eq. (3.70) can be simplified using an Emery-Kivelson transformation that will lead to a phase shift in the spin sector. This transformation acts locally at the impurity site and is parametrized by a real number γ whose exact value will be chosen later:

$$U = e^{i\gamma\phi_s(0)S_z}. \tag{3.71}$$

The action of this unitary transformation on the Hamiltonian in Eq. (3.70) is fully determined by the elementary operator identity

$$[A, B] = DB \text{ and } [A, D] = [B, D] = 0 \quad \Rightarrow \quad e^B A e^{-B} = A - DB \tag{3.72}$$

and the following commutation relations:

$$[b_{qs}, \phi_s(0)S_z] = -\frac{1}{\sqrt{n_q}} e^{-aq/2} S_z \tag{3.73}$$

$$\xrightarrow{3.72} U b_{qs} U = b_{qs} + i\frac{\gamma}{\sqrt{n_q}} e^{-aq/2} S_z, \tag{3.74}$$

$$[\partial_x \phi_s(0)S_z, \phi_s(0)S_z] \overset{3.28}{=} -\frac{i}{2a} \xrightarrow{3.72} U\partial_x\phi_s(0)S_z U^\dagger = \partial_x\phi_s(0)S_z - \frac{\gamma}{2a}, \tag{3.75}$$

$$[S_z, S_\pm] = \pm S_\pm \xrightarrow{3.43} U S_\pm U^\dagger = e^{\pm i\gamma\phi_s(0)} S_\pm, \tag{3.76}$$

$$[\partial_x \phi_s(x), \phi_s(0)S_z] \overset{3.31}{=} -2\pi i\delta(x)S_z, \tag{3.77}$$

$$\xrightarrow{3.72} U\partial_x\phi_s(x)U^\dagger = \partial_x\phi_s(x) - 2\pi\gamma S_z\delta(x). \tag{3.78}$$

Since $\partial_x\phi_s(x)/(2\pi\sqrt{2})$ is the spin density of the conduction band electrons, Eq. (3.78) suggests to think of the Emery-Kivelson transformation as tying a spin of $-\gamma S_z/\sqrt{2}$ of the surrounding conduction band electrons to the impurity spin [46]. Due to Eq. (3.74) the kinetic energy acquires an additional scatterer of the structure $\propto \partial_x\phi_s(0)S_z$ as it is

already present in Eq. (3.70):

$$
\begin{aligned}
UH_0U^\dagger &= \sum_{q>0} Ub_{qs}^\dagger U^\dagger Ub_{qs}U^\dagger \\
&= \sum_{q>0} q \left[b_{qs}^\dagger - i\frac{\gamma}{\sqrt{n_q}}e^{-aq/2}S_z \right] \left[b_{qs} + i\frac{\gamma}{\sqrt{n_q}}e^{-aq/2}S_z \right] \\
&= \sum_{q>0} qb_{qs}^\dagger b_{qs} + i\gamma \sum_{q>0} \frac{q}{\sqrt{n_q}} \left[b_{qs}^\dagger - b_{qs} \right] S_z + \gamma^2 \sum_{q>0} e^{-aq}S_z^2 \\
&= \sum_{q>0} qb_{qs}^\dagger b_{qs} - \gamma\partial_x\phi_s(0)S_z + \frac{\gamma^2}{4a}.
\end{aligned}
\tag{3.79}
$$

Eq. (3.75) shows that U shifts $H_\parallel = J_\parallel/\sqrt{2}\partial_x\phi_s(0)S_z$ by a real number:

$$
\begin{aligned}
UH_\parallel U^\dagger &= \frac{J_\parallel}{\sqrt{2}}U\partial_x\phi_s(0)U^\dagger S_z \\
&= \frac{J_\parallel}{\sqrt{2}}\partial_x\phi_s(0)S_z - \frac{\gamma J_\parallel}{2\sqrt{2}a}.
\end{aligned}
\tag{3.80}
$$

Since the Klein factors commute with all bosonic fields, the only effect of U on $H_\perp$ is a change of the parameter in the exponentials:

$$
\begin{aligned}
UH_\perp U^\dagger &= \frac{J_\perp}{2a} \left[F_\uparrow^\dagger F_\downarrow U e^{i\sqrt{2}\phi_s(0)}S_- U^\dagger + F_\downarrow^\dagger F_\uparrow U e^{i\sqrt{2}\phi_s(0)}S_+ U^\dagger \right] \\
&= \frac{J_\perp}{2a} \left[F_\uparrow^\dagger F_\downarrow e^{i[\sqrt{2}-\gamma]\phi_s(0)}S_- + F_\downarrow^\dagger F_\uparrow e^{-i[\sqrt{2}-\gamma]\phi_s(0)}S_+ \right].
\end{aligned}
\tag{3.81}
$$

In order to simplify the last line of the equation above, one chooses $\gamma = \sqrt{2} - 1$. In this case one arrives at the following expression where constant terms are neglected:

$$
\begin{aligned}
H_K' = UH_KU^\dagger &= \sum_{q>0} qb_{qs}^\dagger b_{qs} + \left[\frac{J_\parallel}{\sqrt{2}} - \gamma \right] \partial_x\phi_s(0)S_z \\
&+ \frac{J_\perp}{2a} \left[F_\uparrow^\dagger F_\downarrow e^{i\phi_s(0)}S_- + F_\downarrow^\dagger F_\uparrow e^{-i\phi_s(0)}S_+ \right].
\end{aligned}
\tag{3.82}
$$

3.2.3 Refermionization

As already mentioned at the end of Sec. (3.1.4), the bosonization identity can also be used to introduce new fermionic fields for given bosonic fields and Klein factors. The structure of the Hamiltonian in Eq. (3.82) suggests to use the bosonic fields $\phi_s(x)$ for the definition of new pseudofermions $\Psi_s(x)$. The goal will be to completely fermionize the Hamiltonian above. For that purpose, a fermionic representation for the spin operators has to be established. Therefore, another unitary transformation $U_2 = e^{i\pi\hat{\mathcal{N}}_s S_z}$ has to be performed [45]. The operator

$$
\hat{\mathcal{N}}_s = \frac{1}{2} \left[\hat{N}_\uparrow - \hat{N}_\downarrow \right]
\tag{3.83}
$$

measures the total spin of the bath of conduction band electrons. The only operators of H_K' that are affected by U_2 are the Klein factors and spin operators $S_\pm$:

$$
\begin{aligned}
U_2 F_\downarrow^\dagger F_\uparrow U_2^\dagger &= e^{-i\pi S_z} F_\downarrow^\dagger F_\uparrow, \\
U_2 S_\pm U_2^\dagger &= e^{\pm i\pi\hat{\mathcal{N}}_s} S_\pm.
\end{aligned}
\tag{3.84}
$$

The transformed Hamiltonian reads:

$$U_2 H'_K U_2^\dagger = \sum_{q>0} q b_{qs}^\dagger b_{qs} + \left[\frac{J_\parallel}{\sqrt{2}} - \gamma \right] \partial_x \phi_s(0) S_z$$

$$+ \frac{J_\perp}{2a} \left[F_\uparrow^\dagger F_\downarrow e^{i\phi_s(0)} e^{i\pi[S_z - \hat{\mathcal{N}}_s]} S_- + S_+ e^{-i\pi[S_z - \hat{\mathcal{N}}_s]} F_\downarrow^\dagger F_\uparrow e^{-i\phi_s(0)} \right]. \tag{3.85}$$

Now, all prerequisites are prepared in order to refermionize the Kondo Hamiltonian. In order to introduce new fermionic fields out of the bosonic fields $\phi_s(x)$, first the appropriate Klein factors $\mathcal{F}_s$ have to be defined:

$$\mathcal{F}_s = F_\downarrow^\dagger F_\uparrow, \qquad \mathcal{F}_s^\dagger = F_\uparrow^\dagger F_\downarrow. \tag{3.86}$$

Using the bosonization identity, see Eq. (3.54), leads to the introduction of new spinless pseudofermions $\Psi_s(x)$ and their corresponding modes c_k:

$$\Psi_s(x) = \frac{1}{\sqrt{a}} \mathcal{F}_s e^{-i\phi_s(x)}, \tag{3.87}$$

$$c_k = \frac{1}{\sqrt{2\pi L}} \int_{L/2}^{L/2} dx \, e^{ikx} \, \Psi_s(x). \tag{3.88}$$

Due to the periodicity condition $\phi_s(x + L/2) = \phi_s(x - L/2)$, the quasi-momenta k take the values [37]:

$$k_n = \frac{2\pi}{L} n \qquad , n \in \mathbb{Z}. \tag{3.89}$$

Additionally, fermionic representations of the spin operators can be defined as a consequence of the unitary transformation U_2:

$$d^\dagger = S_+ e^{i\pi[\hat{\mathcal{N}}_s - S_z]}, \qquad d = e^{-i\pi[\hat{\mathcal{N}}_s - S_z]} S_-. \tag{3.90}$$

Remarkably, despite of both unitary transformations the relation between the spin operator S_z and the new fermionic operators remains simple:

$$\boxed{S_z = d^\dagger d - \frac{1}{2} \qquad (3.91)}.$$

Therefore, the spin expectation value of the local level is a quantity that is easily accessible in this new picture. This is not the case for the original electrons, for example. They are very complicated functions of the new fermions $\Psi_s(x)$. The relation (3.91) will be of great importance for the evaluation of correlation functions. Due to the unitary transformation U_2 the new operators obey fermionic commutation relations since $\hat{\mathcal{N}}_s - S_z$ has integer eigenvalues:

$$\{d, d^\dagger\} = 1, \qquad \{d^\dagger, d^\dagger\} = 0, \tag{3.92}$$

$$\{d, c_k^\dagger\} = 0, \qquad \{c_k, c_{k'}^\dagger\} = \delta_{k,k'}. \tag{3.93}$$

By use of Eq. (3.32) it is easy to see the relation of $\partial_x \phi_s(x)$ to the modes c_k:

$$\partial_x \phi_s(x) =: \Psi_s^\dagger(x)\Psi_s(x) := \frac{2\pi}{L} \sum_{kk'} e^{i(k-k')x} : c_k^\dagger c_{k'} : \tag{3.94}$$

Additionally, Eq.(3.64) is also applicable such that the kinetic energy for the bosonic spin operators transforms to a kinetic energy term for the pseudofermions where the dispersion stays linear:

$$\sum_{q>0} q b_{qs}^\dagger b_{qs} = \sum_k k : c_k^\dagger c_k : . \tag{3.95}$$

After the insertion of all these relations above into $U_2 H_K' U_2^\dagger$ one arrives at an interacting resonant level model for the new pseudofermions where the energy ϵ_d of the resonant level takes the value $\epsilon_d = 0$:

$$\begin{aligned}
H_{\mathrm{IRLM}} = U_2 H_K' U_2^\dagger &= \sum_k k : c_k^\dagger c_k : + \left[\frac{J_\|}{\sqrt{2}} - \gamma \right] \frac{2\pi}{L} \sum_{kk'} : c_k^\dagger c_{k'} : S_z \\
&+ V \sum_k \left[d^\dagger c_k + c_k^\dagger d \right] .
\end{aligned} \tag{3.96}$$

Here, $V = \sqrt{2\pi/L} J_\perp /(2\sqrt{a})$. The resonant level hybridizes with the sea of pseudofermions with width $\Delta = V^2 L/2$ that is connected to the Kondo scale $T_K \propto \Delta$ as will be shown later. The appearance of a factor $1/\sqrt{a}$ in the Hamiltonian may be contradicting the fact that the bosonization identity is only valid in the limit $a \to 0$. In fact, $1/\sqrt{a} \propto \sqrt{D}$ gives the correct dependence on the bandwidth D for the hybridization term in the interacting resonant level Hamiltonian [45]. Therefore, one obtains the correct scaling equations.

3.2.4 Toulouse limit

As is obvious in Eq. (3.96), for a special value of the coupling

$$J_\| = 2 - \sqrt{2} \tag{3.97}$$

i.e. $J_\| = \sqrt{2}\gamma$, the many-body interaction term in the Hamiltonian cancels. As a result, the transformed Kondo Hamiltonian becomes quadratic in the pseudofermions and exactly solvable. The line in parameter space of the couplings $J_\perp$ and $J_\|$ with $J_\| = 2 - \sqrt{2}$ is referred to as the Toulouse limit. As a consequence, one arrives at a noninteracting resonant level model [25]:

$$H_{\mathrm{RLM}} = \sum_k k : c_k^\dagger c_k : + V \sum_k \left[d^\dagger c_k + c_k^\dagger d \right] \tag{3.98}$$

Although no restriction on $J_\perp$ appeared up to now, for the bosonization technique it is important that only low energy physics are described properly mainly due to the linearization of the spectrum. Therefore, the perpendicular coupling $J_\perp$ should provide a low energy scale $J_\perp \ll J_\parallel$ [17]. The parameter V can be connected to the Kondo scale T_K, the only scale in the Kondo problem, via the zero temperature impurity contribution to the Sommerfeld coefficient γ_{imp} [27]. In this way

$$T_K = \pi w \Delta, \qquad \Delta(\epsilon) = \pi \sum_k |V_k|^2 \, \delta(\epsilon_k - \epsilon) = \frac{V^2 L}{2}. \qquad (3.99)$$

Here, $w = 0.4128$ is the Wilson ratio. The hybridization function Δ is the transition rate for the pseudofermions in presence of the resonant level in 2nd order perturbation theory evaluated using Fermi's Golden Rule. If an experiment reveals, that the quantum dot, say, has a Kondo temperature T_K, the appropriate low energy Hamiltonian is a resonant level model where the intrinsic energy scale Δ has to be chosen such that Eq. (3.99) is fulfilled.

3.2.5 Summary

Concluding, the application of an Emery-Kivelson transformation U and a second unitary transformation U_2 simplified the anisotropic Kondo Hamiltonian in the Toulouse limit tremendously. The resulting Hamilton operator of the resonant level model is quadratic in spinless fermions. Those spinless fermions describe the spin degrees of freedom in the Kondo model and are complicated functions of the initial conduction band electrons. Therefore, the action of those operators cannot be easily interpreted in the initial picture. Furthermore, despite the fact that the Emery-Kivelson transformation simplifies the Hamiltonian, observables, in general, become difficult. But there is one important exception. The spin operator S_z commutes with both transformations U and U_2 and can be connected to the operators of the effective Hamiltonian in an easy way, see Eq. (3.91). Consequently, despite of all difficulties, the dynamics of the local spin are analytically accessible.

Throughout the mapping onto a resonant level model, there has been no requirement on $J_\perp$. As a consequence, one can choose $J_\perp$ or equivalently V to be arbitrarily time-dependent. This basic observation will serve as a starting point for the specific nonequilibrium setup that will be analyzed later. Namely, the situation where the spin dynamics in the Kondo Hamiltonian are switched on and off periodically: $J_\perp(t) = J_\perp \theta \left[\sin(\Omega t)\right]$. The mapping itself puts no constraint upon the couplings $J_\perp$ and V, but, initially, the spectrum of the electrons has been linearized for an appropriate use of the bosonization technique. This is a suitable approximation for the low energy properties of the model. Therefore, V and $J_\perp$ should be small enough such that the typical energy transfer for scattered electrons does not exceed the range of validity for linearization. In this case, the effect of curvature in the dispersion relation is negligible. The periodic time dependence of the Hamiltonian, however, leads to another energy scale in the problem, the driving frequency Ω. Electrons can hop off the local level into the conduction band by absorbing or emitting multiple quanta of Ω [21]. As a consequence, the energy gain or loss $\sim \Omega$ for a conduction band electron in a scattering process has to be small enough such that the curvature of the spectrum is negligible.

Chapter 4

Setup: Periodic time-dependent Kondo model

Before the advent of quantum dots, experiments on the Kondo effect were limited to samples where different kinds of magnetic impurities are embedded in various bulk materials. Obviously, the amount of control over such devices is rather restricted. Since one is dealing with bulk samples, a certain concentration of magnetic impurities is needed to observe a significant impact onto bulk properties like the conductance or magnetic susceptibility. Therefore, properties of a single impurity are not accessible in such a measurement. Moreover, the microscopic parameters are fixed for each sample, such that a variation of system parameters can only be achieved by fabricating a whole bunch of samples with different kinds of impurities, for example.

The realization of quantum dots enabled the creation of highly tunable nanodevices. In a certain regime of the microscopic parameters, quantum dots act as magnetic impurities producing Kondo physics [11]. Most importantly, the Kondo effect can be studied at a single impurity with the opportunity to generate nonequilibrium setups because unscreened electrical or magnetic fields can be applied directly to the impurity. Since the Kondo effect is a coherent fragile many-body effect, that can be destroyed easily by temperature in equilibrium for example, a nonequilibrium setting may affect the Kondo effect drastically. One way of creating a nonequilibrium situation is the application of a dc bias across the dot. In this case a window of scattering channels is opened that is not present in an equilibrium setting. Moreover, a nonequilibrium setting may be created by varying microscopic parameters like a back gate voltage or a locally applied magnetic field in time.

4.1   Setup

In this work a scenario will be considered that leads to a periodic switch on and off of the interaction in the Kondo model. A possible experimental realization using a quantum dot with a time-dependent back gate voltage will be presented in Sec. (4.1.2). Moreover, it will be shown that this experimental situation is indeed described by a time-dependent Kondo Hamiltonian in which the Kondo exchange interaction is switched on and off periodically. As a quantum dot can be modeled by a time-dependent Anderson impurity Hamiltonian, one can construct an appropriate time-dependent Schrieffer-
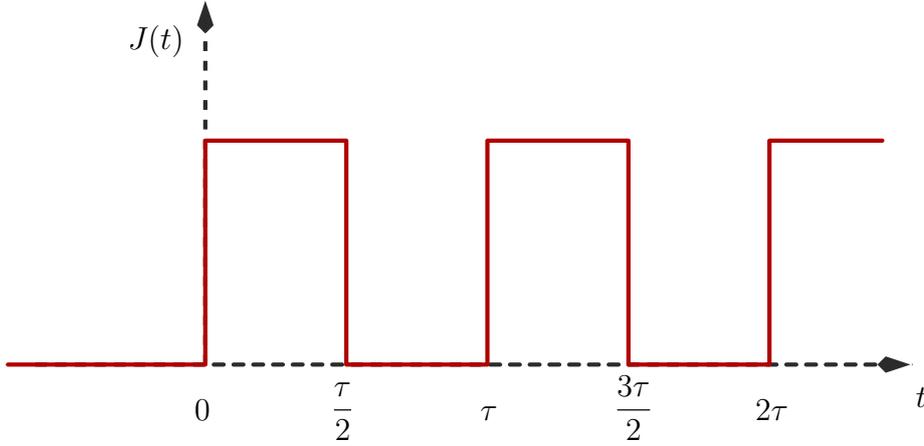
Figure 4.1: Time dependence of the Kondo coupling $J(t)$ in the time-dependent Kondo Hamiltonian under the periodic driving.

Wolff transformation, as will be explained in Sec. (4.1.3), that maps the Anderson impurity Hamiltonian onto the desired Kondo Hamiltonian. As will be shown in Sec. (4.1.1), in the strong coupling limit, a proper anisotropic Kondo Hamiltonian can be used to map the problem onto an exactly solvable one, onto a time-dependent noninteracting resonant level model.

The time-dependent Kondo Hamiltonian whose dynamics will be analyzed in this thesis is the following:

$$H_K = \sum_{k\eta} \varepsilon_k : c_{k\eta}^\dagger c_{k\eta} : + J(t) \sum_{kk'} \left[c_{k\uparrow}^\dagger c_{k'\downarrow} - c_{k\downarrow}^\dagger c_{k'\uparrow} \right] S_z$$
$$+ J(t) \sum_{kk'} \left[c_{k\downarrow}^\dagger c_{k'\uparrow} S_+ + c_{k\uparrow}^\dagger c_{k'\downarrow} S_- \right], \tag{4.1}$$
$$\text{with} \quad J(t) = J\, \theta(t)\, \theta(\sin(\Omega t)).$$

The Kondo coupling $J(t)$ is switched on and off periodically in time as indicated in Fig. (4.1). The protocol according to which the system evolves will be the following. For all times $t < 0$ the Hamiltonian is given by just the free part of the Kondo Hamiltonian describing a decoupled noninteracting Fermi gas and local spin. The system is connected to a heat bath for $t < 0$ whose temperature T is assumed to be small enough to consider the system to be in the ground state, that is a product state of the Fermi sea $|0\rangle$ and a spin wave function $|\chi\rangle$ of the local spin. Therefore, the system is prepared initially in the following state:

$$|\Psi_0\rangle = |0\rangle \otimes |\chi\rangle. \tag{4.2}$$

At time $t = 0$ the system is decoupled from the heat bath and the time-dependent periodic setup starts with an instantaneous switch on of the Kondo interaction. The coupling J is held at a constant value until time $\tau/2$ where the Kondo interaction is switched off and remains off until $t = \tau$. This procedure is repeated until after an infinite number of periods τ one expects a quasi-steady state to build up. The energy scale associated with this periodic switching is the so-called driving frequency Ω:

$$\text{period } \tau, \qquad \text{driving frequency } \Omega = \frac{2\pi}{\tau}. \tag{4.3}$$
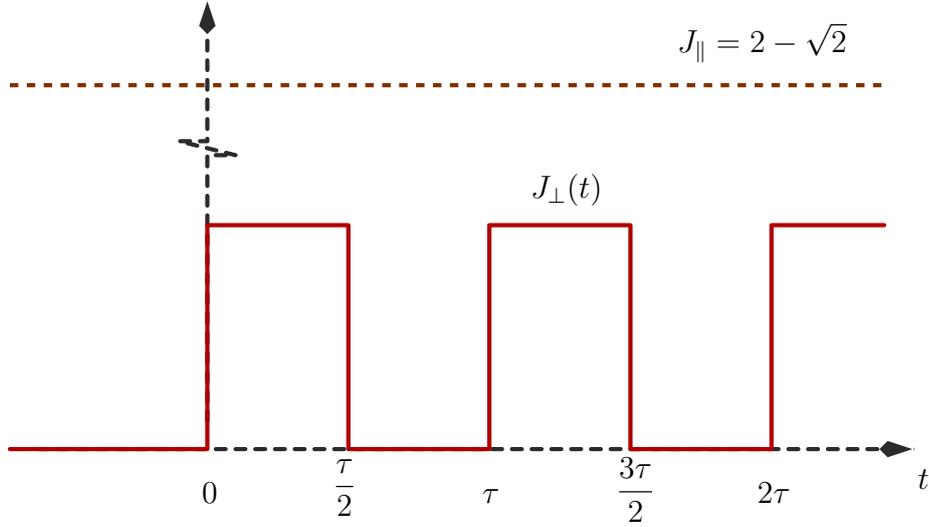
Figure 4.2: Time dependence of the couplings of the periodic time-dependent anisotropic Kondo Hamiltonian.

Due to the time dependence of the Hamiltonian the energy is not a conserved quantity. Moreover, each quench that is performed excites the system such that one can expect that after an infinite number of switches an infinite amount of energy is pumped into the system. Therefore, a dissipation mechanism is needed that absorbs the excitations that are created in the vicinity of the impurity in a periodic fashion. As has been shown by Doyon and Andrei [8], the leads themselves can serve as heat baths in the correct limit. Therefore, no additional dissipation mechanism is needed. They showed rigorously that in a dc bias situation the leads in the Kondo Hamiltonian act as a bath if they are taken as infinitely big. As a consequence, a certain order of taking limits has to be prescribed, namely the thermodynamic limit has to be performed before taking the limit of long times:

$$\lim_{t \to \infty} \lim_{L \to \infty} . \tag{4.4}$$

Doyon and Andrei referred to this order of taking limits as the open system limit. The opposite order of taking limits would lead to a blow up of the occupation distribution $n_k = \langle c_k^\dagger c_k \rangle$ in this setup, where c_k are the modes of the spinless fermions in the resonant level model Hamiltonian, signaling an overheating of the system.

4.1.1 Setup in the effective Hamiltonian picture

For temperatures T much lower than the Kondo temperature, $T \ll T_K$, the Kondo singlet forms, as explained in Sec. (2.1), driving the Kondo system into the strong coupling regime. The effective Hamiltonian describing the dynamics in this limit is obtained by replacing the Kondo Hamiltonian by the appropriate anisotropic counterpart in the Toulouse limit. In the present periodic driving setup the proper time-dependent anisotropic Kondo Hamiltonian reads:
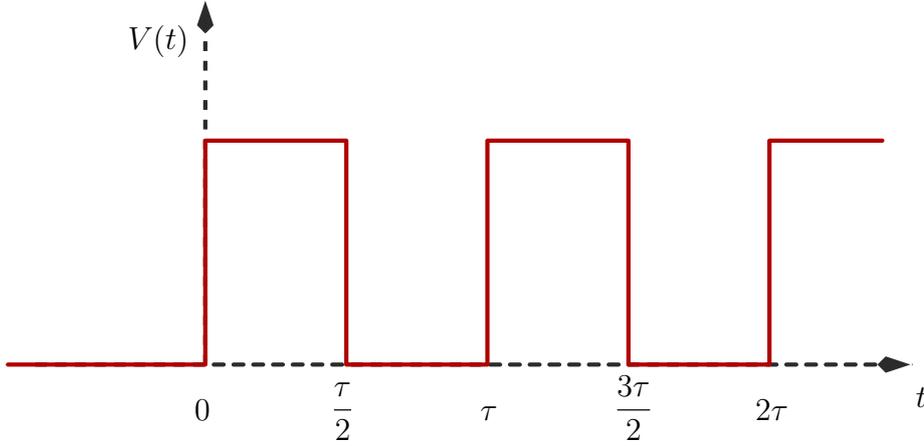
Figure 4.3: Time dependence of the hopping element V of the effective Hamiltonian under the periodic driving

$$H_K = \sum_{\eta=\uparrow\downarrow} \int \frac{dx}{2\pi} : \Psi_\eta^\dagger(x)[-i\partial_x]\Psi_\eta(x) : + \frac{J_\parallel}{2} \left[: \Psi_\uparrow^\dagger(0)\Psi_\uparrow(0) : - : \Psi_\downarrow^\dagger(0)\Psi_\downarrow(0) : \right] S_z,$$

$$+ \frac{J_\perp(t)}{2} \left[\Psi_\uparrow^\dagger(0)\Psi_\downarrow(0)S^- + \Psi_\downarrow^\dagger(0)\Psi_\uparrow(0)S^+ \right]$$

$$J_\perp(t) = J_\perp \, \theta(t), \, \theta(\sin(\Omega t)) \qquad J_\parallel = 2 - \sqrt{2}.$$

$$(4.5)$$

The parallel coupling is fixed at a value $J_\parallel = 2 - \sqrt{2}$, corresponding to the so-called Toulouse limit, see Eq. (3.97). The Kondo scale is solely determined by the perpendicular coupling $J_\perp$, see Eq. (3.99), providing the low energy scale in the problem. The time dependence of the couplings in the effective strong coupling Hamiltonian is shown in Fig. (4.2). As explained in the previous chapter, the anisotropic Kondo Hamiltonian can be mapped onto a resonant level model Hamiltonian of spinless pseudofermions (3.98) in the Toulouse limit by use of the bosonization technique. This mapping does not depend on the actual value of $J_\perp$, such that it can also be performed for a time-dependent coupling $J_\perp(t)$. An anisotropic Kondo Hamiltonian with $J_\perp = 0$ results in the free part of the effective resonant level model Hamiltonian since $V \propto J_\perp$. Therefore, the effective Hamiltonian in the periodic driving setup considered here is a time-dependent resonant level model Hamiltonian, where the coupling to the local level is switched on and off periodically:

$$H_{\text{RLM}}(t) = \sum_k k : c_k^\dagger c_k : + V(t) \sum_k \left[d^\dagger c_k + c_k^\dagger d \right]$$

$$V(t) = V \, \theta(t) \, \theta(\sin(\Omega t))$$

$$(4.6)$$

The Kondo temperature, the only energy scale in the Kondo model, is connected to the hopping element V of the resonant level model by the relation $T_K = \pi w \frac{V^2 L}{2}$ where $w = 0.4128$ is the Wilson number and L the system size, see Eq. (3.99). Reminding the
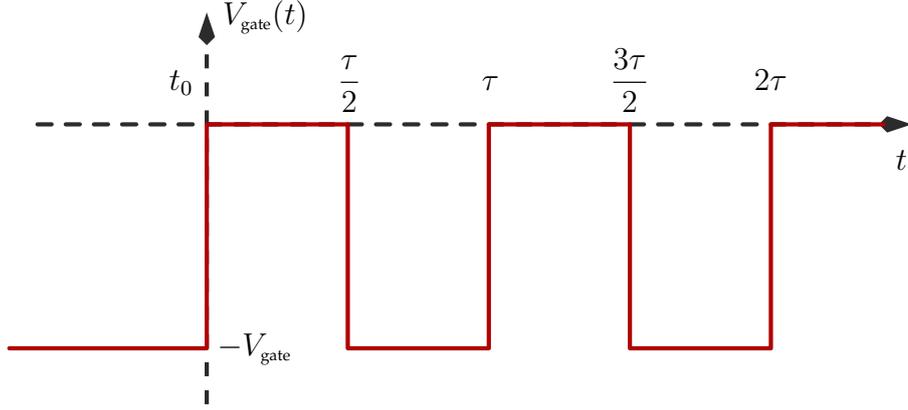
Figure 4.4: Time dependence of the gate voltage

previous paragraphs, the complete protocol according to which the system will evolve in the language of the effective Hamiltonian can be summarized in the following way. Initially, the system is prepared in the ground state of the Hamiltonian for times $t < 0$, that is a product state

$$|\Psi_0\rangle = |0\rangle \otimes |\chi\rangle \tag{4.7}$$

where $|0\rangle$ is the Fermi sea of the spinless fermions and $|\chi\rangle$ an arbitrary wave function of the local level. At time $t = 0$ the periodic quenching process starts where the hopping term is switched on and off periodically with period τ as indicated in Fig. (4.3).

Although all couplings in the Kondo Hamiltonian before the replacement by the anisotropic Kondo Hamiltonian are switched including $J_\parallel$, the parallel coupling is held fixed at a constant value here. As has been shown by Lobaskin and Kehrein [27] for a single interaction quench in the Kondo Hamiltonian, an additional switch off of the parallel coupling induces a potential scattering term for times during which the time-dependent resonant level model Hamiltonian only contains the kinetic part in the present setup as a consequence of the Emery-Kivelson transformation, see Sec. (3.2.2). As one can check, this additional potential scattering term does not affect the spin dynamics in a single interaction quench scenario. The strength of the potential scattering is proportional to the magnetization of the impurity spin $\langle S_z \rangle$. Since the magnetization drops exponentially in the present setup, as will be shown later, one can expect that at least in the steady state after an infinite number of switches this additional potential scattering term will be irrelevant.

4.1.2 Possible experimental realization

As pointed out by Nordlander et al. [32], in contrast to impurities in a bulk it is possible to apply unscreened time-dependent electric or magnetic fields directly to a single impurity by using a quantum dot. The goal of this section will be to show a possible experimental setup for a quantum dot that generates a periodic switch on an off of the Kondo interaction. This can be achieved by periodically modulating the gate voltage as is indicated in Fig. (4.4) with a large amplitude V_{gate}. The Hamiltonian that models such a physical situation is the following time-dependent Anderson impurity model with a

local level whose energy $\varepsilon_d(t)$ changes in time due to the applied gate voltage:

$$H_{\text{AIM}}(t) = H_{el} + H_{dot}(t) + H_t$$

$$
\begin{aligned}
H_{el} &= \sum_{k\eta=\uparrow,\downarrow} \epsilon_k : c_{k\eta}^\dagger c_{k\eta} : \\
H_{dot}(t) &= \sum_\eta \epsilon_d(t) \, d_\eta^\dagger d_\eta + U\hat{n}_\uparrow \hat{n}_\downarrow \\
H_t &= \sum_{k\eta} t_k \left[c_{k\eta}^\dagger d_\eta + d_\eta^\dagger c_{k\eta} \right] \\
\varepsilon_d(t) &= \varepsilon_d + V_{\text{gate}}(t).
\end{aligned}
\tag{4.8}
$$

All energies will be measured with respect to the Fermi energy, i.e. $\varepsilon_F = 0$. The protocol according to which the system evolves is the following. For times $t < 0$, a large negative gate voltage is applied to the quantum dot such that the local level position is shifted far beyond the Fermi level in order to suppress exchange processes that cause the Kondo effect. Furthermore, the Coulomb repulsion U is chosen to be large enough to prevent double occupancy even for large gate voltages, in order to stay in the subspace of single occupation such that one arrives at the following conditions:

$$\varepsilon_d - V_{\text{gate}} \ll \varepsilon_d, \qquad \varepsilon_d - V_{\text{gate}} + U \gg \varepsilon_F. \tag{4.9}$$

A shift of the local level position far below the Fermi surface, the first condition, suppresses the hopping processes between the conduction band and the central region. The probability for exchange processes, causing the spin flips and therefore the Kondo effect, becomes negligible such that the hopping term in the Anderson Hamiltonian as well as the Kondo interaction are effectively switched off. This will be shown rigorously in Sec. (4.1.3).

At time $t = 0$, the local level position is suddenly shifted to a value ε_d where a Kondo effect can build up. For a time $\tau/2$ the system evolves due to a Anderson impurity model in the local moment regime. At $t = \tau/2$, the Hamiltonian is pushed back to the configuration with a large negative gate voltage V_{gate}. This procedure of shifting the local level position, switching the Kondo effect on and off, will be continued further in order to generate the desired time-dependent Kondo Hamiltonian.

The regime where the Kondo effect emerges, the so called local moment regime, is realized when $\varepsilon_d \ll \varepsilon_F, \varepsilon + U \gg \varepsilon_F, \Gamma \ll |\varepsilon_d|, \varepsilon_d + U$, see Eq. (2.4). In equilibrium those conditions are sufficient in order to cause Kondo physics. In the periodic driving setup another condition has to be imposed. By driving the system periodically electrons can hop off the central region into the conduction band by absorbing quanta of the driving frequency Ω [21]. If $\Omega \gtrsim |\varepsilon_d|$, for example, a local electron can easily hop into the lead leaving behind an unoccupied level. Similarly, in the case where $\Omega \gtrsim U + \varepsilon_d$, electrons at the Fermi level can hop onto the dot into the level at $U + \varepsilon_d$ by absorbing quanta of Ω leading to double occupancy. Both processes lead to a destruction of the Kondo effect since they would drive the system out of the subspace of single occupation. Therefore, a restriction on the driving frequency emerges:

$$\Omega \ll |\varepsilon_d|, \varepsilon_d + U, \tag{4.10}$$

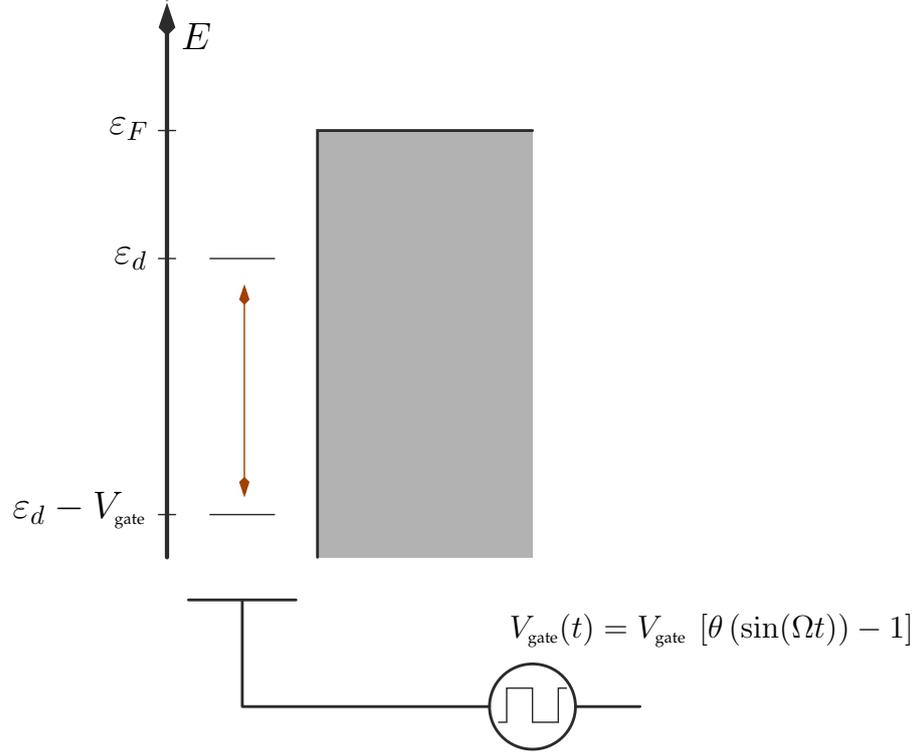to exclude processes in which the dot is ionized.

Figure 4.5: Schematic picture of the periodic modulation of the local level in a quantum dot

4.1.3 Time-dependent Schrieffer-Wolff transformation

In the local moment regime the low-energy sector of the Anderson impurity model can be mapped onto a Kondo Hamiltonian via a Schrieffer-Wolff transformation, see Sec. (2.1.2) for the equilibrium case. This is possible even for time-dependent Anderson Hamiltonians as is the case in the periodic driving setup considered here [13][21]. The Schrieffer-Wolff transformation, however, has to be modified since time-dependent unitary transformations leave the Schrödinger equation invariant only if the Hamilton operator is transformed in the following way, see for example [13]:

$$H_{\mathrm{AIM}} \quad \longrightarrow \quad e^{W} H_{\mathrm{AIM}} e^{-W} + i \frac{\mathrm{d}W}{\mathrm{d}t}. \tag{4.11}$$

Here, $\hbar$ was set equal to 1. In the time-independent case, the generator W of this transformation is chosen such that all terms linear in the tunnel coupling t_k vanish, see Eq. (2.8). This leads to an algebraic equation that can be solved for W. In the time-dependent case, a differential equation has to be solved instead, in order to eliminate all linear in t_k contributions:

$$[W, H_{el} + H_{dot}] + H_t + i \frac{\mathrm{d}W}{\mathrm{d}t} = 0. \tag{4.12}$$

Accordingly, the final Hamiltonian will be of the structure

$$H_K = H_{el} + H_{dot} + \frac{1}{2} \left[[W, H_t] - i \left[W, \frac{\mathrm{d}W}{\mathrm{d}t} \right] \right] \tag{4.13}$$

up to third order terms in the tunnel coupling t_k. Inserting the choice

$$W = \sum_{k\eta} \left[\left(w_k^{(1)}(t)(1 - d_{-\eta}^\dagger d_{-\eta}) + w_k^{(2)}(t) d_{-\eta}^\dagger d_{-\eta} \right) d_\eta^\dagger c_{k\eta} - H.c. \right] \tag{4.14}$$

for W into Eq. (4.12) leads to a differential equation for the functions $w_k^{(1)}(t)$ and $w_k^{(2)}(t)$:

$$\begin{aligned} -i\dot{w}_k^{(1)}(t) &= [\varepsilon_k - \varepsilon_d(t)]\, w_k^{(1)}(t) + t_k, \\ i\dot{w}_k^{(2)}(t) &= [\varepsilon_k - \varepsilon_d(t) - U]\, w_k^{(2)}(t) + t_k. \end{aligned} \tag{4.15}$$

It was shown in the previous section that the driving frequency has to be chosen small compared to the energy scales $|\varepsilon_d|$ and $U - \varepsilon_d$, confirm Eq. (4.10). In this case the differential equations can be solved in the adiabatic approximation since one can assume that the functions w will only vary slowly in each half period such that one can neglect the derivatives on the left hand side [21]:

$$\begin{aligned} w_k^{(1)}(t) &= -\frac{t_k}{\varepsilon_k - \varepsilon_d(t)}, \\ w_k^{(2)}(t) &= \frac{t_k}{\varepsilon_k - \varepsilon_d(t) - U}. \end{aligned} \tag{4.16}$$

If the position of the local level is shifted to a value $\varepsilon_d(t) = \varepsilon_d - V_{\text{gate}}$ well below the Fermi surface the functions $w_k^{(1)}(t)$ and $w_k^{(2)}(t)$ vanish leading to the following relations in the periodic driving setup:

$$\begin{aligned} w_k^{(1)}(t) &= -\theta(\sin(\Omega t)) \frac{t_k}{\varepsilon_k - \varepsilon_d}, \\ w_k^{(2)}(t) &= \theta(\sin(\Omega t)) \frac{t_k}{\varepsilon_k - \varepsilon_d - U}. \end{aligned} \tag{4.17}$$

Inserting these expressions into Eq. (4.13), the Kondo Hamiltonian is given by:

$$\begin{aligned} H_K &= \sum_{k\eta} \varepsilon_k : c_{k\eta}^\dagger c_{k\eta} : + \sum_{kk'} J_{kk'}(t) \left[c_{k\uparrow}^\dagger c_{k'\downarrow} - c_{k\downarrow}^\dagger c_{k'\uparrow} \right] S_z \\ &\quad + \sum_{kk'} J_{kk'}(t) \left[c_{k\downarrow}^\dagger c_{k'\uparrow} S_+ + c_{k\uparrow}^\dagger c_{k'\downarrow} S_- \right] + \sum_{kk'\eta} K_{kk'}(t) c_{k\eta}^\dagger c_{k'\eta}. \end{aligned} \tag{4.18}$$

where the derivative of the generator in Eq. (4.13) has been neglected due to $\dot{w}_k^{(1)}(t)$, $\dot{w}_k^{(2)}(t) \approx 0$ in the adiabatic approximation. In order to arrive at the desired Hamilton operator a further projection onto the subspace of single occupation has to be performed as in the equilibrium case. The couplings $J_{kk'}(t)$ and $K_{kk'}(t)$ obey the following relations:

$$\begin{aligned} J_{kk'}(t) &= \theta(\sin(\Omega t)) \left[\frac{t_k^2}{\varepsilon_k - \varepsilon_d} + \frac{t_k^2}{\varepsilon_k - \varepsilon_d - U} \right], \\ K_{kk'}(t) &= \frac{1}{2} \theta(\sin(\Omega t)) \left[\frac{t_k^2}{\varepsilon_k - \varepsilon_d} - \frac{t_k^2}{\varepsilon_k - \varepsilon_d - U} \right]. \end{aligned} \tag{4.19}$$

The exact dependence of $J_{kk'}(t)$ on the modes is negligible for electrons near the Fermi level. Since the low energy properties of the Kondo model depend only on the electrons near the Fermi surface, one can replace $J_{kk'}$ by the structureless constant $J := J_{00}$.

In the particle-hole symmetric case, i.e. $U = -\varepsilon_d/2$, the potential scattering term in the Kondo Hamiltonian vanishes. Since the potential scattering term does not affect the spin sector of the Kondo Hamiltonian, as already emphasized in Sec. (3.2.1), it can be neglected for the study of the spin observables due to spin charge separation. Accordingly, the particle-hole symmetric case will be assumed from now on. As a result, the effective low energy Hamiltonian of the Anderson impurity model, where the local level is shifted periodically, is given by:

$$H_K = \sum_{k\eta} \varepsilon_k : c_{k\eta}^\dagger c_{k\eta} : + J(t) \sum_{kk'} \left[c_{k\uparrow}^\dagger c_{k'\downarrow} - c_{k\downarrow}^\dagger c_{k'\uparrow} \right] S_z$$
$$+ J(t) \sum_{kk'} \left[c_{k\downarrow}^\dagger c_{k'\uparrow} S_+ + c_{k\uparrow}^\dagger c_{k'\downarrow} S_- \right], \tag{4.20}$$
$$\text{with} \quad J(t) = J\,\theta(\sin(\Omega t)),$$

that is the desired time-dependent Kondo Hamilton operator. Therefore, it was shown that shifting the local level of a quantum dot far beyond the Fermi level switches off the Kondo effect. Accordingly, a periodic shifting in this setup leads to a periodic switch on and off of the Kondo interaction as expected.

4.2 Periodic time-dependent Hamiltonians and Floquet theory

Despite the complexity of time evolution in time-dependent physical systems, Hamiltonians that share a periodic time dependence are provided with a formalism called Floquet theory moving periodic time-dependent systems towards time-independent ones. A Hamiltonian equipped with a discrete symmetry of the form

$$H(t + \tau) = H(t) \tag{4.21}$$

where τ is a positive and finite real number exhibits a set of wave functions called Floquet modes that are the solutions of an eigenvalue equation formally resembling that of a time-independent Schrödinger equation [41] [36]. A simple proof can be found in [34] that is similar to the proof of the Bloch theorem for particles moving in a spatially periodic potential. The basic observation is that there exists a complete set of solutions $|\Psi_\alpha(t)\rangle$, called Floquet states, of the time-dependent Schrödinger equation that is of the following form:

$$|\Psi_\alpha(t)\rangle = e^{-i\varepsilon_\alpha t}|\phi_\alpha(t)\rangle \tag{4.22}$$

where the so called Floquet modes $|\phi_\alpha(t)\rangle$ exhibit a characteristic periodicity property

$$|\phi_\alpha(t + \tau)\rangle = |\phi_\alpha(t)\rangle. \tag{4.23}$$

The structure of the Floquet states resembles the structure of the Bloch states, the single particle eigenstates of particles moving in a spatially periodic potential. As the Bloch states can be characterized by a quasimomentum, the Floquet states can be labeled by the so-called quasienergies ε_α, also called the Floquet characteristic exponents. As a consequence of the periodicity of the Floquet modes, the long time evolution is completely determined by the quasienergies [14]. The dynamics within one period, however, relies on the behavior of the Floquet modes. Insertion of the Floquet states into the

time-dependent Schrödinger equation leads to an eigenvalue equation of the so called Floquet Hamiltonian

$$\mathfrak{H} = H - i\frac{\partial}{\partial t} \tag{4.24}$$

for the Floquet modes with the quasienergies playing the role of the eigenvalues:

$$\mathfrak{H}|\Phi_\alpha(t)\rangle = \varepsilon_\alpha|\Phi_\alpha(t)\rangle. \tag{4.25}$$

Here, the great advantage of the Floquet formalism becomes apparent. Due to the formal similarity to a time-independent Schrödinger equation known theorems for time-independent problems can be simply adopted to the periodic time-dependent case, like the Rayleigh-Ritz variational principle or the Hellman-Feynman theorem [14]. As is the case for the quasimomenta in the Bloch theorem, the quasienergies are not uniquely defined such that one can restrict to a certain "Brioullin zone"

$$-\frac{\Omega}{2} \leq \varepsilon_\alpha \leq \frac{\Omega}{2} \tag{4.26}$$

where $\Omega = 2\pi/\tau$ is the frequency of the driving. Due to the periodicity of the Floquet mode and the Hamilton operator one can perform a Fourier expansion of both quantities such that one can find a time-independent representation of the Schrödinger equation:

$$\sum_m H_{n-m}|\Phi_\alpha^m\rangle = [\varepsilon_\alpha + n\Omega]\,|\Phi_\alpha^n\rangle \tag{4.27}$$

where

$$H_n = \frac{1}{\tau}\int_0^\tau \mathrm{d}t\, e^{in\Omega t}H(t), \qquad |\Phi_\alpha^n\rangle = \frac{1}{\tau}\int_0^\tau \mathrm{d}t\, e^{in\Omega t}\,|\Phi_\alpha(t)\rangle. \tag{4.28}$$

The time evolution operator $U(t, t_0)$ that propagates any state $|\Psi(t_0)\rangle$ at a time t_0 to time t,

$$|\Psi(t)\rangle = U(t, t_0)|\Psi(t_0)\rangle, \tag{4.29}$$

although difficult for time-dependent systems, exhibits special properties in the case of periodic time-dependence. First, it is invariant under a shift of one period τ in both time arguments [23]:

$$U(t + \tau, t_0 + \tau) = U(t, t_0). \tag{4.30}$$

As a consequence, the propagator over multiple periods factorizes into a product of propagators over one period:

$$U(n\tau, 0) = [U(\tau, 0)]^n. \tag{4.31}$$

This property will be used extensively throughout this work. Moreover, the propagator carries all information about the quasienergies. As the time evolution operator is unitary, it can be diagonalized by another unitary transformation W:

$$W^\dagger U(\tau, 0)W = e^{-iD\tau}. \tag{4.32}$$

The diagonal elements of the diagonal matrix D are just the quasienergies ε_α [14]. Since the Floquet states constitute a complete basis of the Hilbert space, any wave function can be decomposed in a way similar to a time-independent situation:

$$|\Psi(t)\rangle = \sum_\alpha c_\alpha e^{-i\varepsilon_\alpha t}|\Phi_\alpha(t)\rangle, \qquad c_\alpha = \langle\Phi_\alpha|\Psi\rangle, \tag{4.33}$$

such that the whole information about the long time behavior is encoded in the quasi-energies.

Correlation functions in a periodic setup also exhibit a distinctive periodicity property. Suppose, that the system of interest is initially prepared in an equilibrium state characterized through a density matrix ρ_0. Then, due to the periodic driving, the state of the system evolves into a quasi-steady state after an infinite amount of periods, that is determined by the following density matrix:

$$\lim_{N \to \infty} [U(\tau)]^N \rho_0 [U^\dagger(\tau)]^N \tag{4.34}$$

where $U(\tau)$ is the time evolution operator over one period. In this state, correlation functions are invariant under a discrete time shift of one period τ in all their time arguments. A two-time correlation function of two observables $\mathcal{O}$ and $\mathcal{P}$ in the quasi-steady state, for example, is given by:

$$\langle \mathcal{O}(t)\mathcal{P}(t') \rangle = \frac{1}{Z} \lim_{N \to \infty} \mathrm{Tr} \left[[U(\tau)]^N \rho_0 [U^\dagger(\tau)]^N \mathcal{O}(t)\mathcal{P}(t') \right] \tag{4.35}$$

where $Z = \mathrm{Tr}[\rho_0]$ is the partition function. The invariance property of two-time correlation functions follows directly:

$$\langle \mathcal{O}(t+\tau)\mathcal{P}(t'+\tau) \rangle = \frac{1}{Z} \lim_{N' \to \infty} \mathrm{Tr} \left[[U(\tau)]^{N'} \rho_0 [U^\dagger(\tau)]^{N'} \mathcal{O}(t)\mathcal{P}(t') \right]$$
$$= \langle \mathcal{O}(t)\mathcal{P}(t') \rangle. \tag{4.36}$$

Here, $N' = N + 1$. In equilibrium two-time correlation functions depend only on the time difference of both time variables such that they are functions of only one time argument, effectively. Therefore, one can find a spectral decomposition in terms of a function of only one frequency. In nonequilibrium time translational invariance is broken such that those two-time correlation functions cannot be reduced to a function of only one argument. Consequently, a spectral representation involves two arguments. In the case of periodic time-dependence, however, a special representation can be found due to the periodicity property, see Eq. (4.36). Exploiting this invariance property one can define a set of two new variables, a relative time coordinate t_{rel} and an average one t_{ave} by [42]

$$t_{rel} = t - t' \qquad t_{ave} = \frac{t + t'}{2} \tag{4.37}$$

such that one can rewrite the two time correlation function in the following way

$$\langle \mathcal{O}(t)\mathcal{P}(t') \rangle = \langle \mathcal{O}(t_{ave} + t_{rel}/2)\mathcal{P}(t_{ave} - t_{rel}/2) \rangle. \tag{4.38}$$

Most importantly, the time average coordinate carries the invariance property $t_{ave} \to t_{ave} + \tau$. With respect to the new time coordinated one can define two spectral decompositions of the two-time correlation function:

$$\langle \mathcal{OP} \rangle(t_{ave}, \varepsilon) = \int_{-\infty}^{\infty} \mathrm{d}t_{rel}\, e^{i\varepsilon t_{rel}} \langle \mathcal{O}(t_{ave} + t_{rel}/2)\mathcal{P}(t_{ave} - t_{rel}/2) \rangle,$$
$$\langle \mathcal{OP} \rangle_n(\varepsilon) = \frac{1}{\tau} \int_0^\tau \mathrm{d}t_{ave}\, e^{in\Omega t_{ave}} \langle \mathcal{OP} \rangle(t_{ave}, \varepsilon). \tag{4.39}$$

Effectively, the first spectral decomposition is a Wigner transform of the correlation function and can be interpreted as the spectral decomposition of the two time correlation function at a given time point t_{ave}. Due to the invariance under a discrete time shift $t_{ave} \to t_{ave} + \tau$ the Wigner transform can be expanded into a Fourier series defining a second spectral representation. With each mode n one can associate processes in which n photons are absorbed ($n > 0$) or emitted ($n < 0$) [23]. The zero mode $n = 0$ Fourier coefficient is equivalent to the time averaged Wigner transform.

One can also regard a modified Wigner transform that can be obtained by the following reasoning:

$$\langle \mathcal{OP} \rangle_n(\varepsilon) = \frac{1}{\tau} \int_0^\tau \mathrm{d}t_{ave} \, e^{in\Omega t_{ave}} \int_{-\infty}^\infty \mathrm{d}t_{rel} \, e^{i\varepsilon t_{rel}} \, \langle \mathcal{O}(t_{ave} + t_{rel}/2)\mathcal{P}(t_{ave} - t_{rel}/2) \rangle$$

$$\overset{t_{ave} \to t_{\underline{ave}} + t_{rel}/2}{=} \int_{-\infty}^\infty \mathrm{d}t_{rel} \, e^{i(\varepsilon + n\Omega/2)t_{rel}} \frac{1}{\tau} \int_{t_{rel}/2}^{\tau + t_{rel}/2} \mathrm{d}t_{ave} \, e^{in\Omega t_{ave}} \langle \mathcal{O}(t_{ave} + t_{rel})\mathcal{P}(t_{ave}) \rangle. \tag{4.40}$$

Since the evaluation of a Fourier component of a periodic function is independent on how one chooses the integral over the period, one can shift the integration limits in the integral over t_{ave} back to 0 and τ. Defining $\bar{\varepsilon} := \varepsilon + n\Omega/2$, one can rewrite the expression above in the following way:

$$\langle \mathcal{OP} \rangle_n(\bar{\varepsilon}) = \frac{1}{\tau} \int_0^\tau \mathrm{d}t_{ave} \, e^{in\Omega t_{ave}} \int_{-\infty}^\infty \mathrm{d}t_{rel} \, e^{i\bar{\varepsilon} t_{rel}} \, \langle \mathcal{O}(t_{ave} + t_{rel})\mathcal{P}(t_{ave}) \rangle \tag{4.41}$$

Therefore, equivalently to the Wigner transform of the two-time correlation function one can consider the following spectral decomposition:

$$\langle \mathcal{OP} \rangle(t_{ave}, \bar{\varepsilon}) = \int_{-\infty}^\infty \mathrm{d}t_{rel} \, e^{i\bar{\varepsilon} t_{rel}} \, \langle \mathcal{O}(t_{ave} + t_{rel})\mathcal{P}(t_{ave}) \rangle \tag{4.42}$$

Chapter 5

Single-particle dynamics in the periodic driving setup

In Chapter 3 it was shown that the anisotropic Kondo Hamiltonian in the Toulouse limit can be mapped onto a noninteracting resonant level model by use of the bosonization technique. Remarkably, this mapping allows for an arbitrary time-dependence of the perpendicular Kondo coupling $J_\perp(t)$ resulting in the corresponding time dependence of the hopping amplitude $V(t) \propto J_\perp(t)$ in the resonant level model. This observation opens the way to analyze the properties of the Kondo model under time-dependent nonequilibrium conditions as has been done in the work by Lobaskin and Kehrein [27][28] for a single interaction quench.

Since the resonant level model Hamiltonian is quadratic in spinless fermionic operators, the time evolution is analytically accessible on all time scales. In this chapter, the dynamics of the single-particle operators will be evaluated in the periodic driving setup presented in the last chapter where the couplings $J_\perp$, and V respectively, are switched on and off periodically. For this purpose, a technical statement will be made at first, namely that the unitarity of time evolution in quantum mechanics evidently translates into a unitary time evolution of the single-particle operators. Based on these considerations, the dynamics of the single particle operators are calculated exactly for all times in the periodic nonequilibrium setup.

Despite the difficulty of time evolution in driven systems, the dynamics in this setup are governed by sequentially time-independent Hamiltonians, alternately a free and a resonant level model Hamiltonian. Effectively, the time evolution can be reduced to an equilibrium time evolution where a state is evolved sequentially by different time-independent Hamiltonians. Moreover, the symmetry of the Hamiltonian $H(t + \tau) = H(t)$ in time can be exploited for the description of the dynamics of the single-particle operators. Due to this periodicity of the Hamiltonian the time evolution operator for an integer number n of periods τ factorizes into a product of n identical operators that evolve the system over one period, see Eq. (4.31). Essentially, the problem of long-time evolution can be reduced to a matrix multiplication problem where the challenge will be to evaluate matrix elements of powers of the period matrix $\mathcal{M}$, that is the matrix that takes the single-particle operators over one period.

5.1   Dynamics of systems with quadratic Hamiltonians

In this section, an elementary property of the time evolution for a wide class of quadratic Hamilton operators will be analyzed. The reason for the exact solvability of quadratic Hamiltonians is the property, that the time evolution of a single-particle operator only involves transitions into other single-particle operators. It can never happen, that they get dressed by particle-hole excitations. As a consequence, the dynamics are restricted to a certain operator subspace. For quadratic Hamiltonians the corresponding transition matrix, whose elements give the probability amplitude for a transition from one operator to the other in course of time, is unitary.

A basis transformation U, like the unitary time evolution, that acts on a Hilbert space $\mathcal{H}$, induces a transformation T_U on the linear operators $\mathcal{O}$:

$$T_U[\mathcal{O}] := U\mathcal{O}U^{-1}. \tag{5.1}$$

In the case where $U^\dagger = e^{-iHt}$ is the time evolution operator for a time-independent Hamiltonian H, the induced transformation T_U is the time evolution operator in the space of operators $T_U = e^{tL}$. The generator L of this transformation is the so-called Liouvillian, that is defined through its action on operators: $L[\Gamma] := i[H, \Gamma]$ where the brackets denote the standard commutator. The aim of this section is to show that, if U is unitary, T_U is unitary, too, if one chooses an appropriate domain. As a first observation, T_U is a linear operator:

$$T_U[\eta\mathcal{O} + \mathcal{P}] = U\left(\eta\mathcal{O} + \mathcal{P}\right)U^{-1} = \eta\,T_U[\mathcal{O}] + T_U[\mathcal{P}] \tag{5.2}$$

where η is a complex number and $\mathcal{O}, \mathcal{P}$ are two arbitrary linear operators. Moreover, for every T_U there exists an inverse transformation T_U^{-1}, because

$$(T_{U^{-1}}\,T_U)[\mathcal{O}] = U^{-1}U\,\mathcal{O}\,U^{-1}U = \mathcal{O}. \tag{5.3}$$

Therefore, the inverse of T_U is the induced transformation of U^{-1}:

$$T_U^{-1} = T_{U^{-1}}. \tag{5.4}$$

Additionally, a product of two operators $\mathcal{O}$ and $\mathcal{P}$ factorizes under T_U:

$$T_U[\mathcal{O}\,\mathcal{P}] = T_U[\mathcal{O}]\,T_U[\mathcal{P}]. \tag{5.5}$$

In order to show the unitarity of T_U, first, a proper domain $\mathcal{D}$ has to be chosen as indicated before. For a fermionic field theory, the operators of interest are the operators $c_l^\dagger, c_l$ that create or annihilate one fermion in state l. Since $c_l^\dagger$ is the Hermitian conjugate of c_l, one can restrict on either one species of them for the purpose of showing the unitarity of T_U. Here, the annihilation operators will be chosen. Define the vector space $\mathcal{D}$ of all linear combinations of the c_l's:

$$\mathcal{D} := \text{span}\left[\{c_l\}\right]. \tag{5.6}$$

If T_U is an endomorphism on $\mathcal{D}$, i.e. for all elements $\mathcal{O}$ of $\mathcal{D}$ $T_U[\mathcal{O}]$ is also an element of $\mathcal{D}$, one can think of T_U as acting on the vector space $\mathcal{D}$:

$$T_U : \mathcal{D} \to \mathcal{D} \qquad \mathcal{O} \to T_U[\mathcal{O}]. \tag{5.7}$$

In the following, only those transformations that fulfill this condition will be considered. For the dynamics of a wide class of quadratic systems this requirement can be met as will be shown below. In order to address the property of unitarity, a scalar product has to be defined on the space $\mathcal{D}$, since unitarity means scalar product conservation. Recalling that a fermionic field theory already owns an additional structure, namely the anticommutation relations of the creation and annihilation operators, the proper inner product on the linear operator space $\mathcal{D}$ can be defined in the following way:

$$\langle \mathcal{O} | \mathcal{P} \rangle := \left\langle \left\{ \mathcal{O}^\dagger, \mathcal{P} \right\} \right\rangle \qquad \forall \mathcal{O}, \mathcal{P} \in \mathcal{D} \tag{5.8}$$

where $\langle ... \rangle$ denotes some average that has not to be specified now, since it is only important to ensure that the outcome of this expression is a complex number. As one can check, the definition above fulfills all requirements for a scalar product. Now all prerequisites are prepared in order to show the unitarity of T_U on the vector space $\mathcal{D}$. Due to the linearity of $\mathcal{D}$ it suffices to restrict to the basis elements c_l:

$$\langle T_U[c_l] | T_U[c_{l'}] \rangle = \left\langle \left\{ U c_l^\dagger U^{-1}, U c_{l'} U^{-1} \right\} \right\rangle = \langle c_l | c_{l'} \rangle = \delta_{l,l'}. \tag{5.9}$$

Consequently, T_U is unitary on $\mathcal{D}$. Using the matrix representation $t(U)$ of T_U, given by:

$$T_U[c_l] = \sum_{l'} t_{ll'}(U) c_{l'}, \tag{5.10}$$

on can rephrase the statement as

$$\sum_j t_{lj}(U) t_{jl'}^*(U) = \delta_{l,l'}. \tag{5.11}$$

In the case of a bosonic field theory, all results apply analogously, except that one has to choose the respective commutation relations instead of anticommutation relations in the definition of the proper scalar product on $\mathcal{D}$.

Up to this point, this section may have been quite technical, but the statement above will be important for the dynamics in the periodic driving setup. Suppose, the time evolution of a physical system is governed by a quadratic Hamilton operator H of the structure

$$H = \sum_{ll'} h_{ll'}(t) c_l^\dagger c_{l'} \tag{5.12}$$

where the matrix elements $h_{ll'}(t)$ may depend on time in an arbitrary fashion. According to Def. (5.6), one can introduce the operator space $\mathcal{D}$ of all linear combinations of the annihilation operators c_l. The time evolution of the c_l's under the Hamiltonian H only leads to transitions to other single-particle annihilation operators. This can be seen by regarding the corresponding Heisenberg equations of motion:

$$\frac{\mathrm{d}}{\mathrm{d}t} c_l(t) = i P^\dagger(t) [H(t), c_l] P(t) = -i \sum_{l'} h_{ll'}(t) c_{l'}(t) \tag{5.13}$$

where $P(t)$ is the time evolution operator. If all the matrix elements $h_{ll'}$ are independent of time, $P = e^{-iHt}$. As the differential equation (5.13) shows, a Hamiltonian of the given structure only induces transitions to all other $c_{l'}$'s. Therefore, the requirement of

Eq. (5.7) is fulfilled. As a direct consequence, the annihilation operators will evolve into a superposition of all other $c_{l'}$'s in course of time where the probability amplitude for a transition $c_l \to c_{l'}$ after a time t is denoted by $\mathcal{G}_{ll'}(t)$:

$$T_P[c_l] = c_l(t) = \sum_{l'} \mathcal{G}_{ll'}(t)\, c_{l'}. \tag{5.14}$$

As a result of the previous considerations, the matrix $\mathcal{G}$ must be unitary [38]. Moreover, there is an explicit expression for this matrix in terms of Green's functions. Due to the fact that there is a scalar product on $\mathcal{D}$, one can expand any operator $\mathcal{O}$ in $\mathcal{D}$ in the basis of annihilation operators:

$$\mathcal{O} = \sum_{l} \left\langle \left\{ \mathcal{O}, c_l^\dagger \right\} \right\rangle c_l. \tag{5.15}$$

Consequently, up to a prefactor of $-i$ the matrix elements $\mathcal{G}_{ll'}(t)$ are the following single-particle Green's functions:

$$\mathcal{G}_{ll'}(t) = \theta(t) \left\langle \left\{ c_l(t), c_{l'}^\dagger \right\} \right\rangle. \tag{5.16}$$

Therefore, the time evolution of the annihilation operators is entirely given by the single particle Green's function where the transition matrix $\mathcal{G}$ is unitary:

$$\boxed{c_l(t) = \sum_{l'} \left\langle \left\{ c_l(t), c_{l'}^\dagger \right\} \right\rangle c_{l'} \qquad (5.17)}.$$

5.2 Green's functions of the resonant level model

Despite the complexity of the dynamics for time-dependent Hamiltonians, the periodic driving as it is considered in this thesis involves two time slices over a half period $\tau/2$ during which the Hamiltonian is constant, see Chapter (4). During the first half period the dynamics are governed by a resonant level model, during the second half period the dynamics are trivial, since the Hamiltonian describes the free time evolution of a noninteracting Fermi gas. As a consequence, the dynamics over one period under this periodic time-dependent Hamiltonian reduces to the time evolution of two subsequent time-independent Hamiltonians. In this section, the time evolution of the first half period will be analyzed. Due to Eq. (5.17) the dynamics of the single-particle operators in the first half period are completely determined by the Green's functions

$$G_{ll'}(t) = -i\theta(t) \left\langle \left\{ c_l(t), c_{l'}^\dagger \right\} \right\rangle, \qquad l, l' \in \{k, d\} \tag{5.18}$$

of the resonant level model:

$$H_{\mathrm{RLM}} = \sum_{k} k : c_k^\dagger c_k : + V \sum_{k} \left[d^\dagger c_k + c_k^\dagger d \right]. \tag{5.19}$$

The transition matrix elements $\mathcal{G}_{ll'}(t)$, see Eq. (5.16), are connected to the Green's functions through $\mathcal{G}_{ll'}(t) = iG_{ll'}(t)$. They can be determined by using the equations of motion approach that relates the derivative of $G_{ll'}(t)$ to the Heisenberg equations of motion for the single-particle operators:

$$\frac{\mathrm{d}}{\mathrm{d}t}G_{ll'}(t) = -i\delta(t)\left\langle\left\{c_l, c_{l'}^\dagger\right\}\right\rangle + \theta(t)\left\langle\left\{[H_{\mathrm{RLM}}, c_l](t), c_{l'}^\dagger\right\}\right\rangle$$
$$= -i\delta_{ll'}\delta(t) + \theta(t)\left\langle\left\{[H_{\mathrm{RLM}}, c_l](t), c_{l'}^\dagger\right\}\right\rangle. \tag{5.20}$$

Using the commutation relations

$$[H_{\mathrm{RLM}}, d] = -V\sum_k c_k, \qquad [H_{\mathrm{RLM}}, c_k] = -kc_k - Vd, \tag{5.21}$$

the equations of motion result in a complete set of coupled differential equations for all Green's functions

$$\frac{\mathrm{d}}{\mathrm{d}t}G_d(t) = -i\delta(t) - iV\sum_k G_{kd}(t)$$

$$\frac{\mathrm{d}}{\mathrm{d}t}G_{kd}(t) = -ikG_{kd}(t) - iVG_d(t)$$

$$\frac{\mathrm{d}}{\mathrm{d}t}G_{dk}(t) = -iV\sum_{k'} G_{k'k}(t) \tag{5.22}$$

$$\frac{\mathrm{d}}{\mathrm{d}t}G_{kk'}(t) = -i\delta_{kk'}\delta(t) - ikG_{kk'}(t) - iVG_{dk'}(t)$$

where the initial conditions that are necessary for the uniqueness of the solution are encoded in the Dirac-δ distributions. A δ-function on the right-hand side corresponds to an initial value of $-i$ whereas the absence corresponds to an initial value 0:

$$G_d(0) = G_{kk}(0) = -i,$$
$$G_{dk}(0) = G_{kd}(0) = G_{k\neq k'}(0) = 0. \tag{5.23}$$

This closed system of coupled differential equations can be solved using Laplace transformation:

$$G(\omega^+) = \int \mathrm{d}t\, e^{i\omega^+ t} G(t) \tag{5.24}$$

where $\omega^+ = \omega + i\varepsilon$. The positive parameter ε is needed to ensure that the Laplace transform exists, since it may be possible that without this additional exponential decay the integral does not converge. At the end of the calculation, however, when the back transformation to the time-dependent Green's functions has been made, one performs the limit $\varepsilon \to 0$. By using Laplace transforms the linear differential equations become algebraic:

i. $\quad \omega^+ G_d(\omega^+) = 1 + V\sum_k G_{kd}(\omega^+)$

ii. $\quad G_{kd}(\omega^+) = \dfrac{V}{\omega^+ - k}G_d(\omega^+)$

iii. $\quad \omega^+ G_{dk}(\omega^+) = V\sum_{k'} G_{k'k}(\omega^+)$ $\qquad\qquad (5.25)$

iv. $\quad G_{kk'}(\omega^+) = \dfrac{\delta_{kk'}}{\omega^+ - k} + \dfrac{V}{\omega^+ - k}G_{dk'}(\omega^+).$

Taking equation **iv**, interchanging k and k', and inserting it into **iii** leads to an algebraic equation for $G_{dk}(\omega^+)$:

$$\omega^+ G_{dk}(\omega^+) = \frac{V}{\omega^+ - k} + G_{dk}(\omega^+)V^2 \sum_{k'} \frac{1}{\omega^+ - k'}. \tag{5.26}$$

The sum appearing on the right hand side can be calculated exactly. Due to Eq. (3.89) the quasi momenta k of the modes c_k take the values $k_n = \frac{2\pi}{L}n$:

$$V^2 \sum_k \frac{1}{\omega^+ - k} = -\frac{V^2 L}{2\pi} \sum_{n=-\infty}^{\infty} \frac{1}{n - \frac{L\omega^+}{2\pi}} = -\frac{\Delta}{\pi} \frac{L\omega^+}{\pi} \sum_{n=1}^{\infty} \frac{1}{n^2 - \left[\frac{L\omega^+}{2\pi}\right]^2} + \frac{2\Delta}{L\omega^+}$$

$$= \Delta \cot\left[\frac{L}{2}\omega^+\right] \xrightarrow{L\to\infty} -i\Delta. \tag{5.27}$$

For this limit to be true it is essential that ω^+ is not purely real. This limit has to be performed at this point because otherwise the back transformation to the time-dependent Green's functions can not be done analytically since the integrals over the corresponding Laplace transforms are not known. Since finally the thermodynamic limit is always taken, the question is if one is allowed to interchange the limiting processes involved here. One can check that the equations of motion for the Green's functions obtained by taking the thermodynamic limit at this stage are fulfilled exponentially fast. Therefore, it is suitable to interchange the limiting processes at this point. Insertion of Eq. (5.27) into Eq. (5.26) solves the coupled system of equations for the function $G_{dk}(\omega^+)$:

$$G_{dk}(\omega^+) = \frac{V}{(\omega^+ - k)(\omega^+ + i\Delta)}. \tag{5.28}$$

With the result for $G_{dk}(\omega^+)$ the solution of $G_{kk'}(\omega^+)$ is easily obtained using Eq. **iv**. Analogously, the remaining functions can be found by inserting **ii** in **i**. Then by use of Eq. (5.27) one can calculate $G_d(\omega^+)$ which in turn enables to compute $G_{kd}(\omega^+)$. Finally, one obtains [16]:

$$\begin{aligned}
G_d(\omega^+) &= \frac{1}{\omega^+ + i\Delta}, \\
G_{dk}(\omega^+) &= \frac{V}{(\omega^+ - k)(\omega^+ + i\Delta)}, \\
G_{kd}(\omega^+) &= \frac{V}{(\omega^+ - k)(\omega^+ + i\Delta)}, \\
G_{kk'}(\omega^+) &= \frac{\delta_{kk'}}{\omega^+ - k} + \frac{V^2}{(\omega^+ - k)(\omega^+ + i\Delta)(\omega^+ - k')}.
\end{aligned} \tag{5.29}$$

The last equation determines the $\mathcal{T}$-matrix that is defined through the relation:

$$G(\omega^+) = G^{(0)}(\omega^+) + G^{(0)}(\omega^+)\mathcal{T}(\omega^+)G^{(0)}(\omega^+) \tag{5.30}$$

where the objects $G(\omega^+), G^{(0)}(\omega^+)$ and $\mathcal{T}(\omega^+)$ are to be understood as matrices with indices k, d. The quantity $G^{(0)}(\omega^+)$ is the unperturbed Green's function of the fermions without the presence of the resonant level. It is diagonal in quasi momentum representation:

$$G_{kk'}^{(0)}(\omega^+) = \frac{\delta_{kk'}}{\omega^+ - k}. \tag{5.31}$$

As a consequence, the $\mathcal{T}$-matrix is independent of the quasi momenta. The origin of this property lies in the structure of the resonant level Hamiltonian. The interaction is pointlike such that the hopping element V itself is independent of k. Due to Eq. (5.17) the $\mathcal{T}$-matrix is given by the following expression:

$$\mathcal{T}_{kk'}(\omega^+) = \mathcal{T}(\omega^+) = \frac{V^2}{\omega^+ + i\Delta}. \tag{5.32}$$

The knowledge of the $\mathcal{T}$-matrix enables the evaluation of the scattering matrix $S(\varepsilon)$ by use of the relation [38]

$$S(\varepsilon) = 1 - 2\pi i \rho(\varepsilon)\mathcal{T}(\epsilon) = \frac{\varepsilon - i\Delta}{\varepsilon + i\Delta} \tag{5.33}$$

where $\rho(\varepsilon) = L/(2\pi)$ is the density of states of the fermions at energy ε that is constant due to the linear spectrum. An important quantity that is related to the S-matrix, is the phase shift $\delta(\varepsilon)$ of a fermion of energy ε that is scattered off the impurity. The phase shifts can be obtained by taking the logarithm of the S-matrix [38]:

$$S(\varepsilon) = e^{2i\delta(\varepsilon)}. \tag{5.34}$$

Therefore, the phase shift at the Fermi energy $\varepsilon_F = 0$ takes the value:

$$\delta(0) = \frac{\pi}{2}. \tag{5.35}$$

This is consistent with the Friedel sum rule, see [16] for example, which states that the phase shift at the Fermi energy divided over π is equal to the screening charge. The screening charge is the amount of charge that is displaced in the bath of fermions by the introduction of the local scatterer. In the resonant level model, the local level will be occupied with a probability $1/2$. Therefore, the bath fermions have to screen an amount of charge of $1/2$ consistent with the above calculation.

The Green's functions in the time domain can be obtained by performing the inverse Laplace transformation:

$$G(t) = \lim_{\varepsilon \to 0} \frac{1}{2\pi} \int_{-\infty}^{\infty} \mathrm{d}\omega e^{-i\omega^+ t} G(\omega^+) \tag{5.36}$$

where it is important to perform the limit $\varepsilon \to 0$ after integration. For the calculation of these integrals one can use the residue theorem yielding:

$$G_d(t) = -ie^{-\Delta t},$$

$$G_{dk}(t) = -i\frac{V}{k + i\Delta}\left[e^{-ikt} - e^{-\Delta t}\right],$$

$$G_{kd}(t) = -i\frac{V}{k + i\Delta}\left[e^{-ikt} - e^{-\Delta t}\right],$$

$$G_{kk'}(t) = -i\delta_{k,k'}e^{-ikt} - iV^2\left[\frac{e^{-ikt}}{(k - k')(k + i\Delta)} + \frac{e^{-\Delta t}}{(k + i\Delta)(k' + i\Delta)} + \frac{e^{-ik't}}{(k' - k)(k' + i\Delta)}\right]. \tag{5.37}$$

Consequently, the transition matrix $\mathcal{G}$ for the resonant level model reads as:

$$\mathcal{G}_d(t) = e^{-\Delta t} \tag{5.38}$$

$$\mathcal{G}_{dk}(t) = \frac{V}{k + i\Delta} \left[e^{-ikt} - e^{-\Delta t} \right] \tag{5.39}$$

$$\mathcal{G}_{kd}(t) = \frac{V}{k + i\Delta} \left[e^{-ikt} - e^{-\Delta t} \right] \tag{5.40}$$

$$\mathcal{G}_{kk'}(t) = \delta_{k,k'} e^{-ikt} + V^2 \left[\frac{e^{-ikt}}{(k - k')(k + i\Delta)} + \frac{e^{-\Delta t}}{(k + i\Delta)(k' + i\Delta)} + \frac{e^{-ik't}}{(k' - k)(k' + i\Delta)} \right] \tag{5.41}$$

The transition matrix $\mathcal{G}$ carries the information of how the scattering states $c_l^\dagger |\rangle$, $l = (k, d)$, behave in time where $|\rangle$ is the true vacuum, see for example [6]:

$$e^{-iHt} c_l^\dagger |\rangle = \sum_{l'} \mathcal{G}_{ll'}(t) \, c_{l'}^\dagger |\rangle, \qquad l = k, d. \tag{5.42}$$

In other words, $\mathcal{G}$ states how a single fermion would behave without the presence of the Fermi sea. The functions in Eq. (5.38) and Eq. (5.39), for example, reveal that a fermion on the local level fully decays into bath fermions after an exponentially short time where the time scale is given by the Kondo scale $1/\Delta \propto 1/T_K$, see Eq. (3.99). The probability $\mathcal{P}_k(t)$ to find the fermion in the bath state k is independent of time for $t \gg 1/\Delta$ where the shape of the probability distribution is a Lorentzian of width Δ, see Fig. (5.1). In the continuum limit, $\mathcal{P}_k(t \gg 1/T_K)$ is given by:

$$\mathcal{P}_k(t \gg 1/T_K) = |\mathcal{G}_{dk}(t \gg 1/T_K)|^2 = \frac{\Delta}{\pi} \frac{1}{k^2 + \Delta^2} \tag{5.43}$$

Since the local state is exactly located at the Fermi level $\varepsilon = 0$, the probability distribution $\mathcal{P}_k$ is centered around $k = 0$. Moreover, it is symmetric because of the particle-hole symmetry of the Hamiltonian in the case of a linearized spectrum. The probability for the inverse process, where a fermion in state $c_k^\dagger |\rangle$ hops onto the resonant level, has to be equal to $\mathcal{P}_k$ due to time reversal symmetry.

The presence of the local level induces transitions of a scattering state $c_k^\dagger |\rangle$ into all other states $c_{k'}^\dagger |\rangle$ in course of time as a result of two subsequent processes. First, the fermion in state k hops onto the resonant level. After some time, it will decay into some bath state k' that may be different from the initial state k. In contrast to $\mathcal{P}_k$, the probability for transitions from $c_k^\dagger |\rangle$ to $c_{k'}^\dagger |\rangle$ oscillates for all times and does not relax.
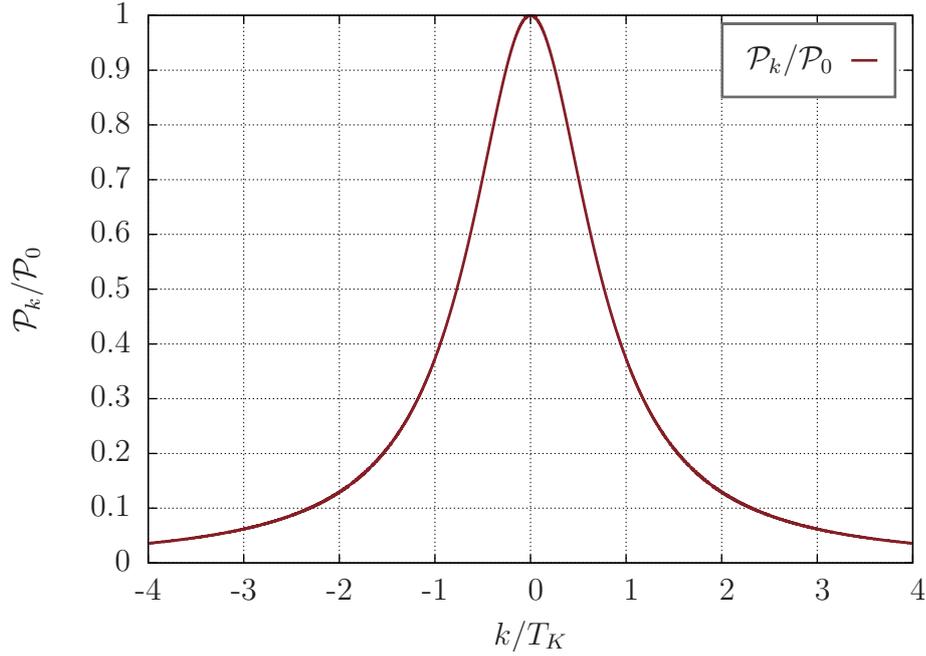
Figure 5.1: Probability $\mathcal{P}_k$ for the scattering state $d^\dagger|\rangle$ to decay into a bath scattering state $c_k^\dagger|\rangle$ after time $t \gg 1/T_K$ in the resonant level model

5.3 Period matrix $\mathcal{M}$

Despite the difficulty of time evolution due to a time-dependent Hamilton operator, the symmetry of the Hamiltonian $H(t+\tau) = H(t)$ can be exploited for the description of the time development of the single-particle operators. The periodicity leads to a separation of time scales, the time evolution over multiple periods and the time evolution within one, see Sec. (4.2). As mentioned in the section before, the time evolution over one period τ is given by the subsequent application of two time-independent Hamiltonians. Firstly, a resonant level Hamiltonian and, secondly, the free Hamiltonian of a gas of noninteracting fermions. In the Schrödinger picture an initial state $|\Psi\rangle$ evolves into the state

$$|\Psi(\tau)\rangle = e^{-iH_0\tau/2} e^{-iH_{\mathrm{RLM}}\tau/2}|\Psi\rangle \tag{5.44}$$

after one period τ. Accordingly, in the Heisenberg picture an operator $\mathcal{O}$ transforms in time in the following way:

$$\mathcal{O}(\tau) = e^{iH_{\mathrm{RLM}}\tau/2} e^{iH_0\tau/2} \mathcal{O} e^{-iH_0\tau/2} e^{-iH_{\mathrm{RLM}}\tau/2}. \tag{5.45}$$

Remarkably, the order of application of the two time evolution operators changes in the Heisenberg picture. At first, the operators are evolved according to the Hamiltonian that acts at last.

For the free Hamiltonian $H_0 = \sum_k k : c_k^\dagger c_k :$ the transition matrix $\mathcal{G}^{(0)}$ for the single-particle operators is diagonal:

$$\mathcal{G}_{kk'}^{(0)}(t) = \delta_{kk'} e^{-ikt}, \qquad \mathcal{G}_{dd}^{(0)} = 1, \qquad \mathcal{G}_{dk}^{(0)} = \mathcal{G}_{kd}^{(0)} = 0. \tag{5.46}$$

According to Eq. (5.45), the transition matrix $\mathcal{M}$ over one period is obtained by a successive application of $\mathcal{G}^{(0)}(\tau/2)$ and the transition matrix $\mathcal{G}(\tau/2)$ of the resonant level model (5.41):

$$\mathcal{M} = \mathcal{G}\left(\frac{\tau}{2}\right)\mathcal{G}^{(0)}\left(\frac{\tau}{2}\right), \qquad c_l(\tau) = \sum_{l'} \mathcal{M}_{ll'} c_{l'}. \qquad (5.47)$$

The operators are first evolved according to the free Hamiltonian followed by the resonant level model. The matrix $\mathcal{M}$ will be called period matrix from now on. Using the results for $\mathcal{G}$ and $\mathcal{G}^{(0)}$, the matrix elements of the period matrix can be obtained by matrix multiplication:

$$\mathcal{M}_d = e^{-\Delta\frac{\tau}{2}} \qquad (5.48)$$

$$\mathcal{M}_{dk} = \frac{V}{k+i\Delta}\left[e^{-ik\frac{\tau}{2}} - e^{-\Delta\frac{\tau}{2}}\right] \qquad (5.49)$$

$$\mathcal{M}_{kd} = \frac{V}{k+i\Delta}e^{-ik\frac{\tau}{2}}\left[e^{-ik\frac{\tau}{2}} - e^{-\Delta\frac{\tau}{2}}\right] \qquad (5.50)$$

$$\mathcal{M}_{kk'} = \delta_{k,k'}e^{-ik\tau} + V^2 e^{-ik\frac{\tau}{2}}\left[\frac{e^{-ik\frac{\tau}{2}}}{(k-k')(k+i\Delta)} + \frac{e^{-\Delta\frac{\tau}{2}}}{(k+i\Delta)(k'+i\Delta)} + \frac{e^{-ik'\frac{\tau}{2}}}{(k'-k)(k'+i\Delta)}\right] \qquad (5.51)$$

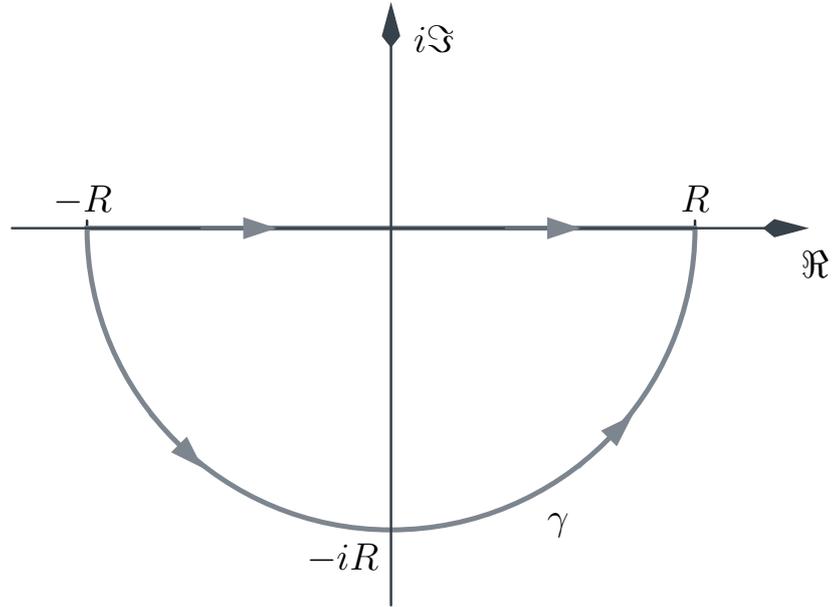## 5.4 Powers of the period matrix

For the long-time behavior of the system all operators have to be evolved over multiple periods. This corresponds to a successive application of the period matrix $\mathcal{M}$ onto the single-particle annihilation operators:

$$c_l(N\tau) = \sum_{l'}\left(\mathcal{M}^N\right)_{ll'} c_{l'}, \qquad (5.52)$$

thereby reducing the problem of long-time evolution to a matrix multiplication problem. The long-time behavior of the annihilation operators is completely determined by the matrix elements of powers of the period matrix $\mathcal{M}$ that will be denoted in the following way:

$$\mathcal{M}_{ll'}^{(N)} := \left(\mathcal{M}^N\right)_{ll'}. \qquad (5.53)$$

In general, the computation of the matrix elements of any power of some matrix can be an arbitrarily difficult task. The matrix $\mathcal{M}$, however, displays nice properties that make the calculation feasible. No element of $\mathcal{M}$ exhibits a pole in the complex plane and the

Figure 5.2: Contour γ

exponentials e^{-ikt} are such that one can always choose integration contours in the lower half plane. Application of the residue theorem then shows that most of the terms do not contribute. The goal will be to derive recursion formulas for the elements $\mathcal{M}_{ll'}^{(N)}$ by a proper splitting of the sums that appear in a matrix multiplication of multiple period matrices $\mathcal{M}$.

5.4.1 Preliminary calculations

As indicated before, the derivation of the matrix elements is based on elementary properties of the period matrix $\mathcal{M}$. Most importantly, there is no matrix element that exhibits a pole in the complex plane. As a consequence, a lot of sums will vanish.

A sum that will appear later is the following:

$$\sum_k \mathcal{M}_{dk}\mathcal{M}_{kd}e^{-i\lambda k\tau} \overset{L \to \infty}{=} \frac{\Delta}{\pi}\int_{-\infty}^{\infty} \mathrm{d}k\, e^{-ik[\lambda+1/2]\tau}\frac{e^{-ik\tau/2}-e^{-\Delta\tau/2}}{k+i\Delta}\frac{e^{-ik\tau/2}-e^{-\Delta\tau/2}}{k+i\Delta}$$

(5.54)

where λ is an arbitrary positive integer. Since the integrand exhibits no pole in the complex plane, the integration contour can be deformed in an arbitrary fashion into the lower complex plane [19], as is indicated in Fig. (5.2). The path γ of the integration contour can be chosen to be:

$$\gamma(s) = -Re^{i\pi s} \qquad s \in [0,1]$$

(5.55)

where the limit $R \to \infty$ is to be taken in the end, since only in this case the integration

over γ is equal to the integration of k over the whole real axis:

$$
\sum_k \mathcal{M}_{dk}\mathcal{M}_{kd}e^{-i\lambda k\tau} = \lim_{R\to\infty} \frac{\Delta}{\pi} \int_0^1 ds \left[-i\pi Re^{i\pi s} \right] e^{iR\cos(\pi s)[\lambda+1/2]\tau - R\sin(\pi s)[\lambda+1/2]\tau} \times
$$

$$
\times \frac{e^{iR\cos(\pi s)\tau/2 - R\sin(\pi s)\tau/2} - e^{-\Delta\tau/2}}{-Re^{i\pi s} + i\Delta} \frac{e^{iR\cos(\pi s)\tau/2 - R\sin(\pi s)\tau/2} - e^{-\Delta\tau/2}}{-Re^{i\pi s} + i\Delta}.
$$

$$\tag{5.56}$$

Since the integrand is at least of the order $1/R$, the integral vanishes in the limit $R \to \infty$:

$$
\sum_k \mathcal{M}_{dk}\mathcal{M}_{kd}e^{-i\lambda k\tau} = 0. \tag{5.57}
$$

As already mentioned, the first index of the period matrix $\mathcal{M}$ marks the initial and the second index the final scattering state in a single particle picture. Therefore, $\mathcal{M}_{dk}$ is for the probability amplitude for a scattering state $d^\dagger|\rangle$ to evolve into $c_k^\dagger|\rangle$ after one period τ. The total probability amplitude for a fermion to stay on the local level after two periods is given by:

$$
\mathcal{M}_{dd}^{(2)} = \mathcal{M}_{dd}\mathcal{M}_{dd} + \sum_k \mathcal{M}_{dk}\mathcal{M}_{kd}. \tag{5.58}
$$

Consequently, the second part of this expression gives the total contribution of all processes where the fermion has hopped into any bath state k after one period and hops back onto the local level a period later. Due to Eq. (5.57), this term vanishes. Therefore, the decay of the local fermion is not influenced by processes that include transitions $d \to k \to d$. Furthermore, the intermediate time evolution of the bath states $c_k^\dagger|\rangle$ due to a free Hamiltonian is irrelevant for the decay. This will be of great importance in the evaluation of correlation functions in the next chapter.

To tackle sums involving $\mathcal{M}_{kk'}$ it is suitable to separate two parts:

$$
\mathcal{M}_{kk'} = \delta_{kk'}e^{-ik\tau} + \mathcal{L}_{kk'},
$$

$$
\mathcal{L}_{kk'} = V^2 e^{-ik\tau/2} \left[\frac{e^{-ik\tau/2}}{(k-k')(k+i\Delta)} + \frac{e^{-\Delta\tau/2}}{(k+i\Delta)(k'+i\Delta)} + \frac{e^{-ik'\tau/2}}{(k'-k)(k'+i\Delta)} \right]. \tag{5.59}
$$

Based on this separation, the evaluation of the sum

$$
\sum_{k'} \mathcal{M}_{dk'}\mathcal{M}_{k'k}e^{-i\lambda k'\tau} = \mathcal{M}_{dk}e^{-i[\lambda+1]k\tau} + \sum_{k'} \mathcal{M}_{dk'}\mathcal{L}_{k'k}e^{-i\lambda k'\tau} \tag{5.60}
$$

reduces to the evaluation of $\sum_{k'} \mathcal{M}_{dk'}\mathcal{L}_{k'k}$ that can be done using a deformed integration contour as before:

$$
\sum_{k'} \mathcal{M}_{dk'}\mathcal{L}_{k'k}e^{-i\lambda k'\tau} \stackrel{L\to\infty}{=} V\frac{\Delta}{\pi} \int dk' \, e^{-i[\lambda+1/2]k'\tau} \frac{e^{-ik'\tau/2} - e^{-\Delta\tau/2}}{k'+i\Delta} \times
$$

$$
\times \left[\frac{e^{-ik\tau/2}}{(k-k')(k+i\Delta)} + \frac{e^{-\Delta\tau/2}}{(k+i\Delta)(k'+i\Delta)} + \frac{e^{-ik'\tau/2}}{(k'-k)(k'+i\Delta)} \right]
$$

$$\tag{5.61}$$

Again, $\mathcal{L}$ has no poles in the complex plain such that the integration contour can be deformed to match γ, see Eq. (5.55), as in the previous case. Analogously, performing

the limit $R \to \infty$ the integral above vanishes such that:

$$\sum_{k'} \mathcal{M}_{dk'} \mathcal{M}_{k'k} e^{-i\lambda k'\tau} = \mathcal{M}_{dk} e^{-i[\lambda+1]k\tau}.$$ (5.62)

The case where the order of k and d is interchanged as well as the case where the summands are $\mathcal{M}_{k\bar{k}}$ and $\mathcal{M}_{\bar{k}k'}$ can be calculated straightforwardly:

$$\sum_{\bar{k}} \mathcal{M}_{k\bar{k}} \mathcal{M}_{\bar{k}k'} e^{-i\lambda\bar{k}\tau} = \sum_{\bar{k}} \left[\delta_{k\bar{k}} e^{-ik\tau} + \mathcal{L}_{k\bar{k}} \right] \left[\delta_{\bar{k}k'} e^{-ik'\tau} + \mathcal{L}_{\bar{k}k'} \right] e^{-i\lambda\bar{k}\tau}$$

$$= \delta_{kk'} e^{-i[\lambda+2]\tau} + \mathcal{L}_{kk'} \left[e^{-ik\tau} + e^{-ik'\tau} \right] e^{-i\lambda\tau} + \sum_{\bar{k}} \mathcal{L}_{k\bar{k}} \mathcal{L}_{\bar{k}k'} e^{-i\lambda\bar{k}\tau}.$$ (5.63)

The sum on the right hand side will vanish since the corresponding integrands do not have poles in the complex plane such that the integration contour γ as in Eq. (5.55) can be used as before. Concluding, the elementary property that the Green's functions do not have any poles made the evaluation of the sums above very simple.

$$\sum_{k} \mathcal{M}_{dk} \mathcal{M}_{kd} e^{-i\lambda k\tau} = 0$$ (5.64)

$$\sum_{k'} \mathcal{M}_{kk'} \mathcal{M}_{k'd} e^{-i\lambda k'\tau} = \mathcal{M}_{kd} e^{-i[\lambda+1]k\tau}$$ (5.65)

$$\sum_{k'} \mathcal{M}_{dk'} \mathcal{M}_{k'k} e^{-i\lambda k'\tau} = \mathcal{M}_{dk} e^{-i[\lambda+1]k\tau}$$ (5.66)

$$\sum_{k"} \mathcal{M}_{kk"} \mathcal{M}_{k"k'} e^{-i\lambda k"\tau} = \delta_{kk'} e^{-i[\lambda+2]k\tau} + \mathcal{L}_{kk'} \left[e^{-i[\lambda+1]k\tau} + e^{-i[\lambda+1]k'\tau} \right]$$ (5.67)

5.4.2 The matrix element $\mathcal{M}_{dd}^{(N)}$

Based on these preliminary calculations the evaluation of powers of the period matrix $\mathcal{M}$ is straightforward. The matrix element that is most easily derived is $\mathcal{M}_{dd}^{(N)}$. Using its definition, see Eq. (5.53), $\mathcal{M}_{dd}^{(N)}$ can be written as a matrix product:

$$\mathcal{M}_{dd}^{(N)} = \sum_{l_1,\dots,l_{N-1}} \mathcal{M}_{dl_1} \mathcal{M}_{l_1 l_2} \dots \mathcal{M}_{l_{N-1}d}$$ (5.68)

where the sums run over all intermediate indices such that for each $l_i = k_i, d$. The sums in this expression can be splitted such that one obtains:

$$
\begin{aligned}
\mathcal{M}_{dd}^{(N)} &= \sum_{l_1,\dots,l_{N-2}} \mathcal{M}_{dl_1}\dots\mathcal{M}_{l_{N-2}d}\mathcal{M}_{dd} + \sum_{l_1,\dots,l_{N-2},k_{N-1}} \mathcal{M}_{dl_1}\dots\mathcal{M}_{l_{N-2}k_{N-1}}\mathcal{M}_{k_{N-1}d} = \\
&= \mathcal{M}_{dd}^{(N-1)}\mathcal{M}_{dd} + \sum_{l_1,\dots,l_{N-3},k_{N-1}} \mathcal{M}_{dl_1}\dots\mathcal{M}_{l_{N-2}d}\mathcal{M}_{dk_{N-1}}\mathcal{M}_{k_{N-1}d} + \\
&\quad + \sum_{l_1,\dots,l_{N-3},k_{N-2},k_{N-1}} \mathcal{M}_{dl_1}\dots\mathcal{M}_{l_{N-3}k_{N-2}}\mathcal{M}_{k_{N-2}k_{N-1}}\mathcal{M}_{k_{N-1}d}.
\end{aligned}
$$

(5.69)

Using Eq. (5.64) the second term in the expression above cancels and one arrives at:

$$
\mathcal{M}_{dd}^{(N)} = \mathcal{M}_{dd}^{(N-1)}e^{-\Delta\tau/2} + \sum_{l_1,\dots,l_{N-3},k_{N-2}} \mathcal{M}_{dl_1}\dots\mathcal{M}_{l_{N-3}k_{N-2}}\mathcal{M}_{k_{N-2}d}e^{-ik_{N-2}\tau}. \quad (5.70)
$$

Again, if $l_{N-3} = d$, the sum over k_{N-2} vanishes as before. As a consequence, only the sum over k_{N-3} remains and a summation over k_{N-2} produces another phase factor according to Eq. (5.65):

$$
\mathcal{M}_{dd}^{(N)} = \mathcal{M}_{dd}^{(N-1)}e^{-\Delta\tau/2} + \sum_{l_1,\dots,l_{N-4},k_{N_3}} \mathcal{M}_{dl_1}\dots\mathcal{M}_{l_{N-4}k_{N-3}}\mathcal{M}_{k_{N-3}d}e^{-i2k_{N-3}\tau}. \quad (5.71)
$$

A successive application of this procedure leads to:

$$
\mathcal{M}_{dd}^{(N)} = \mathcal{M}_{dd}^{(N-1)}e^{-\Delta\tau/2} + \sum_{k_1}\mathcal{M}_{dk_1}\mathcal{M}_{k_1 d}e^{-i[N-2]k_1\tau} = \mathcal{M}_{dd}^{(N-1)}e^{-\Delta\tau/2}. \quad (5.72)
$$

This recursive formula for the sequence $\mathcal{M}_{dd}^{(N)}$ can be solved directly yielding:

$$
\mathcal{M}_{dd}^{(N)} = e^{-N\Delta\tau/2}. \quad (5.73)
$$

In comparison with Eq. (5.17) the matrix element $\mathcal{M}_{dd}^{(N)}$ is connected to a retarded Green's function

$$
\mathcal{M}_{dd}^{(N)} = \mathcal{G}_d(N\tau) = \left\langle \left\{ d(N\tau), d^\dagger \right\} \right\rangle. \quad (5.74)
$$

This Green's function has already been analyzed in the work by Langreth and Nordlander [24] for an arbitrary time dependence of the hopping amplitude V in a resonant level model by solving the corresponding Dyson equations resulting in:

$$
\mathcal{G}_d(N\tau) = e^{-\int_0^{N\tau} d\bar{t},\,\Delta(\bar{t})} = e^{-\Delta N\tau/2} \qquad \Delta(t) = \frac{L}{2}V^2(t) \quad (5.75)
$$

consistent with the calculation above.

5.4.3 The matrix elements $\mathcal{M}_{kd}^{(N)}$ and $\mathcal{M}_{dk}^{(N)}$

The evaluation of $\mathcal{M}_{kd}^{(N)}$ differs from that of $\mathcal{M}_{dd}^{(N)}$ only in one of the last steps. Until Eq. (5.72) the derivation can be simply adopted such that one obtains:

$$
\mathcal{M}_{kd}^{(N)} = \mathcal{M}_{kd}^{(N-1)}\mathcal{M}_{dd} + \sum_{k_1}\mathcal{M}_{kk_1}\mathcal{M}_{k_1 d}e^{-i[N-2]k'\tau} = \mathcal{M}_{kd}^{(N-1)}\mathcal{M}_{dd} + \mathcal{M}_{kd}e^{-i[N-1]k\tau}.
$$

(5.76)

This recursive formula is solved by a geometric series that can be summed up to give:

$$\mathcal{M}_{kd}^{(N)} = \mathcal{M}_{kd} \frac{e^{-iNk\tau} - e^{-N\Delta\tau/2}}{e^{-ik\tau} - e^{-\Delta\tau/2}}. \tag{5.77}$$

The matrix element $\mathcal{M}_{dk}^{(N)}$ can be derived in the same way by splitting the sums from the left hand side:

$$\begin{aligned}
\mathcal{M}_{dk}^{(N)} = \mathcal{M}_{dd} \sum_{l_2,\ldots,l_{N-1}} \mathcal{M}_{dl_2} \ldots \mathcal{M}_{l_{N-1}k} + \sum_{k_1,l_2,\ldots,l_{N-1}} \mathcal{M}_{dk_1} \mathcal{M}_{k_1,l_2} \ldots \mathcal{M}_{l_{N-1}k} = \\
= \mathcal{M}_{dd} \mathcal{M}_{dk}^{(N-1)} + \sum_{k_1,l_3,\ldots,l_{N-1}} \mathcal{M}_{dk_1} \mathcal{M}_{k_1 d} \mathcal{M}_{dl_3} \ldots \mathcal{M}_{l_{N-1}k} + \\
+ \sum_{k_1,k_2,l_3,\ldots,l_{N-1}} \mathcal{M}_{dk_1} \mathcal{M}_{k_1 k_2} \mathcal{M}_{k_2 l_3} \ldots \mathcal{M}_{l_{N-1}k}.
\end{aligned} \tag{5.78}$$

By use of Eq. (5.64) and Eq. (5.66) one arrives at a recursive formula of the same type as for $\mathcal{M}_{kd}^{(N)}$:

$$\mathcal{M}_{dk}^{(N)} = \mathcal{M}_{dd} \mathcal{M}_{dk}^{(N-1)} + \mathcal{M}_{dk} e^{-i[N-1]k\tau}. \tag{5.79}$$

The solution of this relation is determined by a geometric series resulting in:

$$\mathcal{M}_{dk}^{(N)} = \mathcal{M}_{dk} \frac{e^{-iNk\tau} - e^{-N\Delta\tau/2}}{e^{-ik\tau} - e^{-\Delta\tau/2}}. \tag{5.80}$$

5.4.4 The matrix element $\mathcal{M}_{kk'}^{(N)}$

As before, the evaluation of $\mathcal{M}_{kk'}^{(N)}$ starts with a proper splitting of sums:

$$\begin{aligned}
\mathcal{M}_{kk'}^{(N)} = \mathcal{M}_{kd} \sum_{l_2,\ldots,l_{N-1}} \mathcal{M}_{dl_2} \ldots \mathcal{M}_{l_{N-1}k'} + \sum_{k_1,l_2,\ldots,l_{N-1}} \mathcal{M}_{kk_1} \mathcal{M}_{k_1 l_2} \ldots \mathcal{M}_{l_{N-1}k'} \\
= \mathcal{M}_{kd} \mathcal{M}_{dk'}^{(N-1)} + \sum_{k_1,l_3,\ldots,l_{N-1}} \mathcal{M}_{kk_1} \mathcal{M}_{k_1 d} \mathcal{M}_{dl_3} \ldots \mathcal{M}_{l_{N-1}k'} \\
+ \sum_{k_1,k_2,l_3,\ldots,l_{N-1}} \mathcal{M}_{kk_1} \mathcal{M}_{k_1 k_2} \mathcal{M}_{k_2 l_3} \ldots \mathcal{M}_{l_{N-1}k'} \\
= \mathcal{M}_{kd} \mathcal{M}_{dk'}^{(N-1)} + e^{-ik\tau} \mathcal{M}_{kd} \mathcal{M}_{dk'}^{(N-2)} + \sum_{k_1,k_2,l_3,\ldots,l_{N-1}} \mathcal{M}_{kk_1} \mathcal{M}_{k_1 k_2} \mathcal{M}_{k_2 l_3} \ldots \mathcal{M}_{l_{N-1}k'}.
\end{aligned} \tag{5.81}$$

Continuing the procedure of evaluating the contributions where an index d appears leads to:

$$\mathcal{M}_{kk'}^{(N)} = \sum_{j=1}^{N-1} \mathcal{M}_{kd} \mathcal{M}_{dk'}^{(N-j)} e^{-i[j-1]k\tau} + \sum_{k_1,\ldots,k_{N-1}} \mathcal{M}_{kk_1} \ldots \mathcal{M}_{k_{N-1}k'}. \tag{5.82}$$

The first part can be summed up after insertion of the expression for $\mathcal{M}_{dk'}^{(N-j)}$, see Eq. (5.80), by use of the formula for the geometric series:

$$
\sum_{j=1}^{N-1} \mathcal{M}_{dk'}^{(N-j)} e^{-i[j-1]k\tau} =
$$

$$
= \frac{\mathcal{M}_{dk'} e^{ik\tau}}{e^{-ik'\tau} - e^{-\Delta\tau/2}} \sum_{j=1}^{N-1} \left[e^{-i[N-j]k'\tau} e^{-ijk\tau} - e^{-[N-j]\Delta\tau/2} e^{-ijk\tau} \right]
$$

$$
= \frac{\mathcal{M}_{dk'} e^{ik\tau}}{e^{-ik'\tau} - e^{-\Delta\tau/2}} \left[e^{-iNk'\tau} \frac{e^{-i[k-k']\tau} - e^{-iN[k-k']\tau}}{1 - e^{-i[k-k']\tau}} - \right.
$$

$$
\left. - e^{-N\Delta\tau/2} \frac{e^{-ik\tau} e^{\Delta\tau/2} - e^{-iNk\tau} e^{N\Delta\tau/2}}{1 - e^{-ik\tau} e^{\Delta\tau/2}} \right]
\tag{5.83}
$$

$$
= \mathcal{M}_{dk'} \left[\frac{e^{-iNk\tau}}{\left[e^{-ik\tau} - e^{-ik'\tau} \right] \left[e^{-ik\tau} - e^{-\Delta\tau/2} \right]} + \right.
$$

$$
+ \frac{e^{-N\Delta\tau/2}}{\left[e^{-ik\tau} - e^{-\Delta\tau/2} \right] \left[e^{-ik'\tau} - e^{-\Delta\tau/2} \right]}
$$

$$
\left. + \frac{e^{-iNk'\tau}}{\left[e^{-ik'\tau} - e^{-ik\tau} \right] \left[e^{-ik'\tau} - e^{-\Delta\tau/2} \right]} \right].
$$

The matrix $\mathcal{K}$: The second term in Eq. (5.82) can be evaluated by constructing a proper recursion formula. At this point it is suitable to define another object $\mathcal{K}^{(N)}$ as:

$$
\mathcal{K}_{kk'}^{(N)} = \sum_{k_1,\ldots,k_{N-1}} \mathcal{M}_{kk_1} \ldots \mathcal{M}_{k_{N-1}k'}.
\tag{5.84}
$$

By applying Eq. (5.67) to the sum over k_{N-1} one arrives at:

$$
\mathcal{K}_{kk'}^{(N)} = \sum_{k_1,\ldots,k_{N-2}} \mathcal{M}_{kk_1} \ldots \mathcal{M}_{k_{N-3}k_{N-2}} \left[\delta_{k_{N-2}k'} e^{-i2k'\tau} + \mathcal{L}_{k_{N-2}k'} \left(e^{-ik_{N-2}\tau} + e^{-ik'\tau} \right) \right].
\tag{5.85}
$$

The matrix element $\mathcal{L}_{k_{N-2}k'}$ can be rewritten in terms of the period matrix due to Eq. (5.59), $\mathcal{L}_{k_{N-2}k'} = \mathcal{M}_{k_{N-2}k'} - \delta_{k_{N-2}k'} e^{-ik'\tau}$:

$$
\mathcal{K}_{kk'}^{(N)} = \sum_{k_1,\ldots,k_{N-2}} \mathcal{M}_{kk_1} \ldots \mathcal{M}_{k_{N-3}k_{N-2}} \left[\mathcal{M}_{k_{N-2}k'} \left(e^{-ik_{N-2}\tau} + e^{-ik'\tau} \right) - \delta_{k_{N-2}k'} e^{-i[k_{N-2}+k']\tau} \right]
$$

$$
= \mathcal{K}_{kk'}^{(N-1)} e^{-ik'\tau} - \mathcal{K}_{kk'}^{(N-2)} e^{-i2k'\tau} + \sum_{\overline{k}} \mathcal{K}_{k\overline{k}}^{(N-2)} \mathcal{M}_{\overline{k}k'} e^{-i\overline{k}\tau}.
\tag{5.86}
$$

This recursion formula can be solved in an unusual way by considering the following sequence of expressions:

$$
\mathcal{K}_{kk'}^{(N)} = \mathcal{K}_{kk'}^{(N-1)} e^{-ik'\tau} - \mathcal{K}_{kk'}^{(N-l)} e^{-ilk'\tau} + \sum_{\overline{k}} \mathcal{K}_{k\overline{k}}^{(N-l)} \mathcal{M}_{\overline{k}k'} e^{-i[l-1]\overline{k}\tau}
\tag{5.87}
$$

where $l = 2, \ldots, N - 1$. For $l = 2$ this formula is true as it reproduces the derived expression. As will be shown by induction this formula is true for all l. Assuming validity for l, that is true for $l = 2$, validity for $l + 1$ is also given:

$$
\begin{aligned}
\mathcal{K}_{kk'}^{(N)} &= \mathcal{K}_{kk'}^{(N-1)} e^{-ik'\tau} - \mathcal{K}_{kk'}^{(N-l)} e^{-ilk'\tau} + \sum_{\overline{k}} \mathcal{K}_{k\overline{k}}^{(N-l)} \mathcal{M}_{\overline{k}k'} e^{i[l-1]\overline{k}\tau} \\
&= \mathcal{K}_{kk'}^{(N-1)} e^{-ik'\tau} - \mathcal{K}_{kk'}^{(N-l)} e^{-ilk'\tau} + \sum_{\overline{k}\,\overline{k}'} \mathcal{K}_{k\overline{k}'}^{(N-l-1)} \mathcal{M}_{\overline{k}'\,\overline{k}} \mathcal{M}_{\overline{k}k'} e^{-i[l-1]\overline{k}\tau}.
\end{aligned}
\tag{5.88}
$$

The summation over $\overline{k}$ can be carried out by use of Eq. (5.67). According to the previous considerations, $\mathcal{L}$ can be rewritten in terms of the period matrix $\mathcal{M}$ such that one arrives at the desired expression:

$$
\mathcal{K}_{kk'}^{(N)} = \mathcal{K}_{kk'}^{(N-1)} e^{-ik'\tau} - \mathcal{K}_{kk'}^{(N-l-1)} e^{-i[l+1]k'\tau} + \sum_{\overline{k}} \mathcal{K}_{k\overline{k}}^{(N-l-1)} \mathcal{M}_{\overline{k}k'} e^{-il\overline{k}\tau}.
\tag{5.89}
$$

Consequently, insertion of $l = N - 1$ into this formula leads to the recursion formula that allows to determine $\mathcal{K}$ by noting that $\mathcal{K}^{(1)} = \mathcal{M}$:

$$
\begin{aligned}
\mathcal{K}_{kk'}^{(N)} &= \mathcal{K}_{kk'}^{(N-1)} e^{-ik'\tau} - \mathcal{M}_{kk'} e^{-i[N-1]k'\tau} + \sum_{\overline{k}} \mathcal{M}_{k\overline{k}} \mathcal{M}_{\overline{k}k'} e^{-i[N-2]\overline{k}\tau} \\
&= \mathcal{K}_{kk'}^{(N-1)} e^{-ik'\tau} + e^{-i[N-1]k\tau} \mathcal{L}_{kk'}.
\end{aligned}
\tag{5.90}
$$

The solution of this recursion formula with initial condition

$$
\mathcal{K}_{kk'}^{(1)} = \delta_{kk'} e^{-ik\tau} + \mathcal{L}_{kk'}
\tag{5.91}
$$

is given by:

$$
\mathcal{K}_{kk'}^{(N)} = \delta_{kk'} e^{-iNk\tau} + \mathcal{L}_{kk'} \frac{e^{-iNk\tau} - e^{-iNk'\tau}}{e^{-ik\tau} - e^{-ik'\tau}}.
\tag{5.92}
$$

By combining all contributions, the matrix element $\mathcal{M}_{kk'}^{(N)}$ is given by the following formula:

$$
\begin{aligned}
\mathcal{M}_{kk'}^{(N)} = {}& \delta_{kk'} e^{-iNk\tau} + \mathcal{L}_{kk'} \frac{e^{-iNk\tau} - e^{-iNk'\tau}}{e^{-ik\tau} - e^{-ik'\tau}} + \\
&+ \mathcal{M}_{kd} \mathcal{M}_{dk'} \left[\frac{e^{-iNk\tau}}{\left[e^{-ik\tau} - e^{-ik'\tau} \right] \left[e^{-ik\tau} - e^{-\Delta\tau/2} \right]} + \right. \\
&\left. + \frac{e^{-N\Delta\tau/2}}{\left[e^{-ik\tau} - e^{-\Delta\tau/2} \right] \left[e^{-ik'\tau} - e^{-\Delta\tau/2} \right]} \right. \\
&\left. + \frac{e^{-iNk'\tau}}{\left[e^{-ik'\tau} - e^{-ik\tau} \right] \left[e^{-ik'\tau} - e^{-\Delta\tau/2} \right]} \right].
\end{aligned}
\tag{5.93}
$$

5.4.5 Summary

In the preceding parts of this section matrix elements of powers of the period matrix $\mathcal{M}$ have been calculated determining the long-time behavior of the annihilation operators and scattering states. This has been achieved by deriving recursion formulas whose solutions are known. The results are summarized below:

$$\mathcal{M}_{dd}^{(N)} = e^{-N\Delta\tau/2} \tag{5.94}$$

$$\mathcal{M}_{dk}^{(N)} = \mathcal{M}_{dk} \frac{e^{-iNk\tau} - e^{-N\Delta\tau/2}}{e^{-ik\tau} - e^{-\Delta\tau/2}} \tag{5.95}$$

$$\mathcal{M}_{kd}^{(N)} = \mathcal{M}_{kd} \frac{e^{-iNk\tau} - e^{-N\Delta\tau/2}}{e^{-ik\tau} - e^{-\Delta\tau/2}} \tag{5.96}$$

$$\mathcal{M}_{kk'}^{(N)} = \delta_{kk'} e^{-iNk\tau} + \mathcal{L}_{kk'} \frac{e^{-iNk\tau} - e^{-iNk'\tau}}{e^{-ik\tau} - e^{-ik'\tau}} +$$
$$+ \mathcal{M}_{kd} \mathcal{M}_{dk'} \left[\frac{e^{-iNk\tau}}{\left[e^{-ik\tau} - e^{-ik'\tau}\right]\left[e^{-ik\tau} - e^{-\Delta\tau/2}\right]} + \right.$$
$$+ \frac{e^{-N\Delta\tau/2}}{\left[e^{-ik\tau} - e^{-\Delta\tau/2}\right]\left[e^{-ik'\tau} - e^{-\Delta\tau/2}\right]}$$
$$\left. + \frac{e^{-iNk'\tau}}{\left[e^{-ik'\tau} - e^{-ik\tau}\right]\left[e^{-ik'\tau} - e^{-\Delta\tau/2}\right]} \right] \tag{5.97}$$

Remarkably, the decay of a fermion on the local level is unaffected by the driving process, contrary to what one might expect. As in the equilibrium dynamics due to a resonant level model Hamiltonian, see Eq. (5.38), the probability amplitude for a fermion to stay on the local level decays exponentially in time. The time scale of the decay $2/\Delta$, however, is twice the time scale in the equilibrium setup. Remarkably, the decay is solely determined by the total time during which the interaction in the resonant level model is switched on, that is $N\tau/2$ after N periods. This behavior is a consequence of Eq. (5.64) stating that the probability amplitude for a fermion to stay on the local level is not influenced by processes in which the fermion intermediately hops into the continuum of bath states. Therefore, it is only important how much time has passed in which the local dynamics are switched on. This is consistent with the results of Langreth and Nordlander [24] as already discussed before, see Eq. (5.75). In this work the local retarded Green's function $G(t, t') = -i\theta(t - t')\langle\{d(t), d^\dagger(t')\}\rangle$ has been calculated for an arbitrary time dependence of the hopping element V by solving the corresponding Dyson equations. Inserting the particular periodic time dependence into $G(N\tau, 0)$, which is equal to the matrix element $\mathcal{M}_{dd}^{(N)}$, shows perfect agreement.

It is important to note that the whole analysis in this section only applies for the scattering states, i.e. only the dynamics for a single fermion in absence of the bath are considered. The real many-body situation of fermions subject to the bath will be regarded in the next chapter.

The equilibrium Kondo model exhibits only one scale, the Kondo temperature T_K that is connected to the parameters of the resonant level model through $T_K = \pi w \Delta$, see
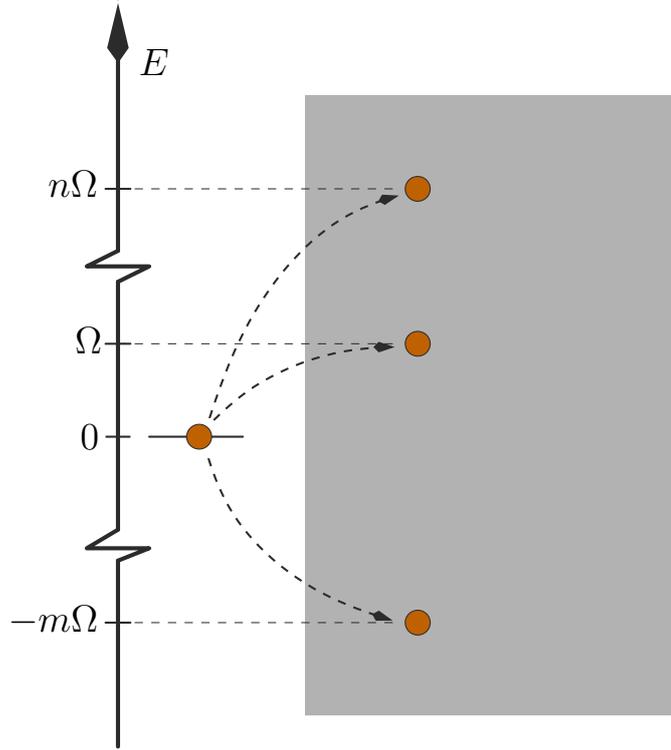
Figure 5.3: Fermions on the local level can hop into the continuum of bath states by absorbing or emitting multiple quanta of Ω

Eq. (3.99). Its inverse

$$t_K = 1/T_K \tag{5.98}$$

is the corresponding internal time scale, the time scale for the buildup of the Kondo correlations [31]. In the present setup another time scale emerges, the time scale of the switching τ with a corresponding energy scale set by the driving frequency $\Omega = 2\pi/\tau$. Remarkably, all matrix elements of $\mathcal{M}^N$ as proper scaled functions depend on the two parameters T_K and τ only through their product. Therefore, it is only important how fast the interaction in the Kondo Hamiltonian is switched in comparison to the internal time scale. Consequently, the only parameter in the present setup is

$$\eta = \frac{\tau}{t_K} \tag{5.99}$$

that compares the speed of switching with the internal time scale.

Regarding the k-dependent matrix elements of $\mathcal{M}^N$, the periodic driving in the resonant level model leads to transitions of fermions where multiple quanta of the driving frequency Ω are absorbed or emitted. This can be seen by analyzing the quantity $\left|\mathcal{M}_{dk}^{(N)}\right|^2$, that is the probability $\mathcal{P}_k^N$ for a scattering state $d^\dagger|\rangle$ to evolve into a bath state $c_k^\dagger|\rangle$ after a time $N\tau$, see Eq. (5.42). Here, $|\rangle$ stands for the true vacuum without any fermion as before. The scattering states describe the time evolution of a single fermion without the presence of a bath in a pure single particle picture. After $N \gg 1/\eta$ periods this probability density becomes stationary and is given by the following expression in
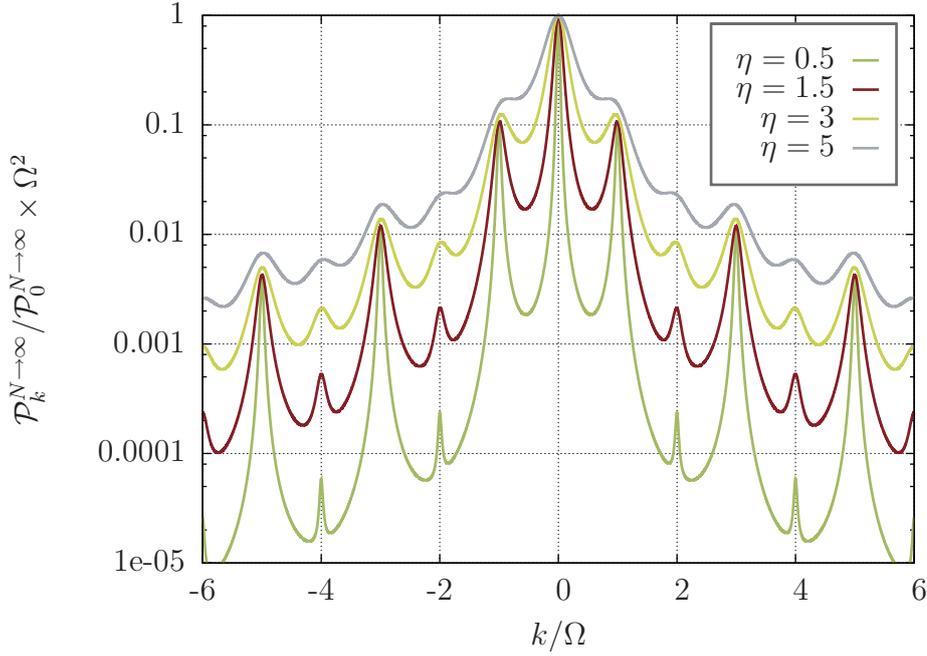
Figure 5.4: Universal curves for the probability $\mathcal{P}_k^{N \to \infty}$ for a scattering state $d^\dagger |\rangle$ to evolve into a state $c_k^\dagger |\rangle$ after $N \gg 1/\eta$ periods

the continuum limit:

$$\mathcal{P}_k^{N \to \infty} = \frac{\Delta}{\pi} \frac{1}{k^2 + \Delta^2} \frac{1 - 2 \cos\left(k\tau/2\right) e^{-\Delta \tau/2} + e^{-\Delta \tau}}{1 - 2 \cos\left(k\tau\right) e^{-\Delta \tau/2} + e^{-\Delta \tau}}. \tag{5.100}$$

Regarding the case of time evolution in a time-independent resonant level model, see Eq. (5.43), this probability distribution gets modified by a multiplicative factor that accounts for processes in which fermions undergo transitions by absorbing or emitting quanta of Ω. A plot of $\mathcal{P}_k^{N \to \infty}$ as a function of k/Ω is shown in Fig. (5.4) for different values of the parameter η, the only parameter in the problem. Clearly, pronounced structures at multiples of the driving frequency Ω are observed. Surprisingly, there is an asymmetry between even and odd multiples of Ω whose origin will be discussed later. The probability distribution $\mathcal{P}_k^{N \to \infty}$ as a function of k/T_K is shown in Fig. (5.5). As a reference the equilibrium curve is included as the dashed line.

The limit $\eta \to \infty$: For slow switching, i.e. large η, the deviation from the equilibrium curve is small. If the period τ is large, the scattering state $d^\dagger |\rangle$ decays completely into bath states in the first half period according to the simple dynamics in a time-independent resonant level model. The probability to find the fermion in state k is given by the equilibrium formula, see Eq. (5.43), that is a Lorentzian of width Δ. The subsequent time evolution due to a free Hamiltonian merely causes the different k-states to acquire their corresponding phase factors in course of time. Eq. (5.62) implies that the additional application of a resonant level model Hamiltonian is not sufficient to cause further transitions. Remarkably, the subsequent time evolution is not affected by the driving process. Consequently, after the first period the scattering state $d^\dagger |\rangle$ has reached its equilibrium configuration that cannot be changed by an additional time
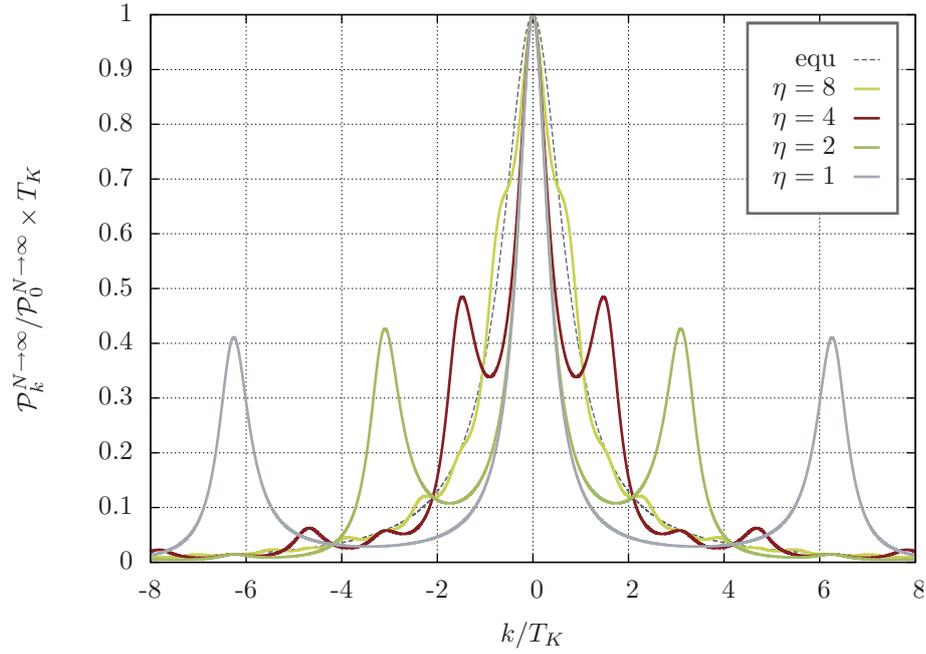
Figure 5.5: Universal curves for the probability $\mathcal{P}_k^{N\to\infty}$ for a scattering state $d^\dagger|\rangle$ to evolve into a state $c_k^\dagger|\rangle$ after $N \gg 1/\eta$ periods for different values of $\eta = \tau T_K$. The equilibrium curve is shown as a reference

evolution with a free or resonant level Hamiltonian. Therefore, in the limit $\eta \to \infty$ the probability distribution $\mathcal{P}_k^{N\to\infty}$ approaches the equilibrium form as can be seen in Fig. (5.5).

Intermediate η: Deviating from this limit, side-peaks appear that are located at odd multiples of the driving frequency Ω such that spectral weight is transferred from the central peak to the satellites. For values of $\eta < \infty$ the scattering state $d^\dagger|\rangle$ is not able to decay completely into bath states after the first half period. With a probability of $e^{-\Delta\tau}$ one can still find the fermion on the local level. According to Eq. (5.39) the probability density for the fermion to be decayed into the scattering state $c_k^\dagger|\rangle$ after the time $\tau/2$ is given by the formula in the continuum limit:

$$|\mathcal{G}_{dk}(\tau/2)|^2 = \frac{\Delta}{\pi}\frac{1}{k^2 + \Delta^2}\left[1 - 2\cos(k\tau/2)e^{-\Delta\tau/2} + e^{-\Delta\tau}\right]. \qquad (5.101)$$

For values of $k_n = (2n + 1)\Omega$, $n \in \mathbb{Z}$, i.e. odd multiples of the driving frequency, this function approaches a local maximum of magnitude $\Delta/\pi[1 + e^{-\Delta\tau}]^2/[k_n^2 + \Delta^2]$. The next half period leads to a trivial time evolution where the modulus of the amplitude for each k stays constant whereas a phase factor of $e^{-ik\tau/2}$ is acquired. Thereafter, the dynamics are again governed by a resonant level model Hamiltonian. According to Eq. (5.66), the further time evolution of a k-state does not lead to additional transitions to other k-states. As in a free time evolution the amplitudes get modified by a phase factor only. Nevertheless, a fermion on the local level can evolve further where the probability for hopping into states $k_n = (2n + 1)\Omega$, $n \in \mathbb{Z}$, is enhanced again. A continued application of this two step time evolution leads to Eq. (5.100) for the probability

distribution $\mathcal{P}_k^{N\to\infty}$. The shorter is the period τ, the smaller the magnitude of the local maxima turns out to be. Due to the increase of the driving frequency Ω the position of the local maxima will move to larger values.

The limit $\eta \to 0$: Formally, this limit can be performed. Nevertheless, one should keep in mind that the mapping from the Anderson impurity model onto the resonant level model is only valid for sufficiently small driving frequencies Ω such that the quantum dot is not ionized, see Eq. (4.10). Consequently, there is a lower bound for the switching period $\tau \gg 1/|\varepsilon_d|, 1/(\varepsilon_d + U)$ where ε_d is the energy of the local level in a quantum dot and U the Coulomb repulsion.

The limit $\tau \to 0$ has to be done with certain care, however, as will be shown in the following. Since $\mathcal{P}_k^{N\to\infty}$ is a probability distribution, it should be normalized to 1:

$$\sum_k \mathcal{P}_k^{N\to\infty} = 1. \tag{5.102}$$

The normalization condition can be proven for all finite τ most easily by using the Fourier series of the multiplicative factor, see Eq. (A.1):

$$\frac{1 - 2\cos(k\tau/2)\,e^{-\Delta\tau/2} + e^{-\Delta\tau}}{1 - 2\cos(k\tau)\,e^{-\Delta\tau/2} + e^{-\Delta\tau}} = \sum_{n\in\mathbb{Z}} c_n e^{ik\tau/2} \tag{5.103}$$

with coefficients

$$c_n = \begin{cases} \dfrac{1 + e^{-\Delta\tau}}{1 - e^{-\Delta\tau}} e^{-|n|\Delta\tau/4} & \text{, for } n \text{ even} \\[4mm] -2\cosh(\Delta\tau/4)\dfrac{e^{-\Delta\tau/2}}{1 - e^{-\Delta\tau}} e^{-|n|\Delta\tau/4} & \text{, for } n \text{ odd.} \end{cases} \tag{5.104}$$

Performing the limit $\tau \to 0$ in Eq. (5.100) leads to an expression that seems to be similar to an equilibrium probability distribution of a resonant level Hamiltonian with different parameters:

$$\lim_{\tau\to0} \mathcal{P}_k^{N\to\infty} = \frac{V^2/4}{k^2 + \Delta^2/4}. \tag{5.105}$$

Integrating $\mathcal{P}_k^{N\to\infty}$ over all k in this limit yields

$$\sum_k \lim_{\tau\to0} \mathcal{P}_k^{N\to\infty} = \frac{1}{2} \tag{5.106}$$

indicating that one has to be careful in taking this limit since a probability distribution should be normalized to 1. Actually, the limit $\tau \to 0$ does not commute with the infinite sum because $\mathcal{P}_k^{N\to\infty}$ is only pointwise convergent. The loss of spectral weight of $\frac{1}{2}$ is caused by shifting the side peaks to $\pm\infty$ in an uncontrolled way. Effectively, by performing the limit directly at the level of the probability distribution, all the spectral weight of the side peaks is lost. Therefore, the limit of $\tau \to 0$ should be performed with care. A more detailed analysis of this limiting behavior will be given in the next chapter.
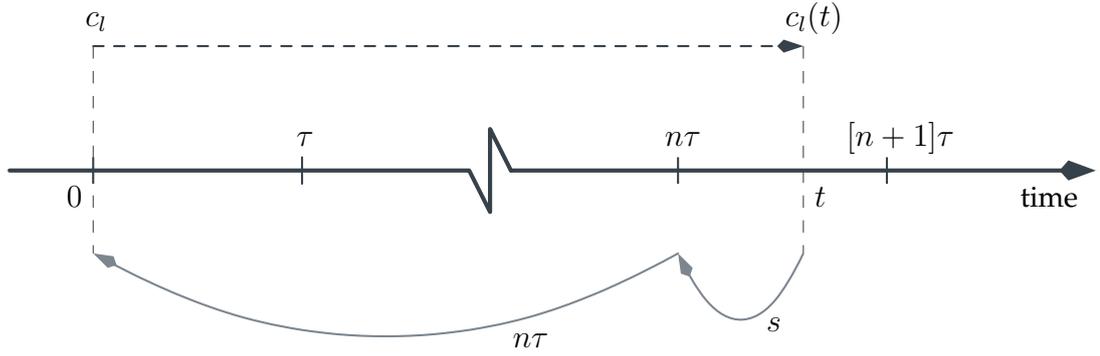
Figure 5.6: Splitting of time evolution in the Heisenberg picture.

5.5 Time evolution of single-particle operators

Based on the previous parts of this section the long-time dynamics of the single-particle operators are analytically accessible by separating the time evolution into two parts, the time evolution over an integer number periods and a short time evolution within one. The order of time evolution, however, is changed for the operators in the Heisenberg picture according to Eq. (5.45), namely the operators are evolved according to the Hamiltonian that acts at last as indicated in Fig. (5.6). Suppose, one is interested in an annihilation operator c_l at some time t. For this purpose it is most convenient to split t into two parts:

$$t = n\tau + s, \qquad 0 \leqslant s < \tau. \tag{5.107}$$

According to this separation the time evolved operator $c_l(t)$ can be written in the following way

$$c_l(t) = P^\dagger(n\tau, 0) \, P^\dagger(n\tau + s, n\tau) \, c_l \, P(n\tau + s, n\tau) \, P(n\tau, 0) \tag{5.108}$$

where $P(t, t_0)$ is the time evolution operator that evolves a state $|\Psi\rangle$ at time t_0 to the final state at time t

$$|\Psi(t)\rangle = P(t, t_0)|\Psi(t_0)\rangle. \tag{5.109}$$

If $s \leqslant \tau/2$ the propagator $P(n\tau + s, n\tau)$ takes a simple form since in the corresponding time window $[n\tau, n\tau + s]$ the Hamiltonian is time-independent and given by the resonant level model Hamiltonian

$$s \leqslant \tau/2 \quad \longrightarrow \quad P(n\tau + s, n\tau) = e^{-iH_{\mathrm{RLM}}s}. \tag{5.110}$$

In the case where $s > \tau/2$, the propagator $P(n\tau + s, n\tau)$ factorizes into two exponentials

$$s > \tau/2 \quad \longrightarrow \quad P(n\tau + s, n\tau) = e^{-iH_0[s-\tau/2]} \, e^{-iH_{\mathrm{RLM}}\tau/2}. \tag{5.111}$$

The operator whose dynamics are the simplest is the operator d of the local level. In the case where $s \leqslant \tau/2$, the time evolution back to $n\tau$ is completely determined by the dynamics of a resonant level model Hamiltonian. According to Eq. (5.17), all the

information about the time evolution of the single-particle operators is encoded in the transition matrix $\mathcal{G}$ where $\mathcal{G}$ is given by Eq. (5.38):

$$P^\dagger(n\tau + s, n\tau)\, d\, P(n\tau + s, n\tau) = \mathcal{G}_d(s)\, d + \sum_k \mathcal{G}_{dk}(s)\, c_k. \tag{5.112}$$

If $s > \tau/2$, the time evolution operator of a free Hamiltonian has to be applied first. Since d commutes with H_0, it commutes with the corresponding propagator, too, such that

$$P^\dagger(n\tau + s, n\tau)\, d\, P(n\tau + s, n\tau) = \mathcal{M}_{dd}\, d + \sum_k \mathcal{M}_{dk}\, c_k. \tag{5.113}$$

Plugging both relations into Eq. (5.108) one obtains:

$$\begin{aligned}
d(t) = \theta\left(\frac{\tau}{2} - s\right)\left[\mathcal{G}_d(s)\, d(n\tau) + \sum_k \mathcal{G}_{dk}(s)\, c_k(n\tau)\right] + \\
+ \theta\left(s - \frac{\tau}{2}\right)\left[\mathcal{M}_{dd}^{(n+1)}\, d + \sum_k \mathcal{M}_{dk}^{(n+1)}\, c_k\right].
\end{aligned} \tag{5.114}$$

Conveniently, one can continue the calculation by regarding s to be in the interval $\left[0, \frac{\tau}{2}\right]$ without caring about the step function θ. The operators on the right hand side of the equation above are known from the last section. They are given by the matrix elements of powers of the period matrix $\mathcal{M}$, see Eq. (5.52):

$$\begin{aligned}
d(n\tau) &= \mathcal{M}_{dd}^{(n)}\, d + \sum_k \mathcal{M}_{dk}^{(n)}\, c_k, \\
c_k(n\tau) &= \mathcal{M}_{kd}^{(n)}\, d + \sum_{k'} \mathcal{M}_{kk'}^{(n)}\, c_{k'}.
\end{aligned} \tag{5.115}$$

Consequently, one obtains:

$$\begin{aligned}
d(t) = \left[\mathcal{G}_d(s)\, \mathcal{M}_{dd}^{(n)} + \sum_k \mathcal{G}_{dk}(s)\, \mathcal{M}_{kd}^{(n)}\right] d + \\
+ \sum_k \left[\mathcal{G}_d(s)\, \mathcal{M}_{dk}^{(n)} + \sum_{k'} \mathcal{G}_{dk'}(s)\, \mathcal{M}_{k'k}^{(n)}\right] c_k.
\end{aligned} \tag{5.116}$$

The sums over intermediate indices in the expressions above can be obtained easily by use of the same techniques as in the calculation of Eq. (5.64) and Eq. (5.66):

$$\begin{aligned}
\sum_k \mathcal{G}_{dk}(s)\, \mathcal{M}_{kd}^{(n)} &= 0, \\
\sum_{k'} \mathcal{G}_{dk'}(s)\, \mathcal{M}_{k'k}^{(n)} &= \mathcal{G}_{dk}(s)\, e^{-ink\tau}.
\end{aligned} \tag{5.117}$$

expressing again the observation that the dynamics of a fermion on the local level are not influenced by processes in which the fermion hops back onto the local level after being in the continuum of bath states intermediately. Therefore, the time evolved single-particle operator $d(t)$ obeys the following relation:

$$
\begin{aligned}
d(t) = {}& \theta\left(\frac{\tau}{2} - s\right) \left[\mathcal{G}_d(s)\, \mathcal{M}_{dd}^{(n)}\, d + \sum_k \left(\mathcal{G}_d(s)\, \mathcal{M}_{dk}^{(n)} + \mathcal{G}_{dk}(s) e^{-ink\tau} \right) c_k \right] \\
& + \theta\left(s - \frac{\tau}{2}\right) \left[\mathcal{M}_{dd}^{(n+1)}\, d + \sum_k \mathcal{M}_{dk}^{(n+1)}\, c_k \right]
\end{aligned}
\tag{5.118}
$$

.

Chapter 6

Correlation functions

In the last section the time evolution in the periodic driving setup has been analyzed in a pure single-particle picture, i.e. the dynamics of the annihilation operators and scattering states of the effective Hamilton picture have been determined without referring to their implications onto the dynamics in the time-dependent nonequilibrium Kondo model. In this chapter the full many-body situation will be considered by analyzing the magnetization $\langle S_z(t) \rangle$ and the spin-spin correlation function $\langle S_z(t) S_z(t') \rangle$. Reminding Chapter 4, the periodic driving setup obeys the following protocol. Initially, the system is prepared in the ground state $|\Psi_{GS}\rangle$ of the Kondo Hamiltonian without spin dynamics that corresponds to the free part of the noninteracting resonant level model. At some time $t = t_0$ the periodic driving process starts where subsequently the spin dynamics in the Kondo Hamiltonian are switched on and off. After an infinite number of periods the system approaches a quasi-steady state, a state in which all correlation functions are invariant under a discrete time shift of one period τ, see Eq. (4.36). The purpose of this work is a characterization of this quasi-steady state by analyzing the influence of the periodic switching onto local properties. The quasi-steady state is generated by shifting t_0 to $-\infty$ by performing the limit $t_0 = -\lim_{N\to\infty} N\tau$. Consequently, the state $|\Phi\rangle$ over which observables are to be averaged is given by:

$$|\Phi\rangle = \lim_{N\to\infty} |\Psi_{GS}(N\tau)\rangle. \tag{6.1}$$

Remarkably, it will be shown that the magnetization of the impurity spin is not affected by the driving process. It decays exponentially where it is only important how much time has passed during which the spin dynamics have been switched on and the spin operator S_z has evolved nontrivially. Therefore, the excitations that are created due to the periodic driving do not influence the impurity spin orientation. This is a consequence of the results of the last chapter for the single-particle dynamics in a time-dependent resonant level model where the probability for a local d fermion to stay on the local level in a single-particle picture is not affected by the periodic driving setup.

Due to the periodic driving, energy is pumped into the system in each period. Because of the built-in dissipation mechanism, the so-called open system limit, see Eq. (4.4), this excess energy can flow away from the central region into the conduction band thereby becoming irrelevant in the thermodynamic limit. Nevertheless, excitations are created in the vicinity of the local level such that one could think of locally heating the system. As a consequence of the analysis of the spin-spin correlation function in the quasi-steady state, the resulting excitations are substantially different from

those that ar induced by temperature. Roughly speaking, the periodic driving leads to a discrete ladder of excitation energies of multiples of the driving frequency Ω. This discrete structure in the excitation spectrum, however, is fundamentally different from that induced by temperature that smears the Fermi surface. As a consequence, the Fermi surface remains sharp under the periodic switching, leading to a long time behavior $\propto t^{-2}$ of the spin-spin correlation as in equilibrium for zero temperature.

The equilibrium Kondo model exhibits only one energy scale, namely the Kondo temperature T_K, with an associated time scale

$$t_K := \frac{1}{T_K}, \tag{6.2}$$

that is the time scale for the build up of the Kondo effect [31]. In the present setup another time scale emerges, the period of the switching τ. As was conjectured by Kaminski et al. [21], the conductance through a quantum dot in the Kondo regime displays a universal description even under time-dependent nonequilibrium conditions despite the appearance of new energy and time scales in a nonequilibrium setup. Remarkably, they found that the Kondo temperature remains the only relevant energy scale. Therefore, the question arises, if quantities like the spin-spin correlation function also display universal behavior in the time-dependent nonequilibrium setup. It will turn out that the spin-spin correlation function indeed exhibits a universal description. The only parameter is

$$\eta = \frac{\tau}{t_K} \tag{6.3}$$

comparing the speed of switching τ with the internal time scale t_K. Additionally, the Kondo temperature remains a meaningful parameter and the only relevant energy scale in the periodic time-dependent setup.

6.1 Asymptotic behavior

6.1.1 The limit of long switching times

The properties of the Kondo system in the case of long switching times, $\tau \to \infty$, are accessible by quite general arguments. As expected, the system relaxes in each half period. Initially, the system is prepared in one of the degenerate ground states of the Kondo Hamiltonian without spin dynamics, i.e. a product state in the effective Hamilton picture:

$$|\Psi_{GS}\rangle = |0\rangle \otimes |\chi\rangle \tag{6.4}$$

where $|0\rangle$ is the Fermi sea of the spinless fermions and $|\chi\rangle$ is a wave function of the local level that has not to be specified at this point. A possible experimental realization using a quantum dot was presented in Sec. (4.1.2). At time $t = t_0$ the spin dynamics in the Kondo Hamiltonian are switched on instantaneously, creating local excitations in the vicinity of the impurity. After a transient time t_K the Kondo correlations are developed and the Kondo singlet has formed [31]. The excess energy in a neighborhood of the local level that has been created by the interaction quench delocalizes and flows away into the bath. After a sufficiently long time, the excitations spread over a large area in the lead. Due to the property of the lead as a heat bath, delocalized excitations of the order of the impurity do not contribute in the thermodynamic limit. Therefore, one can

imagine the system to evolve towards the ground state of the Kondo model after long times. As a result, in the limit $\tau \to \infty$, the system approaches a state that looks like the interacting ground state after a time $\tau/2$. The magnetization of the local level takes a value of $\langle S_z(\tau/2) \rangle = 0$ corresponding to the particle-hole symmetry of the Kondo Hamiltonian [25]. At this point, however, a subtlety arises. As pointed out by Lobaskin and Kehrein [27], the overlap of the time evolved initial state $|\Psi_{GS}(t)\rangle = e^{-iH_{\mathrm{RLM}}t}|\Psi_{GS}\rangle$ with the true ground state Φ_0 of the resonant level model Hamiltonian is constant in time in an interaction quench scenario:

$$\langle \Phi_0 | \Psi_{GS}(t) \rangle = \langle \Phi_0 | \Psi_{GS} \rangle = \text{const.} \tag{6.5}$$

Rigorously speaking, the time evolved nonequilibrium state $|\Psi_{GS}(t)\rangle$ can never evolve into the true ground state of the interacting Hamiltonian. Nevertheless, the time evolved state $|\Psi_{GS}(t)\rangle$ may look like the true ground state for suitable local observables as will be the case for the spin operator S_z. All statements about relaxation of the state itself in the following are to be understood in this sense.

At time $\tau/2$ the spin dynamics are switched off leading to a decoupling of the local dynamics from the conduction band electron's dynamics. Consequently, the local spin is frozen and the Kondo singlet is destroyed. The released binding energy of the order of T_K flows away into the lead. As before delocalized excitations vanish in the thermodynamic limit such that after a whole period the system approaches its noninteracting ground state where the wave function of the level $|\chi'\rangle$ is such that the magnetization takes a value of $\langle S_z \rangle = 0$:

$$|\Psi_{GS}(\tau)\rangle \text{ " = " } |0\rangle \otimes |\chi'\rangle. \tag{6.6}$$

The quotation marks indicate that this equality has to be understood as correct only for certain observables like the S_z operator due to the arguments given above. According to Eq. (6.6), the system's state at the moment where the second interaction quench takes place is similar to the state at the moment of the first quench. Only the local wave function may have changed. Most importantly, the state again is a product state and does not contain any correlations. A further time evolution over another period does not affect the outcoming wave function due to the arguments given above such that the system will always be in the same state after an integer number of periods:

$$|\Psi_{GS}(n\tau)\rangle \text{ " = " } |0\rangle \otimes |\chi'\rangle. \tag{6.7}$$

Concluding, in the limit $\tau \to \infty$ correlation functions involving S_z operators behave as for a single interaction quench setting where the initial state is given by (6.6). This situation was already addressed in a recent work by Lobaskin and Kehrein [27][28] where the magnetization $\langle S_z(t) \rangle$ and spin-spin correlation function $\langle S_z(t)S_z(t') \rangle$ have been analyzed for an interaction quench in the Kondo model.

6.1.2 The limit of fast switching

The opposite limit of taking $\tau \to 0$ requires more care as already emphasized in the last chapter, see Sec. (5.4.5). Strictly speaking, this limit cannot be taken since there is an upper bound on the driving frequency $\Omega \ll |\varepsilon_d|, U + \varepsilon_d$, see Eq. (4.10). If $\Omega \gtrsim |\varepsilon_d|$, for example, the periodic driving is able to ionize the quantum dot by a process where the local electron hops into the conduction band by absorbing an energy quantum Ω

leaving behind a quantum dot without any electron. This situation, however, does not correspond to the Kondo regime that requires a constant occupation of the local level by exactly one electron. Therefore, the driving frequency has to be small enough not to affect the occupation of the central region.

Another important restriction stems from the linearization of the dispersion relation that has to be performed for a proper use of the bosonization technique. The linearization procedure is valid as long as one deals with the low energy properties of the system. Consequently, the excitations of multiples of the driving frequency Ω that are caused in the periodic driving setup should not lead out of the range of validity of the linearization of the spectrum.

Nevertheless, the limit $\tau \to 0$ can be performed formally. Generally, one expects that the system is not able to follow the switching as a consequence of mismatch of time scales. The system is able to adapt to externally forced changes in the system's parameters on an internal time scale, that is the Kondo scale t_K. If parameters are varied faster than the internal time scale, i.e. for $\tau \ll t_K$, the system's behavior cannot adjust within one period. Therefore, correlation functions in the quasi-steady state are expected to show behavior similar to equilibrium as will be shown for the spin-spin correlation function. This, however, does not prohibit the build up of a quasi-steady state since the system may adopt to the external perturbation over a large number of periods.

6.2 Magnetization

One of the quantities characterizing the dynamics of the impurity spin is the spin expectation value $P(t) = \langle S_z(t) \rangle$ called the magnetization. In contrast to the spin-spin correlation function, that will be analyzed in the quasi-steady state, the time dependence of the spin expectation value will be determined starting from the beginning of the driving process. The reason for this different treatment is that the interest of this work is a characterization of the quasi-steady state. As it will turn out, the magnetization does not provide much information about this state, it rather displays the system's behavior in the crossover regime from the initial to the quasi-steady state.

For a factorized initial state $|0\rangle \otimes |\uparrow\rangle$, the magnetization for a single interaction quench has been calculated in numerous works [25] [24] [26] [27] with the result that it decays exponentially in time:

$$P(t) = \frac{1}{2} e^{-t/\mathcal{T}} \tag{6.8}$$

where the time scale $\mathcal{T} = t_K/(2\pi w)$ is set by the Kondo time scale t_K, $w = 0.4128$ denotes the Wilson number. As already emphasized in a previous chapter, see Sec. (3.2.5), the dynamics of the local spin in terms of the operator S_z are accessible analytically. Most importantly, S_z can be connected to the fermionic operators d and $d^\dagger$ of the effective Hamiltonian in the following way, see Eq. (3.91):

$$S_z = d^\dagger d - \frac{1}{2}. \tag{6.9}$$

Moreover, S_z commutes with all unitary transformations that are applied to the anisotropic Kondo Hamiltonian in order to map it onto a resonant level model Hamiltonian. These

observations enable the evaluation of the magnetization $P(t)$ of the impurity spin:

$$P(t) = \langle S_z(t) \rangle. \tag{6.10}$$

By use of the correspondence to the operators of the effective Hamiltonian, see Eq. (6.9), $P(t)$ is completely determined by the occupation $n_d(t) = \langle d^\dagger(t) d(t) \rangle$ of the local d-level in the picture of the effective resonant level model Hamiltonian:

$$P(t) = n_d(t) - \frac{1}{2}. \tag{6.11}$$

As emphasized in Sec. (5.5), it is convenient to divide the time evolution into two parts:

$$t = n\tau + s \qquad , 0 \leqslant s \leqslant \tau/2 \quad \text{or} \quad \tau/2 < s < \tau. \tag{6.12}$$

Due to Eq. (5.118) it is sufficient to restrict s to the interval $[0, \tau/2]$ for the description of the time evolution since the annihilation operator d stays constant in the residual time window $[\tau/2, \tau]$. Inserting the corresponding expression for the dynamics of the d operator into the definition of the level occupation $n_d(t)$ one arrives at:

$$\begin{aligned} n_d(t) = & \langle d^\dagger(t) d(t) \rangle = |\mathcal{G}_d(s)|^2 \left| \mathcal{M}_{dd}^{(n)} \right|^2 \langle d^\dagger d \rangle + \\ & + \sum_k \left| \mathcal{G}_d(s)\, \mathcal{M}_{dk}^{(n)} + \mathcal{G}_{dk}(s)\, e^{-ink\tau} \right|^2 \langle c_k^\dagger c_k \rangle. \end{aligned} \tag{6.13}$$

In the derivation of the last line, the product state character of the initial state provided the vanishing of the following expectation values:

$$\langle d^\dagger c_k \rangle = \langle c_k^\dagger d \rangle = 0. \tag{6.14}$$

This relation accounts for the initial preparation of the system that has been assumed to be completely uncorrelated. As the initial state is the ground state of the free part of the resonant level model Hamiltonian, see Sec. (4.1.1), the expectation value of $\langle c_k^\dagger c_{k'} \rangle$ is equal to the step function:

$$\langle c_k^\dagger c_{k'} \rangle = \delta_{kk'} \theta(-k). \tag{6.15}$$

Consequently, the local level occupation is given by the following expression:

$$\begin{aligned} n_d(t) = & \; n_d\, e^{-n\Delta\tau} e^{-2\Delta s} + e^{-2\Delta s} \sum_{k<0} \left[\left| \mathcal{M}_{dk}^{(n)} \right|^2 + |\mathcal{G}_{dk}(s)|^2 \right] \\ & + e^{-\Delta s} \sum_{k<0} \left[\mathcal{G}_{dk}(s) \mathcal{M}_{dk}^{(n)} e^{-ink\tau} + \mathcal{G}_{dk}^*(s) \mathcal{M}_{dk}^{(n)*} e^{ink\tau} \right]. \end{aligned} \tag{6.16}$$

As one can check, the objects that appear in the sums above exhibit symmetries that allow to extend the $k-$sums to $\pm\infty$:

$$\left| \mathcal{M}_{dk}^{(n)} \right| = \left| \mathcal{M}_{d-k}^{(n)} \right|, \tag{6.17}$$

$$|\mathcal{G}_{dk}(s)| = |\mathcal{G}_{d-k}(s)|, \tag{6.18}$$

$$\mathcal{G}_{dk}^*(s) \mathcal{M}_{dk}^{(n)*} e^{ink\tau} = \mathcal{G}_{d-k}(s) \mathcal{M}_{d-k}^{(n)} e^{ink\tau}. \tag{6.19}$$

Basically, these properties originate from the particle-hole symmetry of the resonant level model Hamiltonian. As one can easily show by using the same techniques as in Sec. (5.4.1), the sum

$$\sum_k \mathcal{G}_{dk}(s)\mathcal{M}_{dk}^{(n)} e^{-ink\tau} = 0 \tag{6.20}$$

vanishes such that the local level occupation is given by the following expression:

$$n_d(t) = n_d\, e^{-n\Delta\tau} e^{-2\Delta s} + \frac{1}{2} e^{-2\Delta s} \sum_k \left[\left|\mathcal{M}_{dk}^{(n)}\right|^2 + |\mathcal{G}_{dk}(s)|^2 \right]. \tag{6.21}$$

Since the matrices $\mathcal{M}^{(n)}$ and $\mathcal{G}$ are unitary, as has been shown in section (5.1) for a wide class of quadratic Hamiltonians, the columns as well as the rows of these matrices have to constitute a set of orthonormal vectors such that the following relations are valid:

$$\sum_k \left|\mathcal{M}_{dk}^{(n)}\right|^2 = 1 - \left|\mathcal{M}_{dd}^{(n)}\right|^2 = 1 - e^{-n\Delta\tau}, \tag{6.22}$$

$$\sum_k |\mathcal{G}_{dk}(s)|^2 = 1 - |\mathcal{G}_d(s)|^2 = 1 - e^{-2\Delta s}. \tag{6.23}$$

Combining all contributions the magnetization of the impurity spin decays exponentially in time:

$$\boxed{\begin{aligned}
P(t) &= \langle S_z(0)\rangle\, \theta\left(\frac{\tau}{2} - s\right) e^{-n\pi w\tau/t_K} e^{-2\pi ws/t_K} \\[2mm]
&\quad + \langle S_z(0)\rangle\, \theta\left(s - \frac{\tau}{2}\right) e^{-[n+1]\pi w\tau/t_K}
\end{aligned}} \tag{6.24}$$

where the relation $T_K = \pi w\Delta$, see Eq. (3.99), has been used. Remarkably, the orientation of the local spin is not affected by the periodic driving process as the analysis of the single-particle dynamics in the previous chapter already indicated. The magnetization decays exponentially where the corresponding time scale is set by the Kondo time scale t_K as for a single interaction quench. The decay only depends on how much time has passed in which the local spin can evolve nontrivially, that is half of the time after an integer number of periods. Physically, there is no spin generating source since the total spin

$$S_T = \hat{\mathcal{N}}_s + S_z \tag{6.25}$$

is a constant of motion [46]. Here, the operator $\hat{\mathcal{N}}_s = \frac{1}{2}\left[\hat{N}_\uparrow - \hat{N}_\downarrow\right] = \sum_k\, :\, c_k^\dagger c_k\, :$ measures the total spin polarization of the bath of conduction band electrons. Initially, the lead is prepared in its ground state, a filled Fermi sea that is not spin polarized. Only the local spin may be oriented. A switch on of the spin dynamics will transport this excess spin away from the central region to infinity. Since no further spin source like a magnetic field is present in this setup, a spin polarization is unable to develop

such that the expectation value of $\hat{\mathcal{N}}_s$ as well as the expectation value of S_z have to average to 0 after a transient regime.

This behavior is consistent with the results of Langreth and Nordlander [24] where the local level occupation in a resonant level model Hamiltonian was calculated for an arbitrary time dependence of the hopping element V. A solution of the corresponding Dyson equations leads to the following expression for the local level occupation:

$$n_d(t) = e^{-2\int_0^t d\bar{t}\,\Delta(\bar{t})}, \qquad \Delta(t) = \frac{L}{2}V^2(t). \qquad (6.26)$$

In the limit $\tau \to \infty$ the impurity spin expectation value decays to zero proportional to $e^{-2\pi wt/t_K}$ already in the first half period corresponding to the single interaction quench situation already addressed in [25] [24][26][27]. The further time evolution does not change the spin expectation value such that the magnetization $P(t)$ stays zero for all later times.

In the limit $\tau \to 0$ the magnetization will decay proportional to $e^{-\pi wt/t_K}$, i.e. with half the time scale compared to the single interaction quench scenario since only half of the time the spin dynamics are switched on. Remarkably, the impurity spin relaxes slower in the case of fast driving.

6.3 Spin-spin correlation function

A dynamical quantity that carries more information about the local two state system than the magnetization is the spin-spin correlation function

$$\langle S_z(t)S_z(t')\rangle. \qquad (6.27)$$

For the purpose of this work it is convenient to separate the real and imaginary part. The real part $C(t,t')$, the symmetrized version of the spin-spin correlator, describes the strength of the fluctuations:

$$C(t,t') = \frac{1}{2}\langle\{S_z(t),S_z(t')\}\rangle. \qquad (6.28)$$

The imaginary part of the spin-spin correlation function, the antisymmetrized part, determines the response $\chi(t,t')$ of the system due to an external classical magnetic field applied to the local spin:

$$\chi(t,t') = i\theta(t-t')\langle[S_z(t),S_z(t')]\rangle. \qquad (6.29)$$

In time-dependent nonequilibrium settings where time reversal symmetry is broken, two-time correlation functions explicitly depend on both time variables. In equilibrium, however, two-time correlation functions depend on both arguments only through their time difference, hence, effectively reducing them to functions of only one variable.

The spin-spin correlation function in equilibrium: In equilibrium the spin-spin correlation function exhibits a characteristic algebraic long-time decay at zero temperature as already mentioned in Sec. (2.3):

$$\langle S_z(t)S_z(0)\rangle \overset{t\to\infty}{\propto} 1/t^2. \qquad (6.30)$$
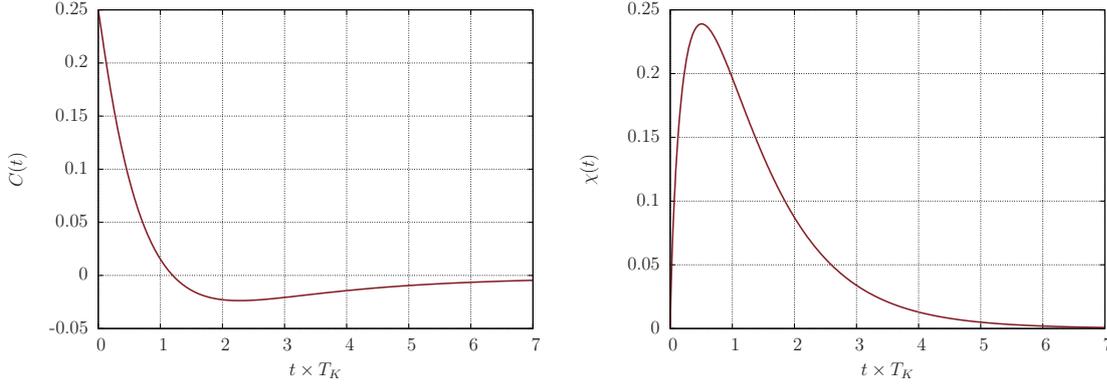
Figure 6.1: Universal curves for the symmetrized part of the spin-spin correlation function $C(t)$ and the response $\chi(t)$ in equilibrium at zero temperature

At finite temperatures the decay is exponential due to the smearing of the Fermi surface. The spin-spin correlation function at zero temperature in equilibrium is given by the following expression, see for example Ref. [27]:

$$\langle S_z(t)S_z(0)\rangle = \langle d^\dagger(t)d(0)\rangle^2, \qquad \langle d^\dagger(t)d(0)\rangle = \frac{1}{2}e^{-\Delta t} - is(t),$$

$$C(t) = \frac{1}{4}e^{-2\Delta t} - s^2(t), \tag{6.31}$$

$$\chi(t) = \theta(t)\,e^{-\Delta t}\,s(t),$$

where the function

$$s(t) = \frac{\Delta}{\pi}\int_0^\infty dk\,\frac{\sin(kt)}{k^2 + \Delta^2} \tag{6.32}$$

is responsible for the long-time algebraic decay since $s(t) \overset{t\to\infty}{\longrightarrow} 1/(\pi\Delta t)$ as is shown in the appendix, see Eq. (A.5). A plot of both $C(t)$ and the response $\chi(t)$ in equilibrium is shown in Fig. (6.1).

As pointed out by Guinea [15], one can identify the correlation function $C(t)$ with the expectation value of a sequence of measurements of the local spin. Suppose that a spin measurement is performed at time $t = 0$ with outcome $+1/2$ such that the system's wave function is given by the projected state $2P_+|\Psi\rangle$. Here, $|\Psi\rangle$ is the initial state and $P_+ = S_z + \frac{1}{2}$ the projector onto the eigenspace corresponding to the eigenvalue $+1/2$. The expectation value of a second spin measurement of the projected state at time t, to be denoted by $\mathcal{P}$, is given by the following expression:

$$\mathcal{P} = 4\left\langle \left[S_z + \frac{1}{2}\right] S_z(t) \left[S_z + \frac{1}{2}\right]\right\rangle = 4\langle S_z S_z(t) S_z\rangle + 4\langle S_z(t)\rangle + 2\langle\{S_z(t), S_z\}\rangle. \tag{6.33}$$

Due to the particle-hole symmetry of the resonant level model Hamiltonian the first two contributions have to vanish such that

$$C(t) = \left\langle \left[S_z + \frac{1}{2}\right] S_z(t) \left[S_z + \frac{1}{2}\right]\right\rangle. \tag{6.34}$$

Therefore, $C(t)$ is proportional to the expectation value of a spin measurement at time t if at time $t = 0$ a spin measurement of the ground state with outcome $+1/2$ has already

been performed.

The spin-spin correlation function after an interaction quench: Lobaskin and Kehrein in their work [27][28] addressed the question of how the spin-spin correlation function behaves after an interaction quench for a factorized initial state, both in the Toulouse limit and the limit of small Kondo couplings. They found that the algebraic long time decay survives for all non-zero waiting times, $t' > 0$, i.e. the first spin measurement is performed after the interaction has been switched. Moreover, they observe that the spin-spin correlation function approaches its equilibrium profile at zero temperature exponentially fast as a function of the waiting time. Since the initial state can never evolve into a true eigenstate of the interacting Hamiltonian due to Eq. (6.5), one cannot conclude that the system really relaxes to the new ground state as a whole. But as one can see by analyzing the nonequilibrium to equilibrium crossover for the spin-spin correlation function, the time evolved state may show equilibration behavior for suitable local observables, as, for example, the spin operator S_z.

6.3.1 The spin-spin correlation function in the periodic driving setup

In the present setup, periodically switching the interaction, one expects that after an infinite amount of periods a quasi-steady state builds up, a state such that all correlation functions are invariant under a discrete time shift of one period τ in all their time arguments, see Eq. (4.36). The existence of this quasi-steady state is ensured by the presence of a sufficient dissipation mechanism, the conduction band in the Kondo Hamiltonian plays the role of a bath that is able to absorb the infinite amount of energy that is pumped into the system by the periodic driving, see Sec. (4.1.1). In this work the quasi-steady state will be characterized by analyzing the spin-spin correlation function. As for the evaluation of the magnetization the time evolution of the spin operator S_z can be traced back to the time evolution of the single-particle operators of the quadratic effective Hamiltonian. Due to the relation $S_z = d^\dagger d - \frac{1}{2}$ the spin-spin correlation function can be written as:

$$\langle S_z(t)S_z(t')\rangle = \langle \hat{n}_d(t)\hat{n}_d(t')\rangle - \frac{1}{2}\left[S_z(t) + S_z(t')\right] - \frac{1}{4} \tag{6.35}$$

where the operator $\hat{n}_d = d^\dagger d$ measures the number of fermions on the local level of the resonant level model Hamiltonian. The average is taken with respect to the quasi-steady state, that is given by, see Eq. (6.1):

$$\langle \mathcal{O} \rangle = \lim_{N\to\infty} \langle \Psi_{GS}(N\tau)|\mathcal{O}|\Psi_{GS}(N\tau)\rangle \tag{6.36}$$

where the initial state $|\Psi_{GS}\rangle = |0\rangle \otimes |\chi\rangle$ is a product state of the Fermi sea for the spinless fermions and an arbitrary wave function $|\chi\rangle$ of the local level. In the following, all expressions will be written down without showing the limit $N \to \infty$ explicitly. The magnetization of the impurity spin in the quasi-steady state is already known from the last section, see Eq. (6.24):

$$S_z(t) = 0 \tag{6.37}$$

such that:

$$\langle S_z(t)S_z(t')\rangle = \langle \hat{n}_d(t)\hat{n}_d(t')\rangle - \frac{1}{4}. \tag{6.38}$$

For the evaluation of $\langle \hat{n}_d(t)\hat{n}_d(t')\rangle$ the time evolution of the single-particle operators d and $d^\dagger$ has to be analyzed. It is convenient to split the time coordinate $t = n\tau + s$ into two parts according to Eq. (5.107) where n is an integer and $0 \le s < \tau$. Moreover, it is sufficient for the whole calculation to assume that $s \le \tau/2$ without any restriction since in the remaining time window $[\tau/2, \tau]$ the local operators stay constant due to the absence of spin dynamics. As a consequence of the periodicity property for two-time correlation functions, see Eq. (4.36), the time coordinate t' can be restricted to the interval $[0, \tau/2]$. The operator d decays completely into bath operators exponentially fast on a times scale t_k, see Eq. (5.118), such that in the quasi-steady state:

$$d(n\tau + s) = \sum_k \left[\mathcal{G}_d(s)\mathcal{M}_{dk}^{(N+n)} + \mathcal{G}_{dk}(s)e^{-i[N+n]k\tau} \right] c_k$$
$$=: \sum_k \zeta_k(n, s)\, c_k. \tag{6.39}$$

Insertion of this relation into Eq. (6.38) yields:

$$\langle S_z(t)S_z(t')\rangle = \sum_{k_1,..,k_4} \zeta_{k_1}^*(n, s)\zeta_{k_2}(n, s)\zeta_{k_3}^*(0, t')\zeta_{k_4}(0, t')\, \langle c_{k_1}^\dagger c_{k_2} c_{k_3}^\dagger c_{k_4}\rangle - \frac{1}{4}. \tag{6.40}$$

By use of Wick's theorem

$$\langle c_{k_1}^\dagger c_{k_2} c_{k_3}^\dagger c_{k_4}\rangle = \delta_{k_1,k_2}\delta_{k_3,k_4} n_{k_1} n_{k_3} + \delta_{k_1,k_4}\delta_{k_2,k_3} n_{k_1} n_{-k_3} \tag{6.41}$$

and the initial condition $n_k = \theta(-k)$, the expression above for the spin-spin correlation function can be rewritten to yield:

$$\langle S_z(t)S_z(t')\rangle = \frac{1}{4}\left[\sum_k |\zeta_k(n, s)|^2\right]\left[\sum_k |\zeta_k(0, t')|^2\right]$$
$$+ \left[\sum_{k<0} \zeta_k^*(n, s)\zeta_k(0, t')\right]^2 - \frac{1}{4} \tag{6.42}$$

where the following property of the functions ζ has been used:

$$\zeta_k^*(n, s) = -\zeta_{-k}(n, s), \tag{6.43}$$

that originates in the corresponding behavior of the matrices $\mathcal{G}$ and $\mathcal{M}^{(N)}$. Due to Eq. (5.9), the transition matrix ζ has to be unitary such that

$$\sum_k |\zeta_k(n, s)|^2 = 1. \tag{6.44}$$

This property can be rephrased in the following way: the probability for a fermion d to transform into a fermion c_k after a time $N\tau + n\tau + s$ is given by $|\zeta_k(n, s)|^2$. Therefore, the probability to find the fermion in any of the final states has to be 1. Insertion into the expression for the spin-spin correlation function yields:

$$\langle S_z(t)S_z(t')\rangle = \left[\sum_{k<0} \zeta_k^*(n, s)\zeta_k(0, t')\right]^2 = \langle d^\dagger(t)d(t')\rangle^2. \tag{6.45}$$
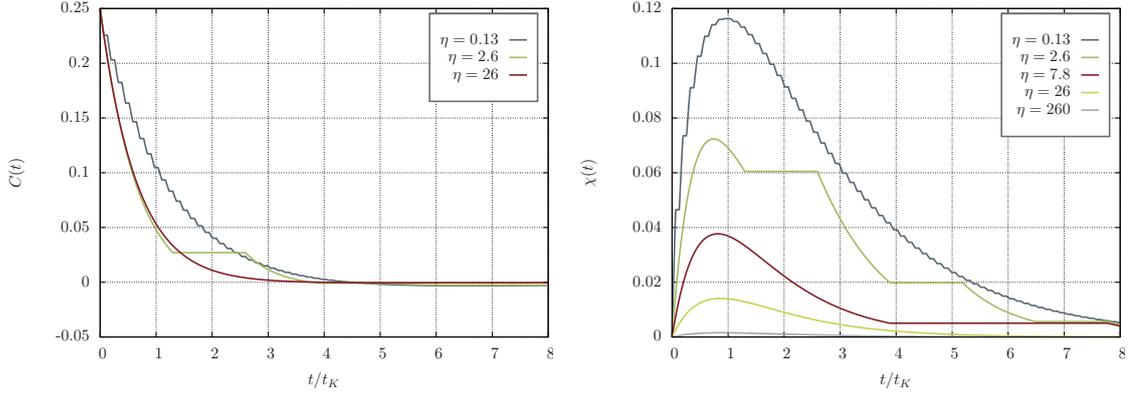
Figure 6.2: Universal curves for the symmetrized spin-spin correlation function $C(t) := C(t, 0)$ and the response $\chi(t) := \chi(t, 0)$ for different values of the parameter η.

Therefore, the evaluation of the spin-spin correlation function, that is a four-point function in terms of the single-particle operators of the effective Hamiltonian, reduces to the evaluation of a two-point function:

$$
\begin{aligned}
\langle d^\dagger(t)d(t')\rangle = V^2 \sum_{k<0} \frac{e^{ink\tau}}{k^2 + \Delta^2} &\left[e^{-\Delta[s+t']} \frac{1 - 2\cos(k\tau/2)e^{-\Delta\tau/2} + e^{-\Delta\tau}}{1 - 2\cos(k\tau)e^{-\Delta\tau/2} + e^{-\Delta\tau}} \right. \\
&+ e^{-\Delta s} \frac{e^{ik\tau/2} - e^{-\Delta\tau/2}}{e^{ik\tau} - e^{-\Delta\tau/2}} \left(e^{-ikt'} - e^{-\Delta t'} \right) \\
&+ e^{-\Delta t'} \frac{e^{-ik\tau/2} - e^{-\Delta\tau/2}}{e^{-ik\tau} - e^{-\Delta\tau/2}} \left(e^{iks} - e^{-\Delta s} \right) \\
&+ \left. \left(e^{iks} - e^{-\Delta s} \right) \left(e^{-ikt'} - e^{-\Delta t'} \right) \right] = \\
\overset{k=z\Delta}{=} \frac{1}{\pi} \int_0^\infty \mathrm{d}z \frac{e^{-iz\Delta n\tau}}{z^2 + 1} &\left[e^{-\Delta[s+t']} \frac{1 - 2\cos(z\eta/2)e^{-\eta/2} + e^{-\eta}}{1 - 2\cos(z\eta)e^{-\eta/2} + e^{-\eta}} \right. \\
&+ e^{-\Delta s} \frac{e^{-iz\eta/2} - e^{-\eta/2}}{e^{-iz\eta} - e^{-\eta/2}} \left(e^{-iz\Delta t'} - e^{-\Delta t'} \right) \\
&+ e^{-\Delta t'} \frac{e^{iz\eta/2} - e^{-\eta/2}}{e^{iz\eta} - e^{-\eta/2}} \left(e^{iz\Delta s} - e^{-\Delta s} \right) \\
&+ \left. \left(e^{-iz\Delta s} - e^{-\Delta s} \right) \left(e^{iz\Delta t'} - e^{-\Delta t'} \right) \right]
\end{aligned}
\tag{6.46}
$$

The real part of this correlator can be calculated analytically as is done in the appendix, see Sec. (B):

$$
\Re\langle d^\dagger(t)d(t')\rangle = \frac{1}{2} \left\langle \left\{ d^\dagger(t), d(t') \right\} \right\rangle = \frac{1}{2} e^{-n\Delta\tau/2} e^{-\Delta[s-t']},
\tag{6.47}
$$

in agreement with the results of Langreth and Nordlander [24]. Since the real part of the $\langle d^\dagger(t)d(t')\rangle$ correlator is proportional to an anticommutator of single-particle operators of the quadratic resonant level model Hamiltonian, it only contains information about the single-particle dynamics of the d operators and is independent of the state.

All the information about the influence of the quasi-steady state onto the spin-spin correlation function is contained in the imaginary part of the $\langle d^\dagger(t)d(t')\rangle$ correlator, that is the average of the commutator of $d^\dagger(t)$ and $d(t')$. The imaginary part is not accessible analytically, but can be evaluated numerically. Reminding that up to now the times s and t' have been restricted to the interval $[0, \tau/2]$, an extension to $[\tau/2, \tau]$ is straightforward since in this time interval the d and S_z operators do not evolve in time due to the switch off of the spin dynamics. Therefore, the spin-spin correlation function remains constant in this time window.

In Fig. (6.2) both the symmetrized correlator $C(t, 0)$ and the response $\chi(t, 0)$ are plotted for different values of the parameter η at zero waiting time in order to give a first impression of the profile of the spin-spin correlation function. A detailed discussion will be given below.

Universality of the spin-spin correlation function: As has been conjectured by Kaminski et al. [21], the conductance through a quantum dot in the Kondo regime displays universal behavior even in a time-dependent nonequilibrium setting despite the appearance of new parameters. Moreover, the Kondo temperature remains a meaningful parameter and is the only relevant energy scale. In terms of time scales this statement implies that t_k is the only relevant time scale. The same is true regarding the spin-spin correlation function in the present time-dependent setup. The Kondo time scale t_K remains a meaningful parameter and the spin-spin correlation function is given by a universal function F as Eq. (6.46) shows:

$$\langle S_z(t)S_z(t')\rangle = F\left[\frac{t}{t_K}, \frac{t'}{t_K}, \frac{\tau}{t_K}\right]. \tag{6.48}$$

Discussion of the $\langle d^\dagger(t)d\rangle$ correlator: In equilibrium one can rewrite the $\langle d^\dagger(t)d\rangle$ correlator at zero temperature in the following way:

$$\langle d^\dagger(t)d\rangle_{eq} = \langle GS|d^\dagger e^{-iH_{\mathrm{RLM}}t}d|GS\rangle = \sum_\lambda e^{-iE_\lambda t}|\langle\lambda|d|GS\rangle|^2 \tag{6.49}$$

where $|GS\rangle$ is the ground state of the resonant level model Hamiltonian H_{RLM} and the $|\lambda\rangle$'s form a complete set of eigenstates with energy E_λ. The energy of the ground state is assumed to be 0. A Fourier transform of this correlation function yields:

$$\langle d^\dagger d\rangle_{eq}(\omega) = \sum_\lambda |\langle\lambda|d|GS\rangle|^2\delta(\omega - E_\lambda),$$
$$\langle d^\dagger(t)d\rangle_{eq} = \int_{-\infty}^{\infty} \mathrm{d}\omega \, \langle d^\dagger d\rangle_{eq}(\omega). \tag{6.50}$$

Therefore, the Fourier transform $\langle d^\dagger d\rangle_{eq}(\omega)$ can be interpreted as the probability density for the ground state with a d hole injected to have energy ω. Alternatively, one can claim the Fourier transform to be the probability density for decreasing ($\omega < 0$) or increasing ($\omega > 0$) the energy in the system by extracting a local fermion. Comparing Eq. (6.31) with Eq. (6.50), the Fourier transform can be read off:

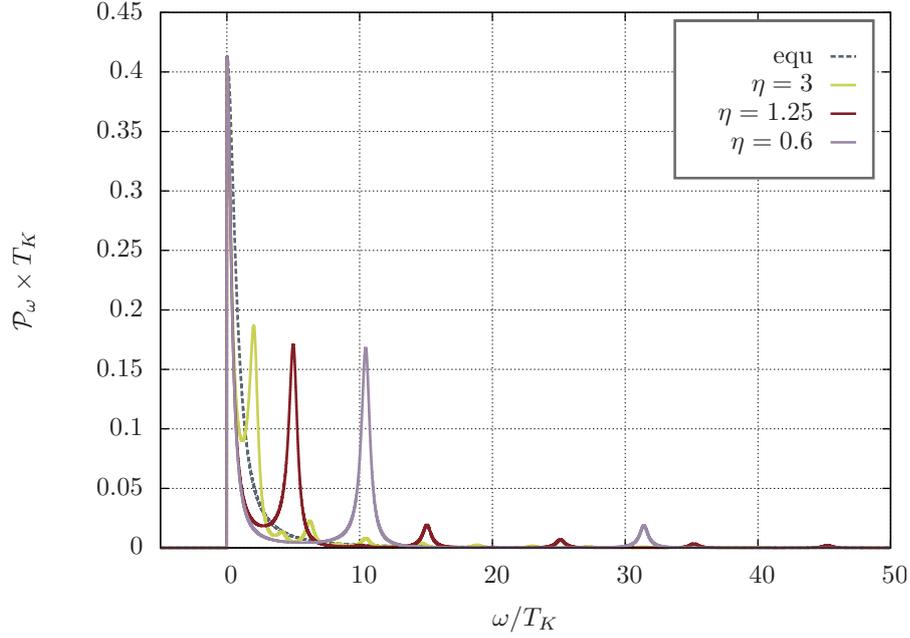$$\langle d^\dagger d\rangle_{eq}(\omega) = \frac{\Delta}{\pi}\frac{\theta(\omega)}{\omega^2 + \Delta^2}. \tag{6.51}$$

Figure 6.3: Probability distribution for a local d fermion to have energy ω

The θ-function ensures that no energy can be gained by the creation of a local hole since the system already is in the ground state such that the bath of surrounding fermions is not able to supply energy to a fermion tunneling out of the local level. It is only possible for the tunneling out fermion to supply energy to the bath. For finite temperatures the θ-function has to be replaced by a Fermi distribution.

In the periodic driving setup the $\langle d^\dagger(t)d(t')\rangle$ correlator depends on two time arguments. As a representative example one can regard the case of zero waiting time, i.e. $t' = 0$, and the case where t takes values of multiples of the period,i.e. $t = n\tau$, such that the time evolution of this correlator is analyzed in a stroboscopic manner. This will display the main features if the period of the switching is not too large compared to the internal time scale such that $\eta \lesssim 1$. In this case:

$$\langle d^\dagger(t)d\rangle = \frac{\Delta}{\pi} \int_0^\infty d\omega \, \frac{e^{-i\omega t}}{\omega^2 + \Delta^2} \frac{1 - 2\cos(\omega\tau/2)e^{-\Delta\tau/2} + e^{-\Delta\tau}}{1 - 2\cos(\omega\tau)e^{-\Delta\tau/2} + e^{-\Delta\tau}} \tag{6.52}$$

Due to the previous considerations, one can regard

$$\mathcal{P}_\omega = \frac{\Delta}{\pi} \frac{\theta(\omega)}{\omega^2 + \Delta^2} \frac{1 - 2\cos(\omega\tau/2)e^{-\Delta\tau/2} + e^{-\Delta\tau}}{1 - 2\cos(\omega\tau)e^{-\Delta\tau/2} + e^{-\Delta\tau}} \tag{6.53}$$

to be the probability density that a local fermion tunneling out of the system lowers ($\omega < 0$) or increases ($\omega > 0$) the energy in the quasi-steady state. A plot of $\mathcal{P}_\omega$ is shown in Fig. (6.3) for different values of the parameter η. A comparison with the equilibrium probability density, see Eq. (6.50), shows that the time-dependent nonequilibrium setup only leads to an additional multiplicative factor. Analogously to the equilibrium case a θ-function appears suggesting to think of the bath as to behave for zero temperature. Therefore, a local fermion tunneling out of the system cannot extract energy from the bath as before. As one can see in the plot, the probability density of increasing the

energy in the system is enhanced at multiples of the driving frequency accounting for processes where multiples of Ω are absorbed. Remarkably, the bath of fermions behaves as for zero temperature although energy is pumped into the system by the periodic driving.

A possible process of extracting a local fermion and later reentering that leads to an increase of energy in the system is the following. Suppose, at time $t = 0$ a local fermion tunnels out of the system leaving behind a hole on the local d level. This vacancy can be filled by a bath fermion around the Fermi surface. By absorbing n quanta of Ω this fermion can hop back into the continuum of bath states. Thus, at time t a fermion is able to tunnel back onto the local level. During this process an energy $n\Omega$ has been put into the system.

At this point one can ask the question why the bath behaves as at zero temperature despite the existence of excitations? As was shown in the previous chapter, the only process that creates excitations driven by the periodic time dependence of the Kondo Hamiltonian, is that fermions can hop onto or hop off the local level by absorbing or emitting multiples of the driving frequency. It is not possible to induce transition for the bath fermions directly. Therefore, excitations can only be created by hopping processes. Due to Eq. (5.64), a fermion that has been on the local level once is not influencing local properties any more after tunneling into the continuum of bath states. Therefore, one can imagine that the excitations are flowing infinitely far away from the local level into the bath without returning such that multiple hopping processes will not take place. Concluding one can state that the excitations that are created in the periodic driving setup always depart from the central region and do not contribute to the local properties any more.

Discussion of the results for the spin-spin correlation function: Here, general features of the spin-spin correlation function will be discussed. The asymptotic behavior will be studied later. In Fig. (6.4), false color plots for the symmetrized spin-spin correlation function $C(t + t', t')$ and for the response $\chi(t + t', t')$ are shown. Both C and χ are invariant under a discrete time shift of τ in both arguments due to Eq. (4.36). Therefore, the time coordinate t' can be restricted to the interval $[0, \tau]$. These plots show how the spin-spin correlation function behaves if the point in time t' of the first measurement is varied over one period.

In the case of fast switching, corresponding to the plot with $\eta = 0.13$, the symmetrized part as well as the response are nearly constant if t' is varied over the period. Therefore, the system is not sensitive to the specific point in time of the first spin measurement. Since the system can change its behavior only on times of the order of the internal time scale, that is t_K in this case, the system's properties like the response to a magnetic field χ cannot vary substantially on a time scale τ in the limit of fast switching. Therefore, the system is not able to adapt within one period.

In the opposite case of large switching times, the $\eta = 13$ plot, the spin-spin correlation function depends crucially on the time coordinate t'. As argued in Sec.(6.1.1), the Kondo system is expected to behave in the same way as for a single interaction quench in the limit of large periods, i.e. $\tau \gg t_K$. This nonequilibrium setting has already been considered in the work by Lobaskin and Kehrein [27]. They found that the spin-spin correlation function approaches its equilibrium behavior exponentially fast as a function of the waiting time t' on a time scale t_K. This can be seen most clearly in the plot
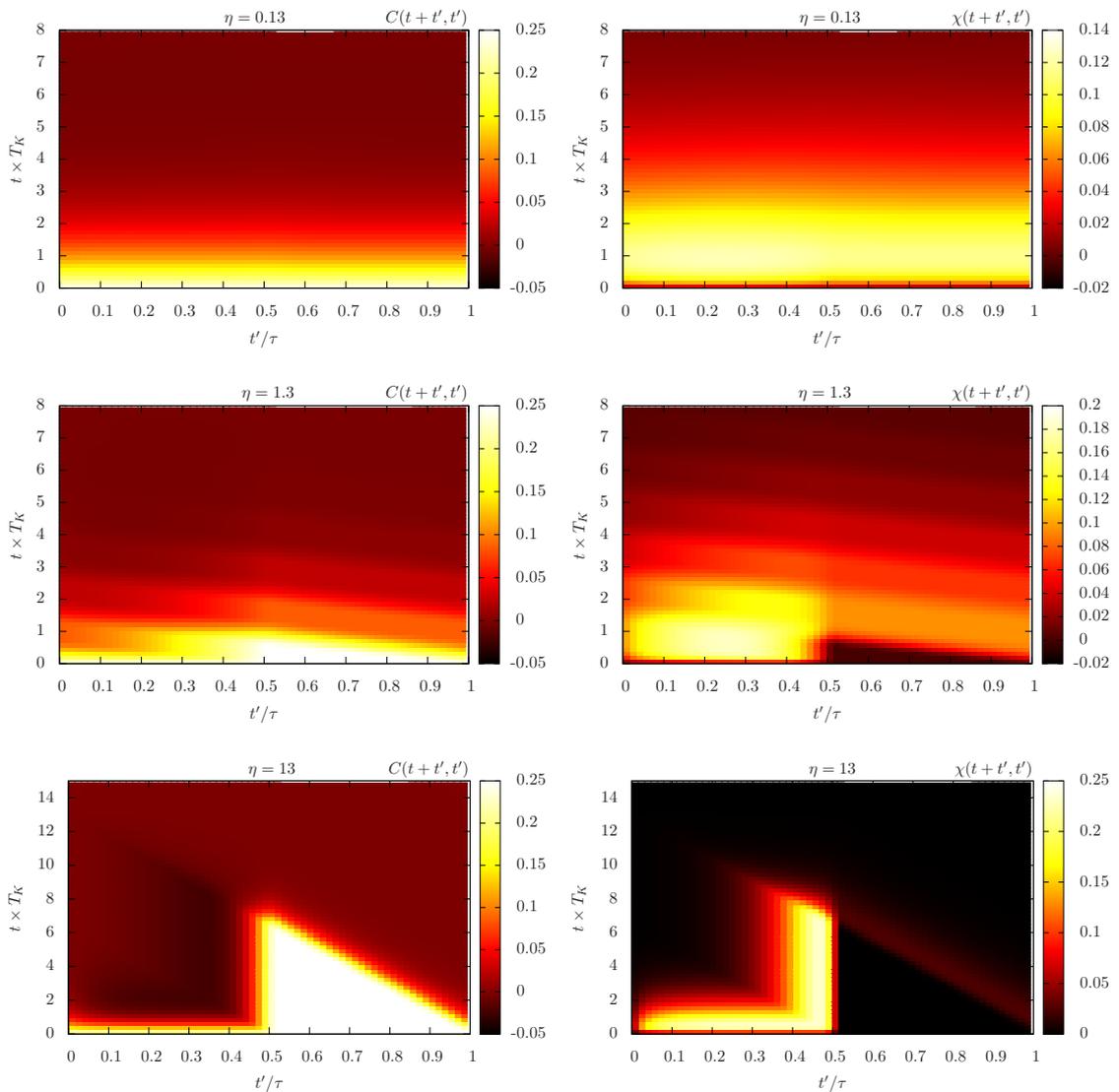
Figure 6.4: False color plot for the symmetrized spin-spin correlation function $C(t + t', t')$ and the response $\chi(t + t', t')$ for three different values of the parameter η where $t > 0$. On the left hand side, the plots for $C(t + t', t')$ are shown in ascending order of the parameter η, on the right hand side the corresponding plots for $\chi(t + t', t')$
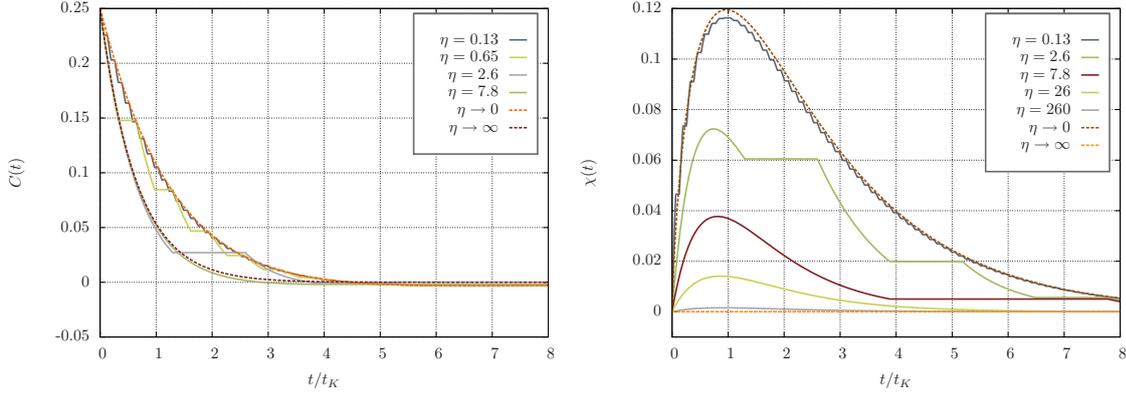
Figure 6.5: Universal curves for C and χ in the fast and slow switching limits

of the dynamical susceptibility. After a transient time of the order t_K, a peak builds up and the dynamical susceptibility evolves into its equilibrium profile that is shown in Fig. (6.1). Near the half period boundary, a new structure appears. Due to the switch off of the spin dynamics during the second half period, the spin operators as well as the spin-spin correlation function are freezed if $\tau > t + t' > \tau/2$ as can be seen in the plot. As a consequence plateaus emerge whose heights depend on the value of C and χ at the moment of the switch off.

If the time scale of the external driving τ is of the same order as the internal time scale t_K, the $\eta = 1.3$ plot, a mixture of both the fast and slow switchings cases is observed. Both C and χ don't vary substantially over one period and one can see the existence of plateaus.

6.3.2   The spin-spin correlation function in the limit of long switching times

As elaborated in Sec. (6.1.1), the general features of correlation functions, involving suitable local observables like the spin operator S_z, in the limit of long switching times $\tau \to \infty$ are accessible by general arguments. Basically, the system relaxes in each half period where relaxation is to be understood in the sense of relaxation of expectation values of suitable observables, as discussed in Sec. (6.1.1). If the system relaxes in each half period, two-time correlation functions are expected to behave analogously to a single interaction quench setting. This will be shown in the following for the spin-spin correlation function.

In the $\tau \to \infty$ limit, it is reasonable to assume for the time coordinates t and t' to take values in the interval $[0, \tau/2]$ such that $n = 0$ in Eq. (6.46). For $\tau \to \infty$, the $\langle d^\dagger(t)d(t)\rangle$ correlator transforms into:

$$
\begin{aligned}
\langle d^\dagger(t)d(t')\rangle \overset{\tau\to\infty}{\approx} \frac{\Delta}{\pi} \int_0^\infty \mathrm{d}k \, &\frac{1}{k^2 + \Delta^2} \left[e^{-\Delta[t+t']} + e^{-\Delta t}e^{ik\tau/2}\left(e^{ikt'} - e^{-\Delta t'}\right) \right. \\
&+ e^{-\Delta t'}e^{-ik\tau/2}\left(e^{-ikt} - e^{-\Delta t}\right) + e^{-ik[t-t']} - e^{-\Delta t'}e^{-ikt} \\
&\left. - e^{-\Delta t}e^{ikt'} + e^{-\Delta[t+t']} \right].
\end{aligned}
\tag{6.54}
$$

As is shown in the appendix, see Eq. (A.5), the integral $\Delta/\pi \int_0^\infty dk\, e^{ik\tau/2}/(k^2 + \Delta^2) \approx$ $2i/(\pi\Delta\tau) \to 0$ vanishes in the $\tau \to \infty$ limit such that the correlator above transforms into:

$$\langle d^\dagger(t)d(t')\rangle \xrightarrow{\tau\to\infty} \frac{\Delta}{\pi} \int_0^\infty dk\, \left[2e^{-\Delta[t+t']} + e^{-ik[t-t']} - e^{-\Delta t'}e^{-ikt} - e^{-\Delta t}e^{ikt'}\right]$$
$$= \frac{1}{2}e^{-\Delta[t-t']} - i\left[s(t-t') + e^{-\Delta t}s(t') - e^{-\Delta t'}s(t)\right] \tag{6.55}$$

where the function $s(t)$ is given by Eq. (6.32). Due to Eq. (6.45), the spin-spin correlation function can be obtained by squaring the $\langle d^\dagger(t)d(t')\rangle$ correlator leading to:

$$\langle S_z(t)S_z(t')\rangle \xrightarrow{\tau\to\infty} \frac{1}{4}e^{-2\Delta[t-t']} - \left[s(t-t') + e^{-\Delta t}s(t') - e^{-\Delta t'}s(t)\right]^2$$
$$- ie^{-\Delta[t-t']}\left[s(t-t') + e^{-\Delta t}s(t') - e^{-\Delta t'}s(t)\right]. \tag{6.56}$$

This result matches precisely the result for the spin-spin correlation function obtained by Lobaskin and Kehrein [27] in a single interaction quench scenario in the Kondo model, exactly as was argued in Sec. (6.1.1). Therefore, the analysis in this regime can be simply adopted from their work. The nonequilibrium to equilibrium crossover is exponentially fast as a function of the waiting time t' on a time scale t_K. For all nonzero waiting times, the spin-spin correlation function decays algebraically $\propto (t-t')^2$ in the limit $t - t' \to \infty$. For $t' = 0$, however, the decay is exponentially fast and the spin-spin correlation function reduces to half of the magnetization after a single quench, a setting that is shown in Fig. (6.5) where the asymptotic curves for $\eta = \infty$ are included. As one can see, the numerical results for the spin-spin correlation function approach the analytical asymptotic behavior. The response $\chi(t)$, proportional to the imaginary part of $\langle S_z(t)S_z\rangle$, declines becoming zero in the $\eta \to \infty$ limit.

6.3.3   The spin-spin correlation function in the limit of fast switching

The opposite limit of fast switching, i.e. $\tau \to 0$, requires more care as already emphasized earlier, see Sec. (6.1.2). In general, the system is not able to follow the fast external driving. Indeed, it will be shown in this section that the spin-spin correlation function approaches a behavior that is similar to an equilibrium setting.

In the beginning, the analysis will focus on the $\langle d^\dagger(t)d(t')\rangle$ correlator since the spin-spin correlation function can be obtained easily from this function, see Eq. (6.45). The real part of the $\langle d^\dagger(t)d(t')\rangle$ correlator is known analytically, see Eq. (6.47), such that the limit can be performed straightforwardly. Since s and t' take values in the interval $[0, \tau/2]$, $s, t' \to 0$ in the limit $\tau \to 0$ such that the $\langle d^\dagger(t)d(t')\rangle$ correlator only depends on one time coordinate $t = n\tau$ signaling that the system approaches an equilibrium-like behavior in the limit of fast switching. The real part of the correlator transforms into:

$$\Re\langle d^\dagger(t)d(t')\rangle \xrightarrow{\tau\to0} \frac{1}{2}e^{-\Delta t/2}, \tag{6.57}$$

that is identical to the real part of the correlator in an equilibrium setting, see Eq. (6.31), except that the time coordinate has to be rescaled, $t \to t/2$, since only half of the time

the d operators can evolve nontrivially. The imaginary part can be obtained in the fast switching limit in the following way:

$$
\begin{aligned}
\Im\langle d^\dagger(t)d(0)\rangle = -\frac{\Delta}{\pi}\int_0^\infty \mathrm{d}k\,\frac{\sin(kt)}{k^2+\Delta^2}\underbrace{\frac{1-2\cos(k\tau/2)e^{-\Delta\tau/2}+e^{-\Delta\tau}}{1-2\cos(k\tau)e^{-\Delta\tau/2}+e^{-\Delta\tau}}}_{\xrightarrow{\tau\to 0}\dfrac{k^2+\Delta^2}{4k^2+\Delta^2}} \\
\xrightarrow{\tau\to 0} -\frac{\Delta}{\pi}\int_0^\infty \mathrm{d}k\,\frac{\sin(kt)}{4k^2+\Delta^2} = -\frac{\Delta}{2\pi}\int_0^\infty \mathrm{d}k\,\frac{\sin(kt/2)}{k^2+\Delta^2} \\
= -\frac{1}{2}s(t/2),
\end{aligned}
\tag{6.58}
$$

also displaying behavior similar to equilibrium. The function $s(t)$ is given by Eq. (6.32). In equilibrium, $\langle d^\dagger(t)d(0)\rangle = \frac{1}{2}e^{-\Delta t} - is(t)$, see Eq. (6.31). The imaginary part of the $\langle d^\dagger(t)d\rangle$ correlator containing the information about the initial state, however, acquires an additional prefactor of $1/2$ compared to the real part where only the time coordinate has been modified. Therefore, the real and imaginary part transform qualitatively different in the fast switching limit. Thus, it is not possible to find a time-independent effective Hamiltonian that generates the same dynamics. Finally, the spin-spin correlation function in the limit $\tau \to 0$ reads:

$$
\langle S_z(t)S_z(0)\rangle \xrightarrow{\tau\to 0} \left[\frac{1}{2}e^{-\Delta t/2} - \frac{i}{2}s(t/2)\right]^2.
\tag{6.59}
$$

A plot of the spin-spin correlation function in this limit can be found in Fig. (6.5). Obviously, the numerical results for the spin-spin correlation function approach the calculated asymptotic behavior for small switching times.

6.3.4   The long-time asymptotic behavior: no effective temperature

As mentioned in the beginning of this chapter, the spin-spin correlation function exhibits a characteristic algebraic long-time decay at zero temperature in equilibrium:

$$
\langle S_z(t)S_z(t')\rangle \overset{t\to\infty}{\propto} (t-t')^{-2}
\tag{6.60}
$$

in contrast to the long-time behavior at finite temperature where the decay is exponential due to a smearing of the Fermi surface. This sensitivity can be used to test if the concept of effective temperature is applicable in the periodic driving setup.

The long-time asymptotics for the spin-spin correlation function can be determined by evaluating the asymptotics for the $\langle d^\dagger(t)d(t')\rangle$ correlator since both correlation functions are connected by quadrature, see Eq. (6.45). The complicated functions of the integrand in Eq. (6.46) are periodic in k with period 2Ω such that they can be expanded into a Fourier series:

$$
\begin{aligned}
\frac{1-2\cos(k\tau/2)e^{-\Delta\tau/2}+e^{-\Delta\tau}}{1-2\cos(k\tau)e^{-\Delta\tau/2}+e^{-\Delta\tau}} = \sum_{n\in\mathbb{Z}} c_n e^{ink\tau/2}, \\
\frac{e^{ik\tau/2}-e^{-\Delta\tau/2}}{e^{ik\tau}-e^{-\Delta\tau/2}} = \sum_{n\in\mathbb{Z}} d_n e^{ink\tau/2}.
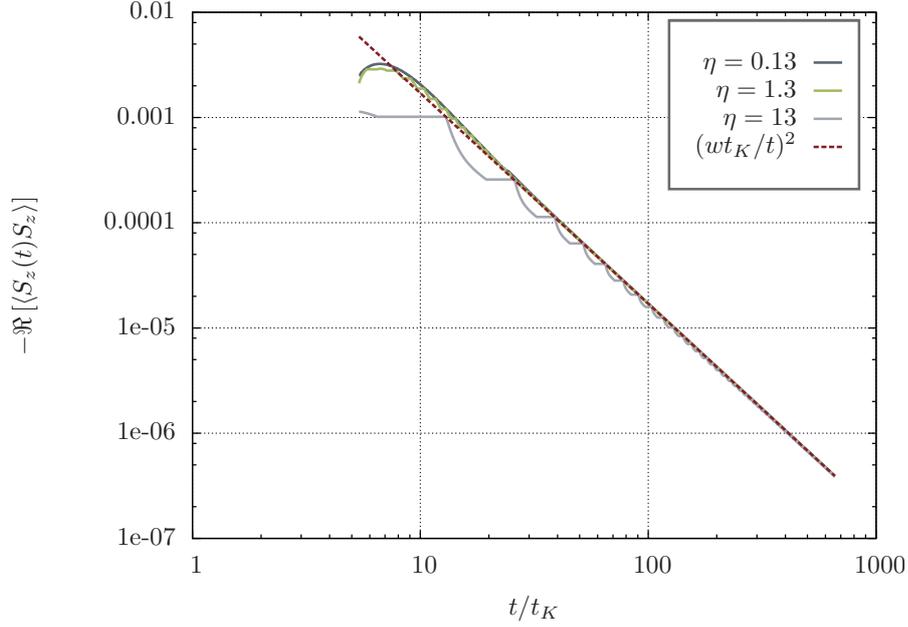\end{aligned}
\tag{6.61}
$$

Figure 6.6: Asymptotic long-time behavior of the spin-spin correlation function

The Fourier coefficients c_n and d_n can be found in the appendix, see Eq. (A.1). Their precise expressions are not important for the evaluation of the desired asymptotics, they decay exponentially as the index n is increased. The long time behavior of the spin-spin correlation function is completely determined by choosing $t = n\tau$ and $s = 0$. Inserting the Fourier series expansions into Eq. (6.46) yields:

$$\langle d^\dagger(t)d(t')\rangle = e^{-\Delta t'} \sum_n [c_n - d_{-n}] \frac{\Delta}{\pi} \int_0^\infty \mathrm{d}k \, \frac{e^{-ik(t-n\tau/2)}}{k^2 + \Delta^2} \\ + \sum_n d_{-n} \frac{\Delta}{\pi} \int_0^\infty \mathrm{d}k \, \frac{e^{-ik(t-t'-n\tau/2)}}{k^2 + \Delta^2}. \tag{6.62}$$

Due to Eq. (A.5), the asymptotic behavior of the integrals as $t \to \infty$ are known such that:

$$\langle d^\dagger(t)d(t')\rangle \xrightarrow{t-t'\to\infty} e^{-\Delta t'} \sum_n [c_n - d_{-n}] \frac{-i}{\pi\Delta t} + \sum_n d_{-n} \frac{-i}{\pi\Delta(t-t')}. \tag{6.63}$$

Since both $\sum_n c_n = 1$ and $\sum_n d_n = 1$, the first term in the expression above vanishes. Due to Eq. (3.99), $T_K = \pi w \Delta$ where $w = 0.4128$ is the wilson number, the $\langle d^\dagger(t)d(t')\rangle$ correlator can be written in terms of the Kondo time scale $t_k = 1/T_K$:

$$\langle d^\dagger(t)d(t')\rangle \xrightarrow{t\to\infty} -i \, \frac{w \, t_K}{t - t'}. \tag{6.64}$$

Therefore, the spin-spin correlation function decays algebraically for long times:

$$\langle S_z(t)S_z(t')\rangle \overset{t-t'\to\infty}{\longrightarrow} -(w\,t_K)^2 \frac{1}{(t-t')^2} \qquad (6.65)$$

.

Remarkably, the asymptotic long-time behavior is independent of the periodic time-dependent setting regardless of the strength of the driving. Moreover, this asymptotic behavior matches exactly the equilibrium behavior at zero temperature. Even the prefactor is identical and is not modified by the driving. In Fig. (6.6) the analytical curve is compared to numerical results for three different values of the parameter η. Obviously, all curves reach the algebraic behavior asymptotically.

The matching of the equilibrium zero temperature long-time decay and the asymptotic behavior in the periodic driving setup indicates that a description of the quasi-steady state in terms of an effective temperature is not possible. As the analysis of the $\langle d^\dagger(t)d(t')\rangle$ correlator showed, the bath of fermions behaves as for zero temperature, it is not possible to extract energy out of it. Nevertheless, excitations are created in the periodically driven system but they are fundamentally different from those that are created by temperature. The excitations in a system periodically in time are excitations of multiples of the driving frequency Ω corresponding to the absorption of multiple quanta of Ω thereby forming a discrete ladder of excitations. At finite temperature, the Fermi surface gets smeared over a width $\sim T$. But as has been shown for the $\langle d^\dagger(t)d(t')\rangle$ correlator, no smearing takes place, the Fermi surface remains sharp. Since the long-time limit of the spin-spin correlation function is dominated by the low energy degrees of freedom, the excitations of multiples of the driving frequency are irrelevant for the asymptotic behavior such that the equilibrium zero temperature behavior is recovered. Therefore, it is not possible to characterize the quasi-steady state by an effective temperature.

6.4 Dynamical spin susceptibility

The result for the magnetization of the impurity spin, see Eq.(6.24), showed that the impurity spin expectation value is zero in the quasi-steady state. There is no source for spin generation in the present setup since the total spin

$$S_T = \hat{\mathcal{N}}_s + S_z \qquad (6.66)$$

is a conserved quantity [7]. The operator $\hat{\mathcal{N}}_s = \frac{1}{2}[\hat{N}_\uparrow - \hat{N}_\downarrow]$ measures the total spin of the bath of conduction band electrons, see Eq. (3.83). A spin generating source can be created, for example, by applying a magnetic field $h(t)$ to the local spin. If one can assume the magnetic field $h(t)$ to be classical such that fluctuations can be neglected, the Hamilton operator reads:

$$H_h(t) = H(t) - h(t)S_z. \qquad (6.67)$$

Here, the leakage of the magnetic field to the conduction band is neglected, it only couples to the local spin. If the amplitude of the field is small, linear response theory
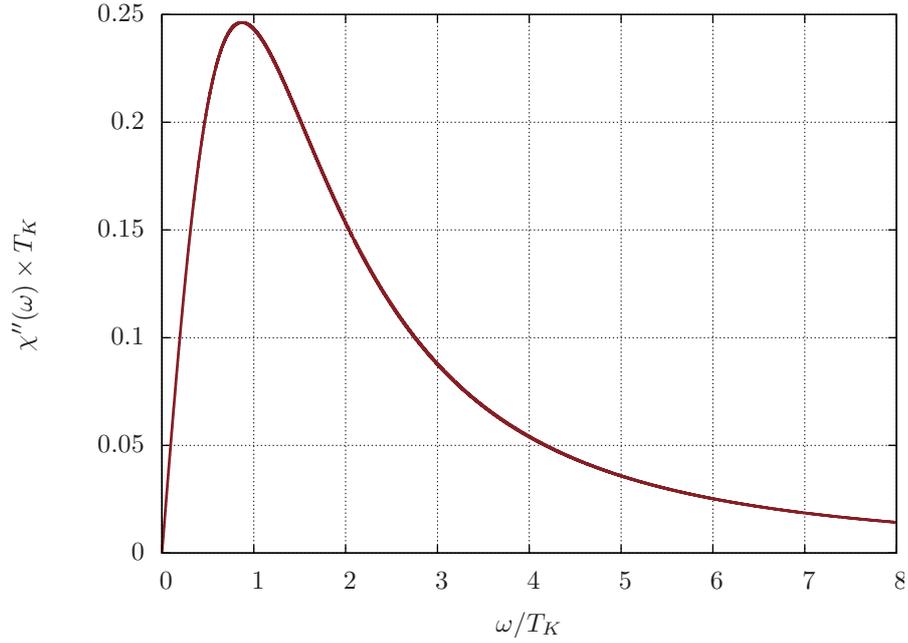
Figure 6.7: Universal curve for the imaginary part of the dynamical spin susceptibility in equilibrium at zero temperature

is applicable predicting for the magnetization of the impurity spin up to second order corrections in the magnetic field:

$$
\langle S_z(t) \rangle_h = \langle S_z(t) \rangle + \int_{-\infty}^{\infty} \mathrm{d}t' \, \chi(t,t')h(t'),
$$
$$
\chi(t,t') = i\theta(t-t')\langle \left[S_z(t), S_z(t') \right] \rangle.
$$
(6.68)

All expectation values that are not marked with an index h are to be evaluated with respect to the unperturbed Hamiltonian without the magnetic field term. The expectation value $\langle S_z(t) \rangle$ vanishes in the quasi-steady state due to Eq. (6.24) such that:

$$
\langle S_z(t) \rangle_h = \int_{-\infty}^{\infty} \mathrm{d}t' \, \chi(t,t') \, h(t').
$$
(6.69)

The response function in equilibrium: The response function $\chi(t,t')$ only depends on the time difference $t - t'$ in equilibrium leading to a reduction to a function of only one argument, i.e. $\chi(t,t') = \chi(t - t')$. Therefore, there exists a spectral representation in terms of only one frequency, called the dynamical spin susceptibility. The imaginary part can be obtained analytically for zero temperature [15] [25]:

$$
\chi(\omega) = \int_{-\infty}^{\infty} \mathrm{d}t \, e^{i\omega t} \chi(t)
$$
$$
\chi''(\omega) = \Im\left[\chi(\omega)\right] = \frac{2\Delta^2}{\pi} \frac{1}{\omega^2 + 4\Delta^2} \left[\frac{1}{\omega} \ln\left(1 + \left(\frac{\omega}{\Delta}\right)^2 \right) + \frac{1}{\Delta} \arctan\left(\frac{\omega}{\Delta}\right) \right]
$$
(6.70)

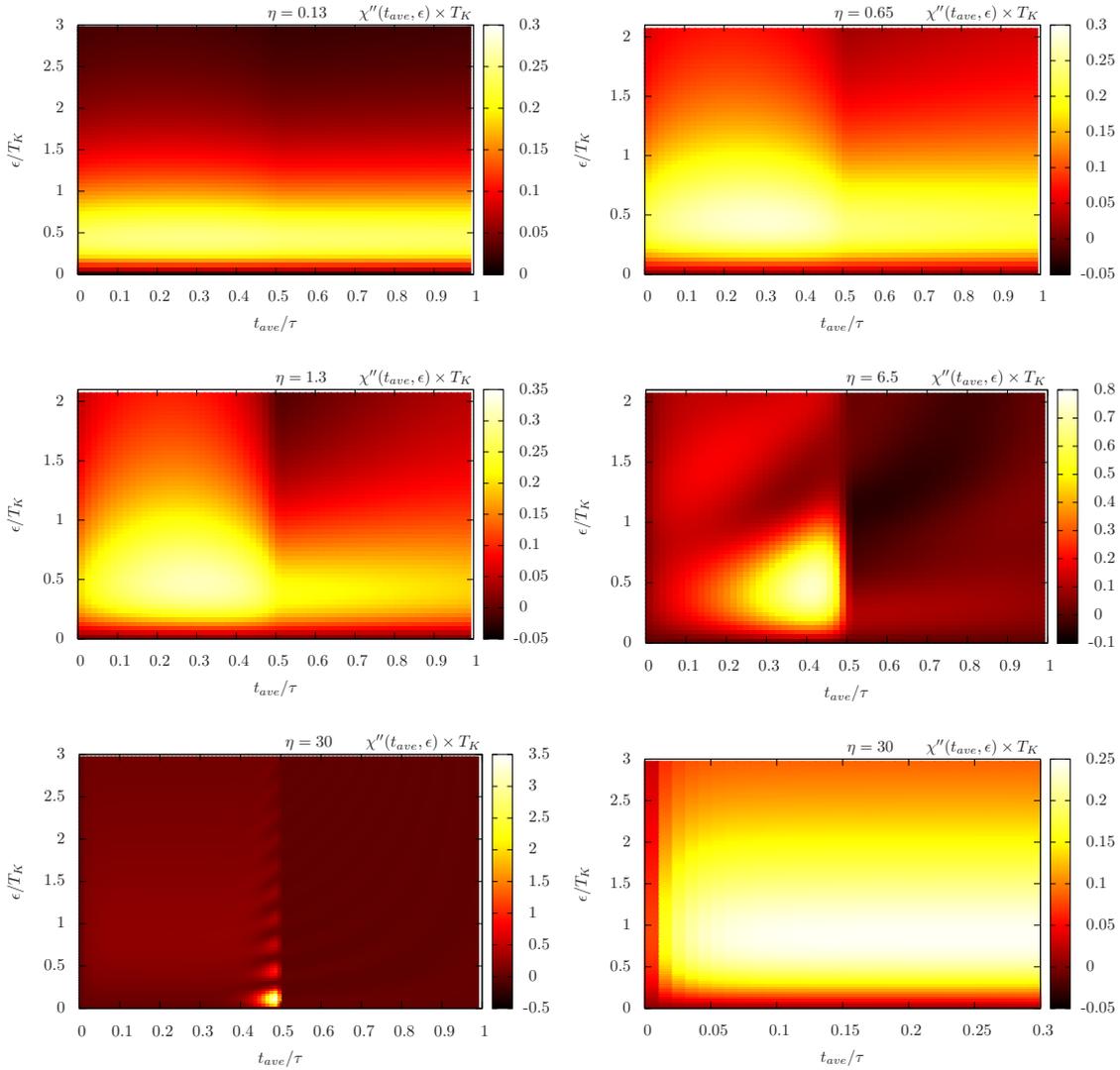A plot of $\chi''(\omega)$ is shown in Fig. (6.7).

Figure 6.8: Spectral decomposition of the imaginary part of the dynamical spin susceptibility $\chi''(t_{ave}, \varepsilon)$ in false color plots for different parameters η. These plots show the low frequency behavior over one period.
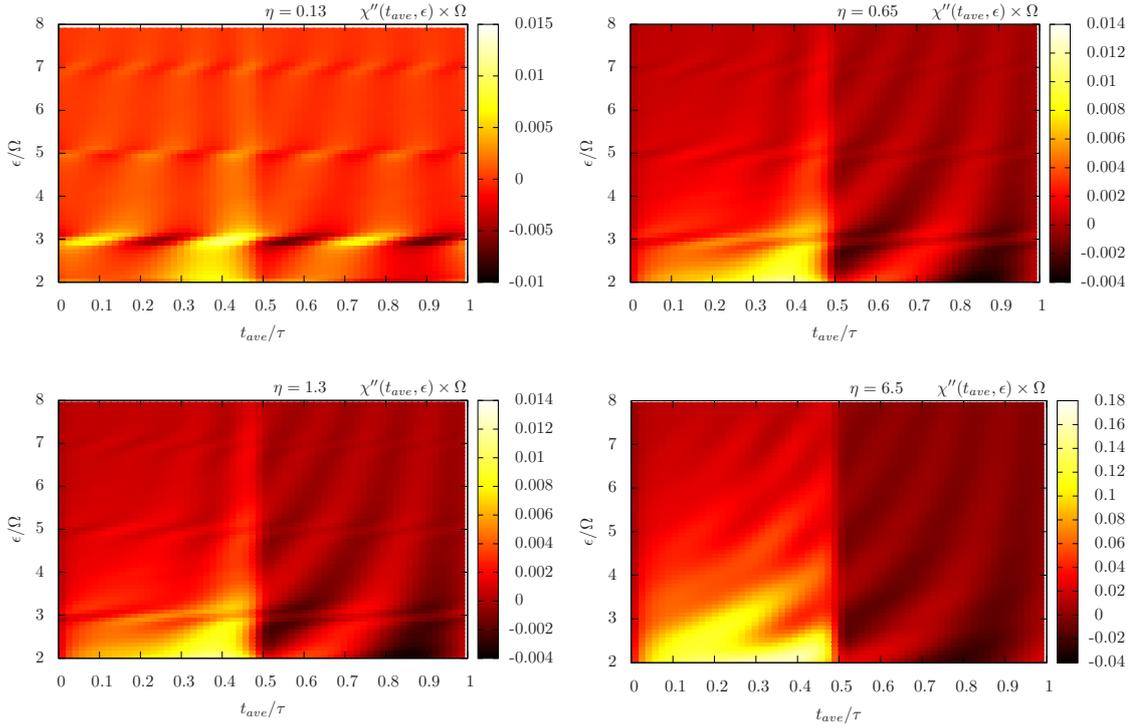
Figure 6.9: Imaginary part of the dynamical susceptibility at high energies for different values of the parameter η.

The response function in nonequilibrium: According to Eq. (4.42), one can derive a spectral decomposition of the response function in the time-dependent nonequilibrium setup:

$$\chi(t_{ave}, \varepsilon) = \int_{-\infty}^{\infty} \mathrm{d}t_{rel}\, e^{i\varepsilon t_{rel}}\, \chi(t_{ave} + t_{rel}, t_{ave}) \tag{6.71}$$

that can be interpreted as the spectral decomposition of the response function at a given point t_{ave} in time. Due to Eq. (4.36), the function $\chi(t_{ave}, \varepsilon)$ is periodic in the time argument with period τ, $\chi(t_{ave} + \tau, \varepsilon) = \chi(t_{ave}, \varepsilon)$, such that t_{ave} can be restricted to the interval $[0, \tau]$.

The dynamical susceptibility cannot be analyzed analytically. Therefore, numerical results are plotted in Fig. (6.8) and Fig. (6.9) as false color plots. The low frequency behavior is shown in Fig. (6.8) whereas the high frequency sector is contained in Fig. (6.9).

The limit of fast switching: For fast switching, the $\eta = 0.13$ plot, the dynamical spin susceptibility approaches a behavior similar to equilibrium, see Sec. (6.3.3). The spectral decomposition of the response function remains nearly constant over the whole period. As explained before, this behavior originates in a mismatch of time scales. Namely, the internal time scale t_k is much larger than the external time scale τ such that the system cannot adapt to the fast change of parameters that is caused by the external driving. In Sec.(6.3.3), an analytical expression for the spin-spin correlation function was derived
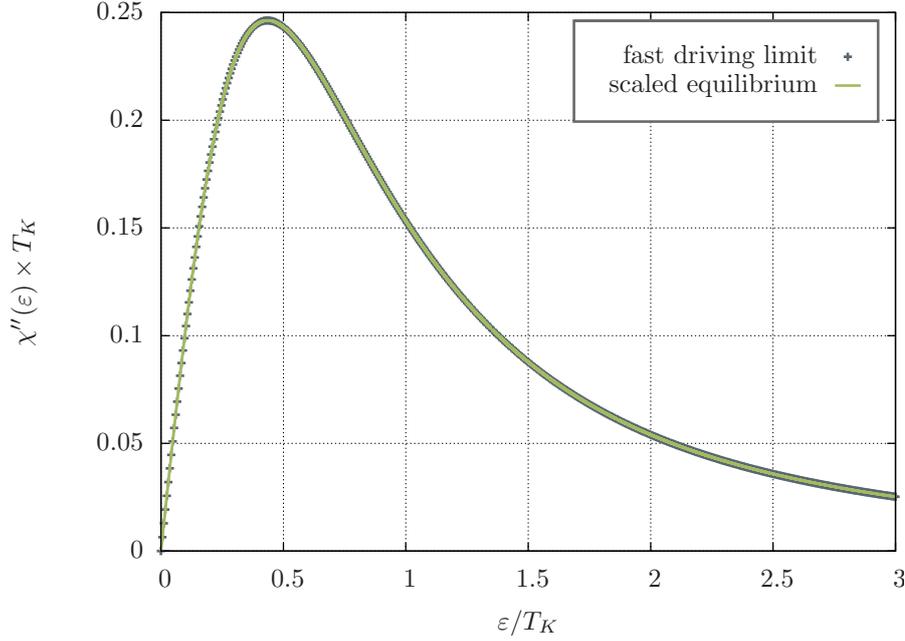
Figure 6.10: Comparison of the scaled equilibrium dynamical susceptibility with the numerical results for the fast switching limit shows perfect agreement.

in the limit of fast driving where the response function obeys the following formula:

$$\chi_{neq}^{\tau \to 0}(t) = \frac{1}{2}\,\theta(t)\,e^{-\Delta t/2}\,s(t/2) \tag{6.72}$$

Note, that in the limit $\tau \to 0$, the response function only depends on one time coordinate indicating the similarity to an equilibrium behavior. Moreover, the response function is identical to an equilibrium response function, see Eq. (6.31), except that the time coordinate is rescaled, $t \to t/2$, and the amplitude is reduced by one half such that one can write:

$$\chi_{neq}^{\tau \to 0}(t) = \frac{1}{2}\chi_{eq}(t/2). \tag{6.73}$$

The rescaling of the time coordinate can be explained by the fact that only half of the time the spin dynamics are switched on, such that the S_z operators only evolve during half of the time. A relation as in Eq. (6.73) in time implies the following relation for the corresponding Fourier transforms:

$$\chi_{neq}^{\tau \to 0}(\omega) = \chi_{eq}(2\omega) \tag{6.74}$$

such that:

$$\chi_{neq}''(\omega) = \frac{\Delta^2}{2\pi}\frac{1}{\omega^2 + \Delta^2}\left[\frac{1}{2\omega}\ln\left(1 + \left(\frac{2\omega}{\Delta}\right)^2\right) + \frac{1}{\Delta}\arctan\left(\frac{2\omega}{\Delta}\right)\right] \tag{6.75}$$

The scaled equilibrium dynamical spin susceptibility is compared with the numerical nonequilibrium result in Fig. (6.10). The plotted fast driving limit curve is obtained by a time average of the $\eta = 0.13$ result in Fig. (6.8). Note the perfect agreement of both
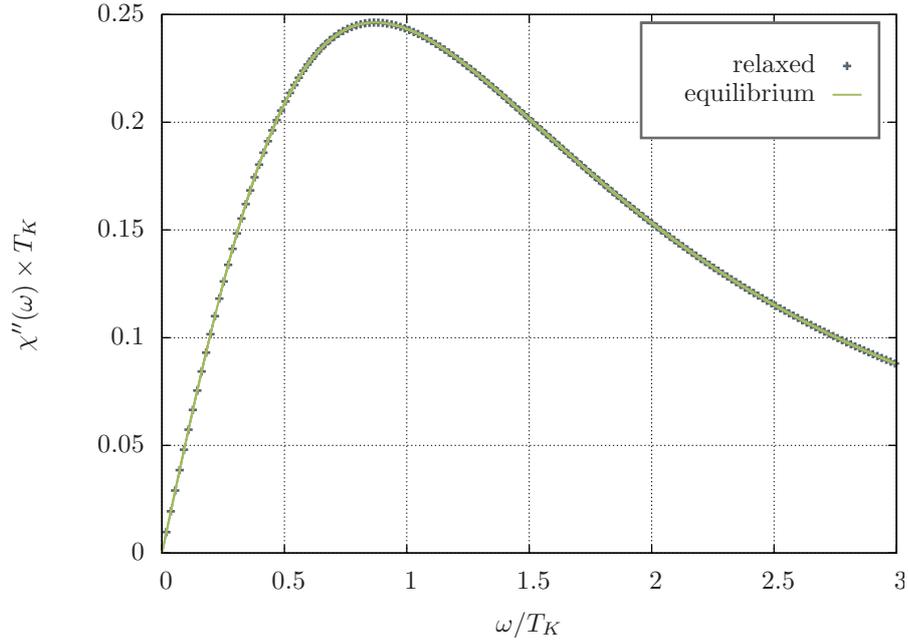
Figure 6.11: Comparison of the relaxed and equilibrium dynamical susceptibility

curves such that the numerical precision of the results for the dynamical susceptibility can be assumed to be very accurate.

In the high energy sector, see Fig. (6.9), pronounced structures can be observed at odd multiples of the driving frequency Ω implying an enhanced response of the local spin for a harmonic external magnetic field with frequency $n\Omega$, n odd. The exclusion of even multiples of the driving frequency seems not very intuitive at first sight since one expects to observe structures at all multiples of the driving frequency. The reason for the restriction to odd multiples of Ω stems from the fact that a square wave, that is the profile of the modulation in the Kondo Hamiltonian, only consists of odd harmonics if one performs a Fourier series expansion:

$$\theta(\sin \Omega t) = -\sum_{n \in 2\mathbb{Z}+1} \cos(n\Omega t). \tag{6.76}$$

Intermediate switching times: Lowering the frequency of the switching, i.e. increasing η, enables the system to adapt to the change in parameters, the dependence of $\chi''(t_{ave}, \epsilon)$ on the coordinate t_{ave} becomes increasingly important. As the spin dynamics are switched on at $t_{ave} = 0$, the Kondo singlet tries to form, the equilibrium shape of the equilibrium dynamical susceptibility tries to build up with a peak located near T_K, see Eq. (6.7). For $\eta \sim 1$, however, it is not possible for the Kondo singlet to fully develop. Towards the half period boundary the dynamical susceptibility collapses and stays nearly constant over the second half period where its profile resembles the dynamical susceptibility of the $\tau \to 0$ limit with a peak located at half of the Kondo temperature.

Regarding the high energy sector, the pronounced structures located at odd multiples of the driving frequency Ω are washed out. Every time the Kondo Hamiltonian is

switched, local excitations in the vicinity of the impurity are created. During the first half period the excitations decay on a time scale t_K. If half of the period exceeds the internal time scale t_K, all excitations have been decayed before the next switch of the interaction. Therefore, it is not possible for the system to establish coherent excitations over the full period like in the case of fast switching.

The limit of long switching times: Increasing the switching time further leads to the appearance of a new structure near the half period boundary. Zooming into the region before the half period boundary, this is the last plot in Fig. (6.8), one can clearly see the dynamics that have been predicted in Sec. (6.1.1) where it was argued that the system behaves as for a single interaction quench in the limit $\tau \to \infty$. After a transient time of the order of t_K, the system approaches its equilibrium ground state properties as can be seen in Fig. (6.11) where the equilibrium and the numerically obtained relaxed dynamical susceptibility are plotted.

Chapter 7

Conclusion and Outlook

In this work a quasi-steady state in the Kondo model has been studied. This quasi-steady state is generated by periodically switching on and off the Kondo interaction at zero temperature. It is shown that the time-dependent Kondo Hamiltonian in the Toulouse limit can be mapped onto a time-dependent noninteracting resonant level model Hamiltonian even under these nonequilibrium conditions. Since the noninteracting resonant level model Hamiltonian is quadratic, its dynamics can be solved analytically on all time scales. This is done by reducing the problem of long-time evolution to a solvable matrix multiplication problem. Based on the exact solution of the single-particle dynamics of the noninteracting resonant level model in the periodic driving setup, correlation functions in the Kondo model are determined exactly.

The quasi-steady state, that builds up after an infinite number of periods, is characterized by the properties of the spin-spin correlation function $\langle S_z(t)S_z(t')\rangle$ and the dynamical spin susceptibility $\chi''(t, \omega)$, that is the spectral decomposition of the spin response function at a given point t in time. Remarkably, the conduction band electrons, that can be thought of as a fermionic bath for the local spin, behave as for zero temperature despite of the creation of excitations in the periodic driving process. This is seen most prominently in the algebraic long-time behavior of the spin-spin correlation function:

$$\langle S_z(t)S_z(t')\rangle \overset{t-t'\to\infty}{\propto} (t-t')^{-2}. \tag{7.1}$$

This behavior matches exactly the equilibrium behavior at zero temperature, even the prefactor is identical. Therefore, the low energy degrees of freedom are not affected by the periodic driving, since they dominate the long-time behavior. As the algebraic long-time decay converts into an exponential decay for an infinitesimal smearing of the Fermi surface, the long-time behavior can be viewed as a sensible measure for the existence of finite temperatures. As a consequence of the result above for the spin-spin correlation, it is not possible to characterize the quasi-steady state by an effective temperature. Basically, the excitations in a periodically driven system are fundamentally different from those induced by finite temperature. A finite temperature leads to a smearing of the Fermi surface whereas a periodic driving creates a discrete ladder of excitations corresponding to the absorption and emission of multiple quanta of the driving frequency.

As proposed by Kaminski et al. [21], the Kondo model is expected to show universality even under nonequilibrium conditions. As is shown in this thesis, the spin-spin correlation function and the related dynamical spin susceptibility indeed display a uni-

versal description. Moreover, it is only important how fast the system is driven in comparison to the internal Kondo time scale revealing that the Kondo scale remains the only relevant energy scale.

The asymptotic behavior of the quasi-steady state in the limits of fast and slow switching can be obtained by quite general arguments. For fast driving, the system is not able to follow the external switching as expected. If external parameters are varied much faster than any internal time scale, the system is not able to adapt to the external perturbation. The spin-spin correlation function as well as the dynamical susceptibility show a profile that is similar to an equilibrium one. A careful analysis, however, reveals that it is not possible to find a time-independent effective Hamiltonian that generates the same spin dynamics. In the opposite limit of slow switching the system relaxes in each half period. Therefore, the system behaves as for a single interaction quench, a setting that has already been considered in the work by Lobaskin and Kehrein [27][28].

For future work, it would be interesting to extend the results presented in this thesis obtained in the Toulouse limit of the Kondo model to the case of small Kondo couplings. For small couplings, the flow equation method can be used to map the Kondo Hamiltonian onto a noninteracting resonant level model as in the Toulouse limit. The hopping amplitude, however, as well as the hybridization function become nontrivial. Moreover, the analysis of further quantities like the local spectral density may provide a deeper understanding of the quasi-steady state in the present setting.

Appendix A

Some mathematical expressions

A.1 Fourier series expansions

In this paragraph, the Fourier series expansion of two important periodic functions will be listed:

i.
$$\frac{1 - 2\cos(k\tau/2)e^{-\Delta\tau/2} + e^{-\Delta\tau}}{1 - 2\cos(k\tau/2)e^{-\Delta\tau/2} + e^{-\Delta\tau}} = \sum_n c_n e^{ink\tau/2}$$

$$c_n = \begin{cases} \dfrac{1 + e^{-\Delta\tau}}{1 - e^{-\Delta\tau}}e^{-|n|\Delta\tau/4} & \text{, for } n \text{ even} \\[4mm] -2\cosh(\Delta\tau/4)\dfrac{e^{-\Delta\tau/2}}{1 - e^{-\Delta\tau}}e^{-|n|\Delta\tau/4} & \text{, for } n \text{ odd.} \end{cases}$$

(A.1)

ii.
$$\frac{e^{ik\tau/2} - e^{-\Delta\tau/2}}{e^{ik\tau} - e^{-\Delta\tau/2}} = \sum_{n\in\mathbb{Z}} d_n e^{ink\tau/2}$$

$$d_n = \begin{cases} -e^{-|n|\Delta\tau/4} & \text{, for } n \text{ even and } n < 0 \\[2mm] e^{\Delta\tau/4}e^{-|n|\Delta\tau/4} & \text{, for } n \text{ odd and } n < 0 \\[2mm] 0 & \text{, } n \geqslant 0 \end{cases}$$

A.2 Long time asymptotics of the function $s(t)$

Here, the asymptotic behavior for $t \to \infty$ of the following integral will be determined:

$$\frac{\Delta}{\pi} \int_0^\infty dk \, \frac{e^{ikt}}{k^2 + \Delta^2} = \frac{1}{\pi} \int_0^\infty dz \, \frac{\Delta t}{z^2 + (\Delta t)^2} e^{iz}.$$
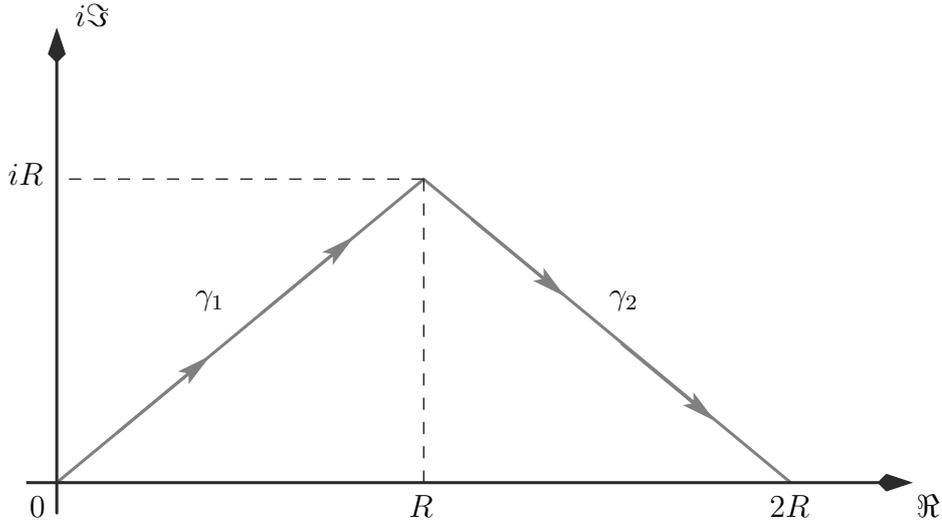
(A.2)

Figure A.1: Integration contour

The poles of the integrand $\pm i\Delta$ lie on the imaginary axis in the complex plain such that one can deform the integration contour as shown in Fig. (A.1):

$$\frac{1}{\pi}\int_0^\infty \mathrm{d}z\, \frac{\Delta t}{z^2+(\Delta t)^2}e^{iz} = \frac{1}{\pi}\int_{\gamma_1} \mathrm{d}z\, \frac{\Delta t}{z^2+(\Delta t)^2}e^{iz} + \frac{1}{\pi}\int_{\gamma_2} \mathrm{d}z\, \frac{\Delta t}{z^2+(\Delta t)^2}e^{iz}, \quad \text{(A.3)}$$
$$\gamma_1(s) = (1+i)Rs, \qquad \gamma_2(s) = (1+i)R + (1-i)s$$

where the limit $R \to \infty$ has to be performed in order to reproduce the correct integration contour:

$$\frac{1}{\pi}\int_{\gamma_1} \mathrm{d}z\, \frac{\Delta t}{z^2+(\Delta t)^2}e^{iz} = \frac{1}{\pi}\int_0^\infty \mathrm{d}x\, \frac{\Delta t}{(1+i)^2x^2+(\Delta t)^2}e^{ix}e^{-x}$$
$$\xrightarrow{t\to\infty} \frac{1+i}{\pi\Delta t}\int_0^\infty e^{ix}e^{-x} = \frac{i}{\pi\Delta t}$$
$$\frac{1}{\pi}\int_{\gamma_2} \mathrm{d}z\, \frac{\Delta t}{z^2+(\Delta t)^2}e^{iz} = \frac{1}{\pi}\int_0^1 (1-i)\Delta t\frac{R}{R^2(2-s+is)^2+(\Delta t)^2}e^{iR(2-s)}e^{-Rs}$$
$$\xrightarrow{R\to\infty} 0$$

$$\text{(A.4)}$$

Concluding:

$$\frac{\Delta}{\pi}\int_0^\infty \mathrm{d}k\, \frac{e^{ikt}}{k^2+\Delta^2} \xrightarrow{t\to\infty} \frac{i}{\pi\Delta t}$$
$$\frac{\Delta}{\pi}\int_0^\infty \mathrm{d}k\, \frac{e^{-ikt}}{k^2+\Delta^2} \xrightarrow{t\to\infty} \frac{-i}{\pi\Delta t}$$

$$\text{(A.5)}$$

Appendix B

The correlator $\langle\{d^\dagger(t), d(t')\}\rangle$

Here, the correlator

$$\langle\{d^\dagger(t), d(t')\}\rangle \tag{B.1}$$

will be determined. Due to Eq. (5.118) one can write $t = n\tau + s$, n being an integer and $s \in [0, \tau/2]$. The time coordinate t' can be chosen to be in the time interval $[0, \tau/2]$ due to the periodicity property of two-time correlation functions, see Eq. (4.36). In order to determine the correlator above, four different expressions have to be evaluated:

$$
\begin{aligned}
&\text{i.} && \frac{\Delta}{2\pi}e^{-\Delta(s+t')}\int_{-\infty}^{\infty}\mathrm{d}k\,\frac{\cos(nk\tau)}{k^2+\Delta^2}\frac{1-2\cos(k\tau/2)e^{-\Delta\tau/2}+e^{-\Delta\tau}}{1-2\cos(k\tau)e^{-\Delta\tau/2}+e^{-\Delta\tau}}\\[2mm]
&\text{ii.} && \frac{\Delta}{2\pi}e^{-\Delta s}\int_{-\infty}^{\infty}\mathrm{d}k\,\frac{e^{-i(n+1)k\tau}}{k^2+\Delta^2}\frac{e^{-ik\tau/2}-e^{-\Delta\tau/2}}{e^{-ik\tau}-e^{-\Delta\tau/2}}\left[e^{ikt'}-e^{-\Delta t'}\right]\\[2mm]
&\text{iii.} && \frac{\Delta}{2\pi}e^{-\Delta t'}\int_{-\infty}^{\infty}\mathrm{d}k\,\frac{e^{i(n+1)k\tau}}{k^2+\Delta^2}\frac{e^{-ik\tau/2}-e^{-\Delta\tau/2}}{e^{-ik\tau}-e^{-\Delta\tau/2}}\left[e^{iks}-e^{-\Delta s}\right]\\[2mm]
&\text{iv.} && \frac{\Delta}{2\pi}\int_{-\infty}^{\infty}\mathrm{d}k\,\frac{e^{ink\tau}}{k^2+\Delta^2}\left[e^{iks}-e^{-\Delta s}\right]\left[e^{-ikt'}-e^{-\Delta t'}\right]
\end{aligned}
\tag{B.2}
$$

that can be obtained by taking the real part of the expression appearing in Eq. (6.46). An integral that will automatically emerge is:

$$\frac{\Delta}{\pi}\int_{-\infty}^{\infty}\mathrm{d}k\,\frac{e^{ik\mathcal{T}}}{k^2+\Delta^2} = e^{-\Delta|\mathcal{T}|} \tag{B.3}$$

The expression above can be evaluated by using Eq. (A.1) and Eq. (B.3):

i. $e^{-\Delta(s+t')} \sum_m c_m \dfrac{\Delta}{2\pi} \displaystyle\int_{-\infty}^{\infty} dk \, \dfrac{e^{i(n+m/2)k\tau}}{k^2 + \Delta^2} = \dfrac{1}{2} e^{-\Delta(s+t')} \sum_m c_m e^{-|2n+m|\Delta\tau}$

$\qquad = \dfrac{1}{2} e^{-n\Delta\tau/2} e^{-\Delta(s+t')}$

ii. $e^{-\Delta s} \sum_m d_{-m} \dfrac{\Delta}{2\pi} \displaystyle\int_{-\infty}^{\infty} dk \, \dfrac{e^{i(m/2-n)k\tau}}{k^2 + \Delta^2} \left[e^{ikt'} - e^{-\Delta t'} \right]$

$\qquad = \dfrac{1}{2} e^{-\Delta s} \sum_m d_{-m} \left[e^{-|(m/2-n)\tau + t'|\Delta} - e^{-\Delta t'} e^{-|m/2-n|\Delta\tau} \right]$ (B.4)

$\qquad = \dfrac{1}{2} e^{-\Delta s} \begin{cases} e^{-n\Delta\tau/2} \left[e^{\Delta t'} - e^{-\Delta t'} \right] & , \text{ for } n > 0 \\ 0 & , \text{ otherwise} \end{cases}$

iii. $\dfrac{1}{2} e^{-\Delta t'} \begin{cases} e^{-n\Delta\tau/2} \left[e^{\Delta s} - e^{-\Delta s} \right] & , \text{ for } n < 0 \\ 0 & , \text{ otherwise} \end{cases}$

iv. $\dfrac{1}{2} \begin{cases} e^{-\Delta(s-t')} - e^{-\Delta(s+t')} & , \text{ for } n = 0 \\ 0 & , \text{ otherwise} \end{cases}$

Collecting all contributions one obtains:

$$\langle d^\dagger(t) d(t') \rangle = \dfrac{1}{2} e^{-n\Delta\tau/2} e^{-\Delta(s-t')}$$ (B.5)

Bibliography

[1] P.W. Anderson, *Phys. Rev.* **124** (1961), 41.

[2] P.W. Anderson, *J. Phys. C: Solid St. Phys.* **3** (1970), 2436.

[3] P.W. Anderson, G. Yuval and D.R. Hamann, *Phys. Rev. B* **1** (1970), 4464.

[4] N. Andrei, *Phys. Rev. Lett.* **45** (1980), 379.

[5] M.A. Cazalilla, *Phys. Rev. Lett.* **97** (2006), 156403.

[6] N. d'Ambrumenil and B.A. Muzykantskii, *Phys. Rev. B* **71** (2005), 045326.

[7] J. von Delft, G. Zarand and M. Fabrizio, *Phys. Rev. Lett.* **81** (1998), 196.

[8] B. Doyon and N. Andrei, *Phys. Rev. B* **73** (2006), 245326.

[9] M. Eckstein and M. Kollar, *Phys. Rev. Lett.* **100** (2008), 120404.

[10] A. Faribault, P. Calabrese and J.S. Caux, *J. Stat. Mech.* (2009), P03018.

[11] D. Goldhaber-Gordon, H. Shtrikman, D. Mahalu, D. Abusch-Magder, U. Meirav and M.A. Kastner, *Nature* **391** (1998), 156.

[12] Y. Goldin and Y. Avishai, *Phys. Rev. Lett.* **81** (1998), 5394.

[13] Y. Goldin and Y. Avishai, *Phys. Rev. B* **61** (2000), 16750.

[14] M. Grifoni and P. Hänggi, *Phys. Rep.* **304** (1998), 229.

[15] F. Guinea, *Phys. Rev. B* **32** (1985), 4486.

[16] A.C. Hewson: *The Kondo Problem to Heavy Fermions*. Cambridge University Press, 1997.

[17] W. Hofstetter: *Renormalization Group Methods for Quantum Impurity Systems*. University of Augsburg, PhD thesis, July 2000.

[18] A. Imambekov and L. Glazman, *Science* **323** (2009), 228.

[19] K. Jänich: *Einführung in die Funktionentheorie*. Springer-Verlag, 1977.

[20] A. Kaminski, Y.V. Nazarov and L. Glazman, *Phys. Rev. Lett.* **83** (1999), 384.

[21] A. Kaminski, Y.V. Nazarov and L. Glazman, *Phys. Rev. B* **62** (2000), 8154.

[22] M. Khodas, M. Pustilnik, A. Kamenev and L. Glazman, *Phys. Rev. B* **76** (2007), 155402.

[23] S. Kohler, J. Lehmann and P. Hänggi, *Phys. Rep.* **406** (2005), 379.

[24] D.C. Langreth and P. Nordlander, *Phys. Rev. B* **43** (1991), 2541.

[25] A.J. Leggett, S. Chakravarty, A.T. Dorsey, M.P.A. Fisher, A. Garg and W. Zwerger, *Rev. Mod. Phys.* **59** (1987), 1.

[26] F. Lesage and H. Saleur, *Phys. Rev. Lett.* **80** (1998), 4370.

[27] D. Lobaskin and S. Kehrein, *Phys. Rev. B* **71** (2005), 193303.

[28] D. Lobaskin and S. Kehrein, *J. Stat. Phys.* **123** (2006), 301.

[29] R. Lopez, R. Aguado, G. Platero and C. Tejedor, *Phys. Rev. Lett.* **81** (1998), 4688.

[30] M. Möckel and S. Kehrein, *Phys. Rev. Lett.* **100** (2008), 175702.

[31] P. Nordlander, M. Pustilnik, Y. Meir, N.S. Wingreen and D.C. Langreth, *Phys. Rev. Lett.* **83** (1999), 808.

[32] P. Nordlander, N.S. Wingreen, Y. Meir and D.C. Langreth, *Phys. Rev. B* **61** (2000), 2146.

[33] P. Nozieres and C.T. De Dominicis, *Phys. Rev.* **178** (1969), 1097.

[34] G. Platero and R. Aguado, *Phys. Rep.* **395** (2004), 1.

[35] M. Pustilnik, M. Khodas, A. Kamenev and L. Glazman, *Phys. Rev. Lett.* **96** (2006), 196405.

[36] H. Sambe, *Phys. Rev. A* **7** (1973), 2203.

[37] H. Schöller and J. von Delft, *Ann. Phys. (Leipzig)* **7** (1998), 225.

[38] K.D. Schotte and U. Schotte, *Phys. Rev.* **185** (1969), 509.

[39] K.D. Schotte and U. Schotte, *Phys. Rev.* **182** (1969), 479.

[40] J.R. Schrieffer and P. Wolff, *Phys. Rev.* **149** (1966), 491.

[41] J.H. Shirley, *Phys. Rev.* **138** (1965), B979.

[42] N. Tsuji, T. Oka and H. Aoki, *Phys. Rev. B* **78** (2008), 235124.

[43] P.B. Wiegmann, *Phys. Lett. A* **80** (1980), 179.

[44] K.G. Wilson, *Rev. Mod. Phys.* **47** (1975), 773.

[45] G. Zarand and J. von Delft, *arXiv:cond-mat/9812182* (1998).

[46] G. Zarand and J. von Delft, *Phys. Rev. B* **61** (2000), 6918.

Selbstständigkeitserklärung

Hiermit erkläre ich, dass ich die vorliegende Arbeit selbstständig angefertigt und nur die angegebenen Quellen und Hilfsmittel verwendet habe.

München, den 7. April 2009

Markus Philip Ludwig Heyl